R-08-121

Effects on surface hydrology and near-surface hydrogeology of an open repository in Forsmark

Results of modelling with MIKE SHE

Lars-Göran Gustafsson, Ann-Marie Gustafsson,
Maria Aneljung, Ulrika Sabel
DHI Sverige AB

September 2009

Svensk Kärnbränslehantering AB
Swedish Nuclear Fuel
and Waste Management Co

Box 250, SE-101 24 Stockholm
Phone +46 8 459 84 00

ISSN 1402-3091
SKB Rapport R-08-121

Effects on surface hydrology and near-surface hydrogeology of an open repository in Forsmark

Results of modelling with MIKE SHE

Lars-Göran Gustafsson, Ann-Marie Gustafsson,
Maria Aneljung, Ulrika Sabel
DHI Sverige AB

September 2009

Abstract

This report presents the methodology and the results from the modelling of an open repository for spent nuclear fuel in Forsmark. Thus, the present work analyses the hydrological effects of the planned repository during the construction and operational phases when it is open, i.e. air-filled, and hence may cause a disturbance of the hydrological conditions in the surroundings. The numerical modelling is based on the MIKE SHE SDM-Site Forsmark model.

The modelling was divided into three steps. The first step was to update the SDM-Site Forsmark model for hydrology and near surface hydrogeology. The main updates concerned the hydraulic properties of the deep bedrock down to 990 metres below sea level and a refined vertical discretisation of the computational layers in the bedrock. This model was used to simulate undisturbed natural conditions.

The next step was to describe the open repository conditions, using Forsmark layout D2 (version 1.0, from April 2008), by implementing the access tunnel, the repository tunnels and shafts to the model, and to simulate the consequences on the surface hydrology caused by an open repository under different conditions. The final step was a sensitivity analysis that aimed to investigate the sensitivity of the model to the properties of the upper bedrock, the interface between the Quaternary deposits and the bedrock, and the sediments under the lakes and the sea, with respect to the effects of the open repository.

The model covers an area of 37 km^2. The surface water divides were assumed to coincide with the groundwater divides; thus, a no-flow boundary condition was used at the horizontal boundaries, except in the sea where a time varying head boundary, equal to observed sea elevation, was applied. Also the bottom boundary was described as a no-flow boundary. The transient top boundary condition was based on meteorological data gathered at the local SKB stations during the period 2005–2006.

The groundwater modelling was performed with the MIKE SHE code, a process-based modelling tool that calculates the groundwater flow in three dimensions. It takes the whole hydrological cycle into consideration and describes the water flow from rainfall to river flow. The coupling to the pipe flow model MOUSE was used to implement the repository. The repository was described as a number of pipe links in MOUSE and the inflow of water from MIKE SHE to MOUSE, i.e. the flow of water from the aquifer to the tunnels, was calculated. The shafts were described as cells with atmospheric pressure.

The results from the updated MIKE SHE model for undisturbed condition agrees with the results obtained from the SDM Forsmark model presented in the final (SDM-Site) version of the site description. The average specific runoff in the simulation for the year 2006 was calculated to 128 mm and the total evapotranspiration was calculated to 421 mm. The groundwater table in the area is shallow; the mean depth to the groundwater table for the year 2006 was calculated to 1.1 m below ground surface (the sea area excluded). The discharge in the water courses is transient during the year and is dependent on the weather conditions.

The impact of the open repository on the groundwater table in the Quaternary deposits is rather mild compared to the head change in the bedrock, and concentrated to outcrop areas around steeply dipping deformation zones in the bedrock above the repository. The largest drawdown of the groundwater table is developed north-east of the Forsmark nuclear power plant.

The calculated groundwater table drawdown and the size of the associated influence area (here defined as the area where the drawdown is larger than 0.3 m) are highly dependent on the level of grouting in the access tunnel and the deposition tunnels. Three levels of grouting were tested corresponding to hydraulic conductivities of $1 \cdot 10^{-7}$ m/s, $1 \cdot 10^{-8}$ m/s and $1 \cdot 10^{-9}$ m/s. The lowest level of grouting leads to an influence area of 1.6 km^2, as an average for 2006. When the highest level of grouting is applied to the repository walls, the average influence area is calculated to 0.5 km^2 for the year 2006.

The temporal variation of the influence area during a year is large, with more than two times larger maximum influence area during 2006 compared to the minimum influence area during that year. The water levels in the lakes, as well as the discharges in the water courses, are only affected to a very small extent by the open repository, and only in areas where the groundwater table is affected (i.e. at Lake Bolundsfjärden and Lake Gällsboträsket).

The simulated total inflows to the open repository vary between 10 L/s and 36 L/s depending on the applied level of grouting. Nearly half of the repository inflow comes from an increased recharge from the sea. The influence areas and inflows specified above refer to a case with the whole repository open, i.e. with all the transport tunnels and deposition tunnels open at the same time. However, this is a hypothetical worst case scenario, because the repository will be constructed and taken into operation in three development phases. Also these individual development phases have been investigated in the present modelling study.

Sammanfattning

Denna rapport ger en presentation av metodiken och resultaten från modelleringen av ett öppet förvar i Forsmark. Det huvudsakliga syftet var att beskriva effekterna av tillfartstunneln, det öppna slutförvaret och hiss- och luftschakt på den ytnära hydrologin. Den numeriska modelleringen baseras på MIKE SHE-modellen från SDM-Site Forsmark, vilket är den ythydrologiska modell som togs fram som en del den sista platsbeskrivande modellen av Forsmark (SDM-Site) som producerades under platsundersökningsskedet.

Modelleringen har delats in i tre huvuddelar. Första delen utgjordes av en uppdatering av den numeriska modellen. Uppdateringen bestod främst i att komplettera modellen med data för det djupa berget ner till nivån 990 meter under havet, samt att förfina modellens vertikala indelning i beräkningslager. Med denna modell simulerades opåverkade förhållanden.

Nästa steg var att beskriva det öppna förvaret, varvid Forsmark layout D2 användes (version 1.0, från april 2008), med tillfartstunnlar och schakt i modellen, samt att simulera och beskriva effekterna på den ytnära hydrologin av det öppna förvaret under olika förhållanden. Slutligen gjordes en känslighetsanalys som syftade till att undersöka modellens känslighet för det ytliga bergets egenskaper, egenskaperna i övergången mellan jord och berg, samt sedimenten under sjöarna och havet, med avseende på påverkan från ett öppet förvar.

Modellen täcker ett område på 37 km^2. Yt- och grundvattendelare antas sammanfalla. Därför har en tät rand (en rand med nollflöde) ansatts vid de horisontella ränderna, förutom i havet där en tidsvarierande tryckrand lika med uppmätt havsnivå ansatts. Även bottenranden har beskrivits med en tät rand. Det övre randvillkoret beskrivs med hjälp av nederbörd och potentiell avdunstning. Meteorologidata från SKB:s lokala väderstationer för åren 2005–2006 har använts som indata.

Grundvattenmodelleringen har genomförts med modellkoden MIKE SHE, ett processbaserat modellverktyg som beräknar grundvattenflödet i tre dimensioner. MIKE SHE beskriver hela den hydrologiska cykeln, från nederbörd till avrinning i bäckar och vattendrag. Kopplingen till modellverktyget MOUSE (utvecklat för beskrivning av ledningsnät) användes för att implementera förvaret i modellen. Förvaret beskrevs som ett antal ledningar i MOUSE och vattenflödet mellan MIKE SHE och MOUSE, det vill säga vattenflödet från akviferen till tunnlarna, beräknades. Hiss- och ventilationsschakt beskrevs i modellen som celler med atmosfärstryck.

Resultaten från den uppdaterade MIKE SHE modellen, som syftar till att beskriva hydrologin i området under ostörda förhållanden, stämmer bra överens med de resultat som presenterades platsbeskrivningen SDM-Site Forsmark. Avrinningen för år 2006 är beräknad till 128 mm och den totala evapotranspirationen beräknades till 421 mm. Grundvattenytan i området ligger nära markytan; medeldjupet till grundvattenytan i hela området (exklusive havet) för den simulerande perioden 2006 är 1.1 m under markytan. Flödena i områdets vattendrag varierar mycket under året och starkt kopplade till de meteorologiska förhållandena i området.

Påverkan av det öppna förvaret på grundvattenytan i jordlagren är ganska begränsad i jämförelse med portrycksändringen i berget, och koncentreras till de områden ovan förvaret där de brantstående deformationszonerna har sitt utgående. Den största avsänkningen av grundvattenytan sker nordost om kärnkraftverket.

Avsänkningen av grundvattenytan och storleken på påverkansområdet, vilket här definieras som det område där grundvattenytan sänks av mer än 0.3 m, visade sig vara mycket beroende av vilken grad av tätning som appliceras på tunnelväggarna. Tre tätningsfall testades motsvarande hydrauliska konduktiviteter på $1 \cdot 10^{-7}$ m/s, $1 \cdot 10^{-8}$ m/s och $1 \cdot 10^{-9}$ m/s i den tätade zonen runt tunnlar och schakt. För den lägsta tätningsnivån med $K = 1 \cdot 10^{-7}$ m/s beräknades påverkansområdet till i medeltal ca 1.6 km^2 för året 2006. När den högsta tätningsnivån tillämpas på tunnelväggarna i modellen ($K = 1 \cdot 10^{-9}$ m/s) fås ett påverkansområde på i medeltal ca 0.5 km^2 för året 2006.

Påverkansområdets tidsmässiga variation är stor under ett år, med mer än dubbelt så stor area för det maximala påverkansområdet under 2006, jämfört med arean för det minsta påverkansområdet

under samma år. Varken sjönivåerna eller flödet i vattendragen påverkas i någon större omfattning av förvaret, och då endast inom de områden där grundvattenytan påverkas (vid sjöarna Bolundsfjärden och Gällsboträsket).

De beräknade totala inflödena till det öppna förvaret varierar mellan 36 L/s och 10 L/s beroende på vilket tätningsfall som studeras. Nästan hälften av inflödet till förvaret härstammar från ett ökat läckage från havet. De angivna påverkansområdena och inflödena ovan baseras på ett beräknings-fall där hela djupförvarsanläggningen antas vara öppen, vilket innebär att alla transport- och deponeringstunnlar är öppna samtidigt. Detta är dock ett hypotetiskt värsta fall som inte kommer att inträffa i verkligheten. Förvaret kommer att anläggas och tas i drift i tre utbyggnadsfaser. Även beräkningsfall med stegvis utbyggnad och drift av förvaret har studerats i modelleringen.

Contents

1 Introduction

1.1 Background

The Swedish Nuclear Fuel and Waste Management Company (SKB) has performed site investigations at two different locations in Sweden, referred to as the Forsmark and Laxemar areas, with the objective of siting a final repository for spent nuclear fuel. Data from the site investigations are used in a variety of modelling activities, and the results are utilised within the frameworks of Site Descriptive Modelling (SDM), Safety Assessment (SA), and Environmental Impact Assessment (EIA). The SDM provides a description of the present conditions at the site, and is used as a basis for developing models intended to describe the future conditions in the area. This report presents model results of numerical flow modelling of surface water and near-surface groundwater and the effects of an open repository at the Forsmark site.

The numerical modelling was performed with the modelling tools MIKE SHE and MOUSE, and is based on the conceptual description of the Forsmark site provided in /Johansson 2008/ and /Follin et al. 2008/. The modelling performed in this project is based on the SDM-Site Forsmark model /Bosson et al. 2008/. All the different subject areas within the site descriptive modelling project are summarised in /SKB 2008/; the surface systems are described in more detail in /Lindborg (ed) 2008/.

During the construction and operational phases, there will be atmospheric pressure in the open tunnels and shafts and rock caverns in the repository. This will cause disturbances in the pressure field around the subsurface constructions and inflow of groundwater. The size of this inflow and its possible effects on surrounding groundwater and surface water systems need to be quantified. The issues related to the effects of the open repository concern both the conditions in the repository (inflows and hydrochemical conditions) and in the surrounding environment (groundwater levels, surface water levels and discharges). Thus, the open repository modelling will provide results to both SA and EIA. The modelling work presented here is focused on the effects on the surface hydrology and near-surface hydrogeology, i.e. on the surrounding environment, which constitutes a primary input to the EIA.

1.2 Scope and objectives

Using the MIKE SHE SDM-Site Forsmark model as a starting point, the present work can be subdivided into the following three parts:

1. Update of the SDM-Site Forsmark numerical flow model (mainly an increase of the vertical extent of the model domain and an enhanced vertical model resolution), and simulation of undisturbed conditions.
2. Implementation of the open repository description in the flow model. Analysis of the hydrological effects of an open repository (effects on surface hydrology and the hydrogeological conditions in the Quaternary deposits and the upper bedrock).
3. Analysis of the sensitivity of the model to the properties of the upper bedrock, the properties in the interface between the Quaternary deposits and the bedrock, and the sediments under the lakes and the sea, with respect to the effects of the open repository.

The general objectives of the present modelling are the following:

- Develop and present an open repository flow model based on the MIKE SHE SDM-Site Forsmark model.
- Provide qualitative and quantitative results to be used in the SA biosphere modelling (SR-Site) and in the EIA (evaluation of open repository effects).
- Evaluate the influence of the open repository on groundwater levels, surface water levels and surface water discharges within the model area.
- Evaluate the inflow to different parts of the open repository construction under different conditions; in particular, for three different levels of grouting.

1.3 Setting

The Forsmark area is located approximately 120 km north of Stockholm, in northern Uppland within the municipality of Östhammar. Figure 1-1 shows parts of the regional model area and the candidate area subjected to site investigation and site descriptive modelling. It also shows some lakes and other objects of importance for the hydrological modelling.

The candidate area is the area initially prioritised for potentially hosting the geological repository, which means that the repository possibly could be built somewhere within this area, not that it would occupy the whole area. This implies that more detailed investigations have been performed within the candidate area than outside it, at least for some of the site investigation disciplines, see /SKB 2008/ for details.

The candidate area is situated in the immediate vicinity of the Forsmark nuclear power plant and the underground repository for low- and medium-active nuclear waste, SFR. It is located along the shoreline of Öregrundsgrepen (a part of the Baltic), and extends from the nuclear power plant and the access road to the SFR facility in the northwest to the Kallrigafjärden in the southeast. The candidate area is approximately 6 km long and 2 km wide.

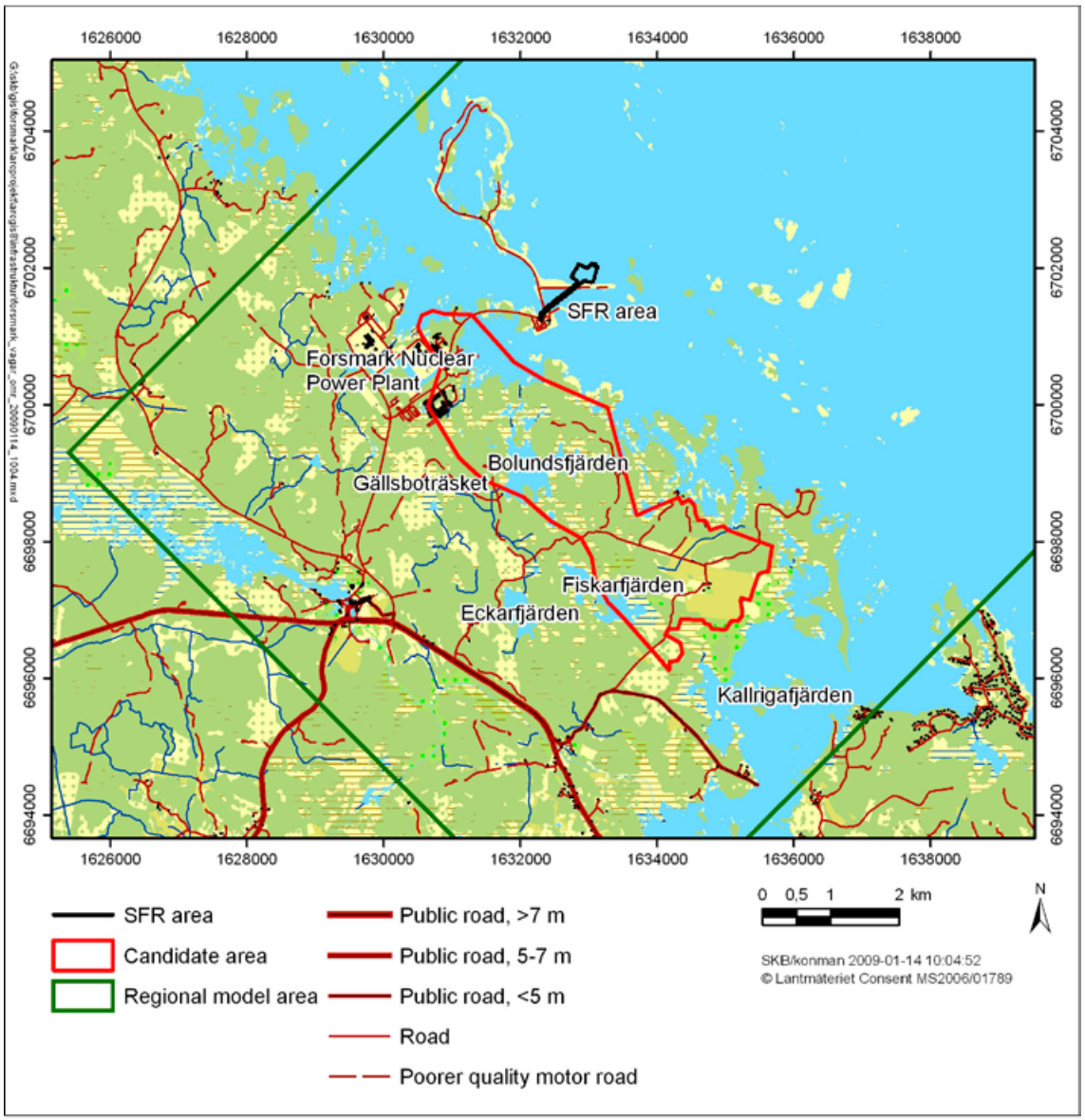

Figure 1-1. *Detailed map of the land part of the regional model area and some objects of particular interest for the hydrological modelling.*

A description of the climate, and the hydrological and hydrogeological conditions in the Forsmark area is presented in /Johansson 2008/. /Lindborg (ed) 2008/ gives a description of the whole surface and near-surface system, including the most current models of, e.g. the topography and the Quaternary deposits.

In this report, the datum plane is RHB70. Depending on type of data presented, levels will be given in metres above sea level (m.a.s.l.) or metres below sea level (m.b.s.l.) according to the RHB70 system.

1.4 Modelling procedure

The modelling work is based on the MIKE SHE SDM-Site Forsmark model /Bosson et al. 2008/. A reference simulation was defined as an updated version of the calibrated final model version as described in /Bosson et al. 2008/. The reference simulation was used as a base model for the tunnels, shafts and rock caverns introduced into the modelling work to investigate how these constructions will affect the near-surface hydrology in the model area. The last step was a sensitivity analysis which aimed to investigate the sensitivity to the level of grouting of the tunnel walls.

1.5 Related modelling activities

Several modelling activities have provided the various external input data and models required for the present modelling. Whereas most of these inputs are described in /Bosson et al. 2008/, we discuss here briefly the interactions with the hydrogeological activities that consider flow modelling of the integrated bedrock-Quaternary deposits system and the modelling activities analysing the influences of an open repository and the design work of the planned repository.

The numerical model was developed using the MIKE SHE tool, coupled with the modelling tool MOUSE describing the geometry of the repository and the interactions with the surrounding groundwater system. The ground surface, as obtained from the topographic model (DEM) of the site, was the upper model boundary and the lower boundary was set at 990 m.b.s.l. The modelling activities that provided inputs to the various parts of this work can be summarised as follows:

- The SDM Forsmark version 2.2 hydrogeological modelling performed with the ConnectFlow modelling tool /Follin et al. 2007/ delivered the hydrogeological properties of the bedrock.
- The SDM-Site conceptual modelling of the hydrology and near-surface hydrogeology at the Forsmark site /Johansson 2008/ provided a basic hydrogeological parameterisation and a hydrological-hydrogeological description to be tested in the numerical modelling. The relations between the near-surface and bedrock hydrogeological models are discussed in /Follin et al. 2008/ and /SKB 2008/.
- The MIKE SHE SDM-Site Forsmark numerical modelling of the surface hydrology and near-surface hydrogeology /Bosson et al. 2008/. All the simulations in this report are based on an update of the final version of the MIKE SHE model described in /Bosson et al. 2008/.
- The open repository simulations performed with DarcyTools /Svensson 2005, Svensson and Follin 2009/. This modelling is focused on the bedrock and the conditions at repository depth, with detailed studies of the inflow to tunnels and the re-saturation after closing the repository.
- The repository layout D2, version 1.0 from April 2008, including 27% loss of deposition holes, was used in the open repository simulations described in this report.

1.6 This report

This report provides an integrated presentation of the modelling activities listed in Section 1.2. Chapter 2 describes the modelling tool and the numerical flow model. In Chapter 3, the model updates, simulation specifications and results of a reference simulation for undisturbed conditions are presented. Chapter 4 describes the conditions and simulation cases for disturbed conditions, i.e. with the open repository included in the model. Chapter 5 presents results from the simulations of disturbed conditions. Chapter 6 describes and presents results from a sensitivity analysis with respect to the effects of the open repository, and Chapter 7 presents the conclusions of the work.

2 Overview of modelling tools

2.1 MIKE SHE

MIKE SHE (Système Hydrologique Europeen) is a physically based, distributed model that simulates water flows from rainfall to river flow. It is a commercial code, developed by the Danish Hydraulic Institute (DHI). This sub-section summarises the basic processes and the governing equations in MIKE SHE. The code used in this project is software release version 2008. For a more detailed description, see the user's guide and technical reference /DHI Software 2008a/.

MIKE SHE describes the main processes in the land phase of the hydrological cycle. The precipitation can either be intercepted by leaves or fall to the ground. The water on the ground surface can infiltrate, evaporate or form overland flow. Once the water has infiltrated the soil, it enters the unsaturated zone. In the unsaturated zone, it can either be extracted by roots and leave the system as transpiration, or it can percolate down to the saturated zone (Figure 2-1). MIKE SHE is fully integrated with a channel-flow code, MIKE 11. The exchange of water between the two modelling tools takes place during the whole simulation, i.e. the two programs run simultaneously.

MIKE SHE is developed primarily for modelling of groundwater flow in porous media. In the present modelling, the bedrock is included as a porous medium. The bedrock is parameterised by use of data from the SDM-Site Forsmark model /Bosson et al. 2008/.

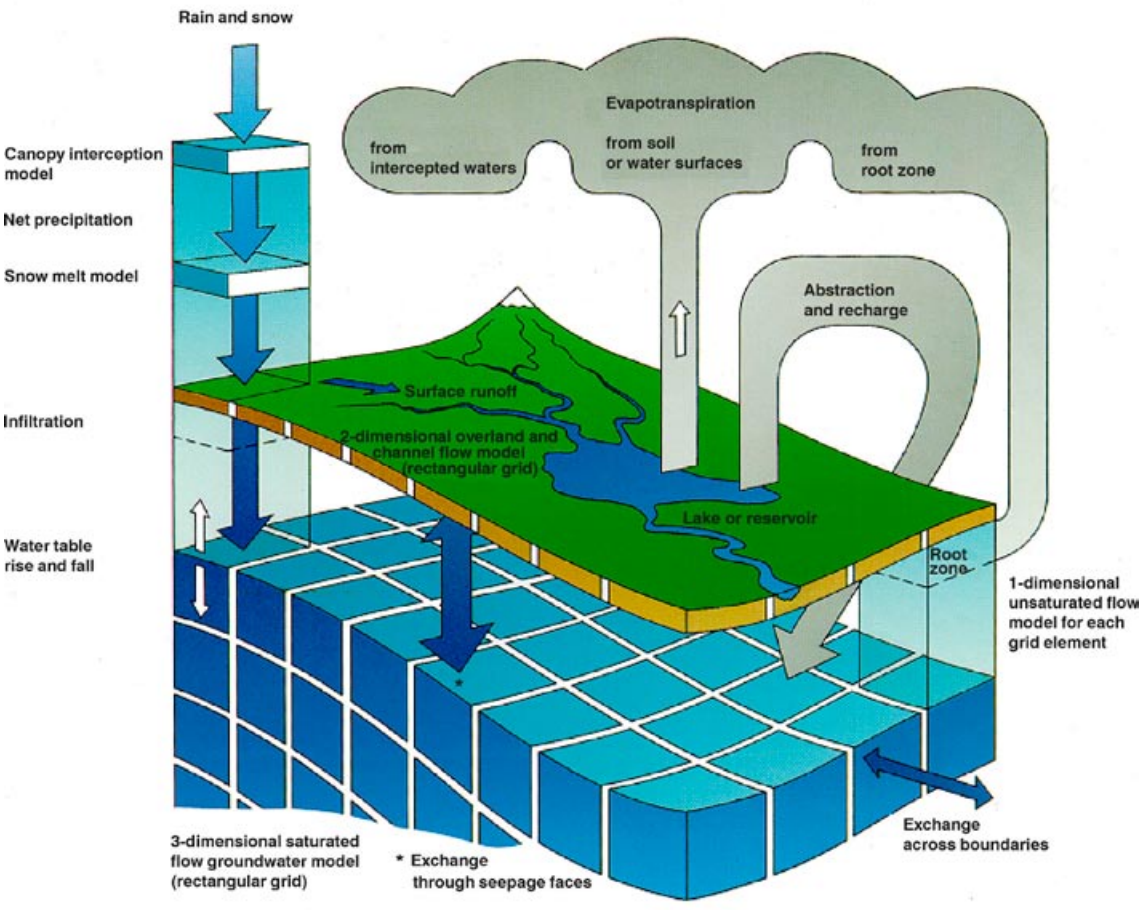

Figure 2-1. *Overview of the MIKE SHE model /DHI Software 2008a/.*

MIKE SHE consists of the following model components:

- Precipitation (rain or snow).
- Evapotranspiration, including canopy interception, which is calculated according to the principles of /Kristensen and Jensen 1975/.
- Overland flow, which is calculated with a 2D finite difference diffusive wave approximation of the Saint-Venant equations, using the same 2D mesh as in the horizontal mesh used in the (3D) groundwater flow component. Overland flow interacts with rivers, the unsaturated zone, and the saturated (groundwater) zone.
- Channel flow, described through the river modelling component, MIKE 11, which is a modelling system for river hydraulics. MIKE 11 is a dynamic, 1D modelling tool for the design, management and operation of river and channel systems. MIKE 11 supports any level of complexity and offers simulation tools that cover the entire range from simple Muskingum routing to high-order dynamic wave formulations of the Saint-Venant equations.
- Unsaturated water flow, which in MIKE SHE is described as a vertical soil profile model that interacts with both the overland flow (through ponding) and the groundwater model (the groundwater table provides the lower boundary condition for the unsaturated zone). MIKE SHE offers three different modelling approaches, including a simple two-layer root-zone mass balance approach, a gravity flow model, and a full Richards's equation model.
- Saturated (groundwater) flow, which allows for 3D flow in a heterogeneous aquifer, with conditions shifting between unconfined and confined. The spatial and temporal variations of the dependent variable (the hydraulic head) are described mathematically by the 3D Darcy equation and solved numerically by an iterative implicit finite difference technique.

For a detailed description of the processes included in MIKE SHE and MIKE 11, see /DHI Software 2008a/.

2.2 The coupling between MIKE 11 and MIKE SHE

The coupling between MIKE 11 and MIKE SHE is made via river links, which are located on the edges that separate adjacent grid cells. The location of each river link is determined from the co-ordinates of the MIKE 11 river points. Since the MIKE SHE river links are located on the edges between grid cells, the details of the MIKE 11 river geometry can be only partly included in MIKE SHE, depending on the grid size. The smaller the grid size, the more accurately the river network can be reproduced. This also leads to the restriction that each MIKE SHE grid cell can only be coupled to one coupling reach in MIKE 11 per river link in MIKE SHE.

2.2.1 Overland water

The communication between the river network in MIKE 11 and the overland component in MIKE SHE can be defined in two different ways:

- using so called flood codes, where water levels from MIKE 11 simply are transferred to MIKE SHE,
- using a two-way communication based on a so-called overbank spilling option.

In this version of the Forsmark model, the two-way overbank spilling option is applied. This option allows river water to spill onto the MIKE SHE model as overland flow. The overbank spilling option treats the river bank as a weir. When the overland flow water level or the river water level is above the left or right bank elevation, water will spill across the bank based on the weir formula in Equation 2-1. The principle is illustrated in Figure 2-2.

$$Q = dx \cdot C \cdot (H_{us} - H_w)^k \cdot \left[1 - \left(\frac{H_{ds} - H_w}{H_{us} - H_w}\right)^k\right]^{0.385} \qquad \text{(Equation 2-1)}$$

Q	Flow across the weir (m^3/s)
dx	Grid size (m)
C	Weir coefficient (-), set to the default value 1.838
H_{us}	Height of water on the upstream side of the weir (m)
H_{ds}	Height of water on the downstream side of the weir (m)
H_w	Height of the weir (m)
k	Head exponent (-), set to the default value 1.5, in order to account for both the flow area and the head gradient according to the Manning equation

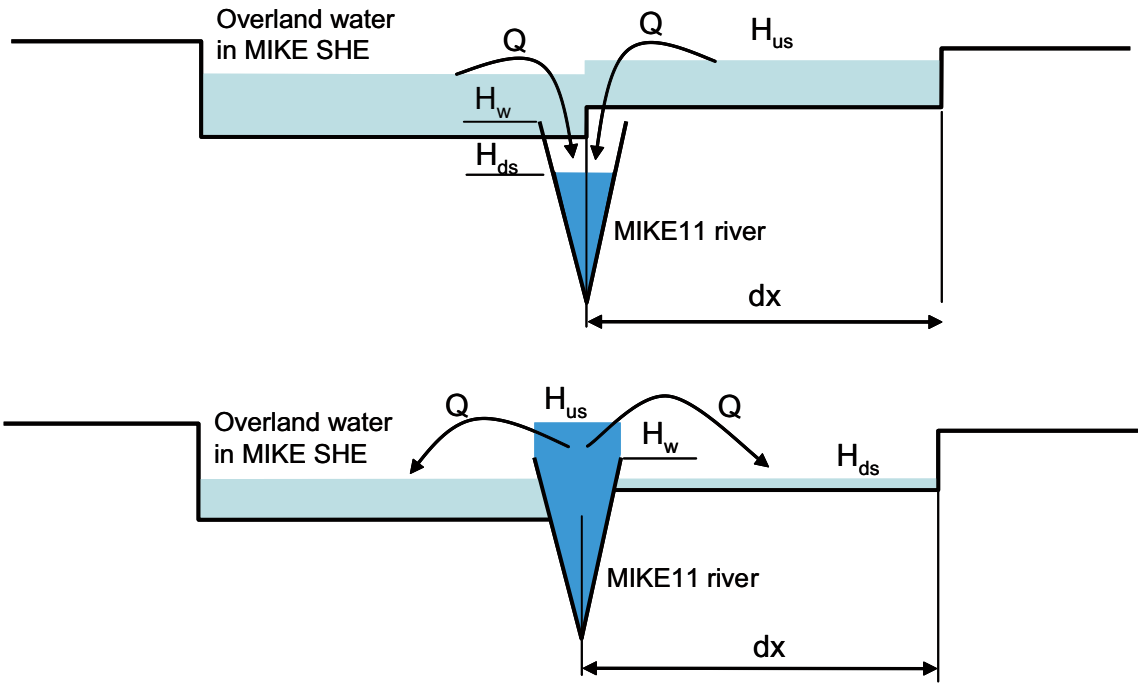

Figure 2-2. *Illustration of the overland coupling between MIKE11 and MIKE SHE, and representation of relevant parameters used for calculating the exchange of water.*

Note that Equation 2-1 is calculated twice, i.e. once for each cell on either side of the river link. This allows for different flow to/from either side of the river if there is an overland water level gradient across the river, or if the right and left river bank levels are different.

If overland water levels are such that overland water is flowing to the river, overland flow to the river is added to MIKE 11 as lateral inflow. If the water level in the river is higher than the level of ponded water, river water will spill onto the MIKE SHE cell and become part of the overland flow. If the upstream water depth over the weir approaches zero, the flow over the weir becomes undefined. Therefore, the calculated flow is reduced to zero linearly when the upstream height goes below a threshold.

2.2.2 Groundwater

The communication between the river network and the groundwater aquifer is calculated in the same way as in previous versions of the code /DHI Software 2008a/. The groundwater coupling between MIKE 11 and MIKE SHE is made via river links, which are located on the edges that separate adjacent grid cells. The exchange flow between a saturated zone grid cell, with contact to the river system, and a river link is included as a source/sink term in the governing flow equation for three-dimensional saturated flow. The exchange flow is calculated as a conductance multiplied by the head difference between the river and the grid cell according to Equation 2-2. The principle is illustrated in Figure 2-3.

$Q_{cell} = dh \cdot C$ (Equation 2-2)

Q_{cell} Exchange flow from one neighbouring grid cell to the river link (m^3/s)

dh Head difference between the river link and the neighbouring grid cell (m)

C Total conductance (m^2/s)

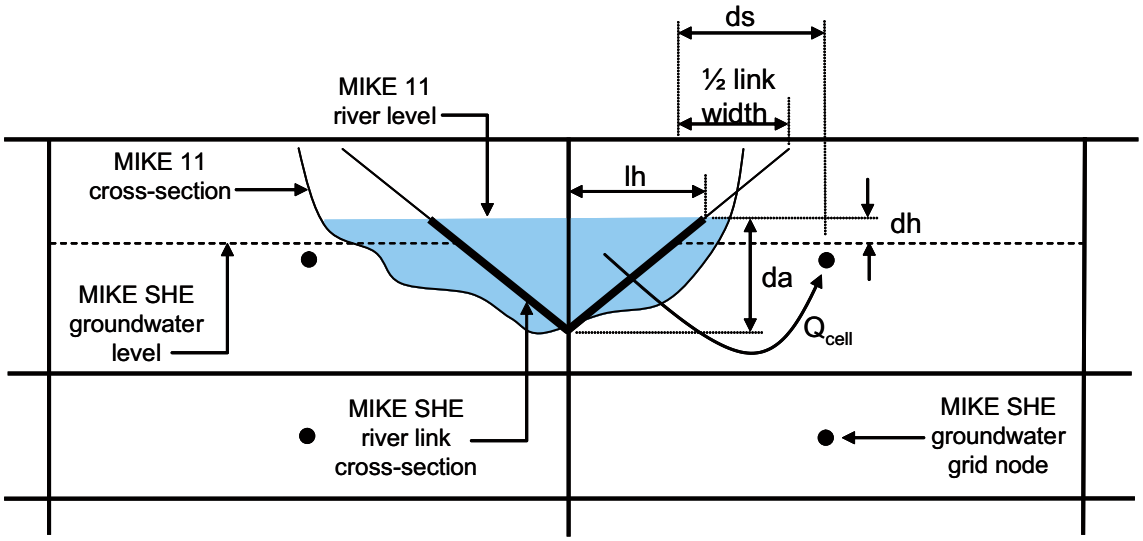

Figure 2-3. *Illustration of the groundwater coupling between MIKE11 and MIKE SHE, and representation of relevant parameters used for calculating the exchange of water.*

Note that Equation 2-2 is calculated twice, once for each cell on either side of the river link. This allows for different flow to/from either side of the river if there is a groundwater head gradient across the river, or if the aquifer properties are different. The conductance between the grid cell and the river link is a function of the water level in the river, the river width, the elevation of the riverbed, as well as the hydraulic properties of the riverbed and the aquifer material, according to Equation 2-3 and Figure 2-3.

$$C = \frac{1}{\frac{ds}{K_h \cdot da \cdot dx} + \frac{1}{LC \cdot P \cdot dx}}$$ (Equation 2-3)

K_h Horizontal hydraulic conductivity (m/s)

da Vertical surface available for exchange flow (m)

dx Grid size (m)

ds Average flow length (m), i.e. the distance from the grid node to the middle of the river bank

P Wetted perimeter of the cross-section (m), assumed to be equal to the sum of the vertical (da) and horizontal (lh) lengths available for exchange flow (Figure 2-3)

LC Leakage coefficient of the bed material (s^{-1})

The MIKE 11 hydraulic model uses the precise cross-sections, as defined in MIKE 11, for calculating the river water levels and the river volumes. However, the exchange of water between MIKE 11 and MIKE SHE is calculated based on the river-link cross-section, which is a simplified, triangular cross-section. The top width is equal to the distance between the left and right bank in the cross-section. The elevation of the bottom of the triangle equals the smallest depth of the MIKE 11 cross-section, see Figure 2-3.

2.3 The coupling between MOUSE and MIKE SHE

In the present open repository modelling, the program MOUSE /DHI Software 2008b/ has been used for modelling inflow to the repository tunnels. MOUSE is a modelling tool developed for urban hydrology and pipe flow hydraulics. The coupling between MOUSE and MIKE SHE is primarily used for calculating groundwater infiltration to sewers. In this project, the access tunnel from the ground down to the repository, the tunnels and rock caverns in the central area, the transport tunnels and the deposition tunnels have been described as a number of pipe links in MOUSE. The program calculates the flow of water between the MIKE SHE groundwater model and the MOUSE model, i.e. the inflow of water to the tunnels, according to Section 2.3.1.

In the present version of the coupling between MOUSE and MIKE SHE, inflow of water to vertical shafts (manholes in MOUSE) is not allowed. Therefore, the inflow of water to the shafts is calculated in MIKE SHE only, according to Section 2.3.2.

2.3.1 Description of different levels of grouting for tunnels

A development of the code has been performed for the present open repository modelling work. The new code was first applied in an earlier stage of the Forsmark open repository modelling /Bosson and Berglund 2006/. The exchange flow between a saturated zone grid cell (MIKE SHE) and a tunnel link (MOUSE) intersecting the grid cell, is included as a source/sink term in the governing flow equation for three-dimensional saturated flow. The exchange flow is calculated according to Equation 2-4. The principle is illustrated in Figure 2-4.

$$Q_{cell} = dh \cdot L \cdot P \cdot LC \qquad \text{(Equation 2-4)}$$

Q_{cell} Leakage flow from grid cell to tunnel (m^3/s)

dh Head difference between groundwater head, h_{aq} (in the grid cell where the tunnel is located), and the water head in the tunnel link, h_t (m)

L Length of a tunnel segment intersecting the grid cell (m)

P Wetted perimeter of the tunnel cross-section (m)

LC Total leakage coefficient (s^{-1})

When calculating the exchange of water between MIKE SHE and MOUSE, the properties of the tunnel (including the grout) and the aquifer are both taken into consideration. The total leakage coefficient, LC, is calculated based on the sum of the flow resistances in the grouted zone (equal to the inverse of the tunnel leakage coefficient, LC_{grout}) and the bedrock in the grid cell where the tunnel segment is located (equal to the inverse of the "average leakage coefficient" of the grid cell, LC_{aq}) according to Equation 2-5.

$$\frac{1}{LC} = \frac{1}{LC_{grout}} + \frac{1}{LC_{aq}} \qquad \text{(Equation 2-5)}$$

LC Total leakage coefficient (s^{-1})

LC_{aq} Leakage coefficient of the aquifer (s^{-1})

LC_{grout} Leakage coefficient of the grouted zone (s^{-1})

LC_{aq} is calculated under the assumption that the exchange water flows to/from the centre of the grid cell as horizontal and/or vertical flow. The current implementation of the MOUSE-SHE coupling does not include a detailed geometric calculation of the flow path; a MOUSE pipe can have any location in a grid cell. Instead, an average flow length is used, 0.25×grid size, dx, for horizontal flow and 0.25×cell height, dz, for vertical flow. The leakage coefficient of the grid cell is calculated as shown in Equation 2-6.

$$LC_{aq} = LC_{aq(h)} + LC_{aq(v)} = \frac{K_h}{0.25 \cdot dx} + \frac{K_v}{0.25 \cdot dz} \qquad \text{(Equation 2-6)}$$

$LC_{aq(h)}$ Horizontal leakage coefficient of the aquifer (s^{-1})

$LC_{aq(v)}$ Vertical leakage coefficient of the aquifer (s^{-1})

dx Cell size (m)

dz Cell height (m)

K_h Horizontal hydraulic conductivity (m/s)

K_v Vertical hydraulic conductivity (m/s)

The tunnel leakage coefficient, LC_{grout}, is an input parameter in the MOUSE model code, and may be specified as a unique value for each tunnel link. This tunnel leakage coefficient should be interpreted as the known level of grouting, expressed as hydraulic conductivity, divided by the thickness of the grouting material (Equation 2-7).

$$LC_{grout} = \frac{K_{grout}}{d_{grout}} \qquad \text{(Equation 2-7)}$$

K_{grout} Hydraulic conductivity of the grouting level, i.e. the conductivity of the bedrock after grouting to a certain level (m/s)

d_{grout} Thickness of the grouted zone (m)

In this open repository modelling work, different levels of grouting have been applied to the tunnel walls. These different grouting cases are described in Section 4.2.

To summarise, Equation 2-5 means that the leakage coefficients of the tunnel grouting and the aquifer are both taken into consideration when calculating the total inflow to the tunnel (Equation 2-4). The leakage coefficient for the aquifer is dependent on which calculation layer the tunnel is intersecting. As a result, the leakage coefficient for the aquifer, LC_{aq}, varies with depth and is set according to the hydraulic conductivities in the calculation layer (Equation 2-6). The exchange of water also depends on the head difference between the tunnel and the aquifer, as well as the circumference of the tunnel (Equation 2-4). The only input data needed for the coupled MOUSE-MIKE SHE simulation, except for the geometry and location of the tunnel, is the leakage coefficient of the tunnel grouting, LC_{grout}, which may be specified as a unique value for each tunnel link.

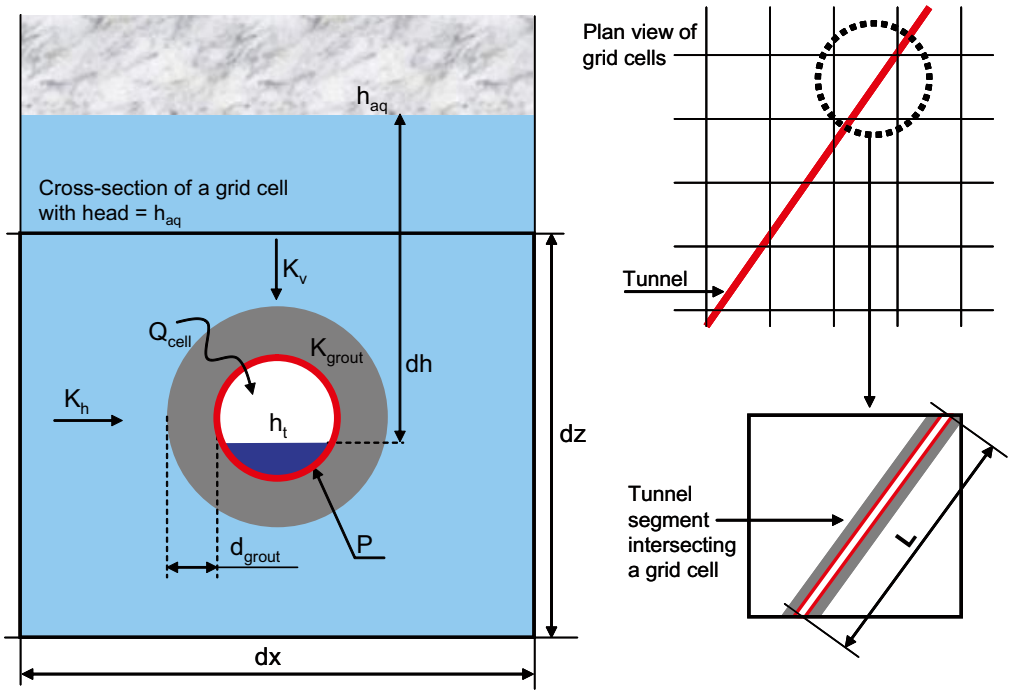

Figure 2-4. *Illustration of the groundwater coupling between MOUSE and MIKE SHE, and representation of relevant parameters used for calculating the exchange of water.*

In the present open repository modelling, the same tunnel leakage coefficient, LC_{grout}, has been applied to all tunnel links, according to the chosen grouting level. This means that also those tunnel links intersecting with grid cells with a lower hydraulic conductivity of the bedrock than the chosen grouting level, receives the higher hydraulic conductivity defined by the grouting level (although grouting will not occur in these cases in practice). In these cases, however, the hydraulic conductivities of the bedrock will have the major influence on the total leakage coefficient, LC, according to Equation 2-5 and Equation 2-6, with minor (or no) influence from the applied tunnel leakage coefficient. The opposite will hold when the grouting level is set to a lower hydraulic conductivity than the bedrock properties.

2.3.2 Description of different grouting levels for shafts

The shafts are described in MIKE SHE as grid cells with a specified head, corresponding to atmospheric pressure, in the calculation layers intersected by the shafts. The leakage flow from the aquifer to a shaft is then calculated as the sum of flows from each calculation layer intersecting the shaft, based on a specified conductance, C, for each calculation layer. The leakage flow from a saturated zone grid cell, containing one or several shafts, is included as a sink term in the governing flow equation for three-dimensional saturated flow. The leakage flow is calculated according to Equation 2-8. The principle is illustrated in Figure 2-5.

$$Q_{cell} = dh \cdot C \qquad \text{(Equation 2-8)}$$

Q_{cell} Leakage flow from grid cell containing the shaft (m^3/s)

dh Difference between the calculated head in the grid cell containing the shaft (h_{aq}), and the specified head boundary (equal to the lower level of the calculation layer when the shaft is deeper than the lower level of the calculation layer, and equal to the bottom of the shaft if the bottom is above the lower level of the calculation layer)

C Total conductance (m^2/s)

The total conductance, C, takes the different levels of grouting into consideration, as well as the hydraulic conductivity of the bedrock, according to Equation 2-9. The total leakage coefficient, LC, is calculated using Equations 2-10 to 2-12.

$$C = LC \cdot dz \cdot 2 \cdot \pi \qquad \text{(Equation 2-9)}$$

$$\frac{1}{LC} = \frac{1}{LC_{grout}} + \frac{1}{LC_{aq}} \qquad \text{(Equation 2-10)}$$

$$LC_{aq} = \frac{K_h}{dx} \qquad \text{(Equation 2-11)}$$

$$LC_{grout} = \frac{K_{grout}}{d_{grout}} \qquad \text{(Equation 2-12)}$$

LC Total leakage coefficient (s^{-1})

LC_{aq} Leakage coefficient of the aquifer (s^{-1})

LC_{grout} Leakage coefficient of the grouted zone (s^{-1})

dz Height of calculation layer (or height of the shaft contained in the layer, if the shaft bottom is above the lower level of the calculation layer) (m)

r Radius of the shaft (m)

K_h Horizontal hydraulic conductivity of the grid cell (m/s)

dx Grid size (m)

K_{grout} Hydraulic conductivity of the grouted zone, i.e. conductivity of the bedrock after grouting (m/s)

d_{grout} Thickness of the grouting zone (m)

The total conductance, C, for each calculation layer, is given in Appendix 1 for each shaft and for the different grouting cases.

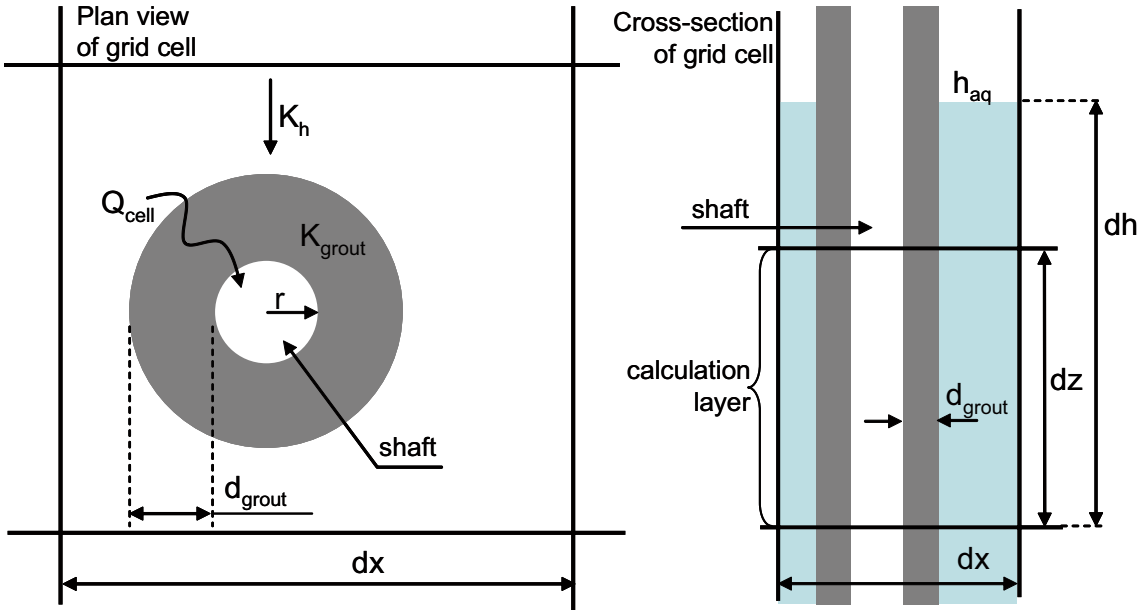

Figure 2-5. *Illustration of how the exchange of water is calculated for the shafts.*

3 Modelling of undisturbed conditions

The first step in the modelling process was to update the MIKE SHE SDM-Site Forsmark model /Bosson et al. 2008/. The main model updates consisted of an increase of the total depth of the model and an enhanced vertical resolution of computational layer structure in the model (see Section 3.1.1). These changes were made in order to avoid boundary effects of the repository being situated close to the original bottom boundary.

Except for the updates mentioned above, the model description follows the SDM-Site Forsmark model as described in /Bosson et al. 2008/. The simulation period and chosen initial conditions are described in Section 3.1.2. A reference simulation with the above mentioned updates to the SDM-Site Forsmark model was run for the chosen simulation period. The results from these simulations are presented in Section 3.2.

3.1 Description of the numerical model and initial base case

3.1.1 Boundaries and grid

Most of the on-shore part of the Forsmark regional model area is included in the MIKE SHE model area as described in /Bosson et al. 2008/. The upstream (inland) boundary follows the water divide towards the river Forsmarksån catchment, rather than the boundary of the regional model area. The MIKE SHE model area, which has a size of 37 km^2, is shown in Figure 3-1. The vertical extent of the reference set up of the model has been extended from 600 m.b.s.l. (in the SDM-Site model) to reach from the ground surface down to 990 m.b.s.l.

The vertical resolution of computational layers was also enhanced in order to resolve the vertical changes in head elevation at different depths above the repository. The original single layer between 250 m.b.s.l. and 600 m.b.s.l. was split into five layers, and the bedrock further down to 990 m.b.s.l. was divided into three layers. The horizontal resolution of the calculation grid is 40 m by 40 m in the whole model area. A detailed description of the geological layers and calculation layers included in the SDM-Site Forsmark model is given in /Bosson et al. 2008/.

The groundwater divides are assumed to coincide with the surface water divides, which means that a no-flow boundary condition is used for the on-shore part of the model boundary. The sea forms the uppermost calculation layer in the off-shore parts of the model. Since large volumes of overland water can cause numerical instabilities, the sea is described as a geological layer consisting of highly conductive material. The hydraulic conductivity of this material is set to 0.001 m/s. The sea part of the uppermost calculation layer, as well as the outer sea boundary for all calculation layers, has a time varying fixed head boundary condition, set equal to the measured time varying sea level.

The top boundary condition is expressed in terms of the precipitation and potential evapotranspiration (PET). The precipitation and PET are assumed to be uniformly distributed over the model area, and are given as time series. The actual evapotranspiration is calculated during the simulation. The bottom boundary of the model is set to a no-flow boundary.

Two existing constructions in the area, the nuclear power plant and SFR (a central facility for disposal of Swedish short-lived low- and intermediate-level waste), were previously described as pumping wells in the SDM-Site Forsmark model /Bosson et al. 2008/. As the well describing SFR was found to be inactive during parts of the simulation period due to lack of water (i.e. the pumping cells dried out), this well was replaced with an internal head boundary, with a prescribed head in the bedrock according to the results with the SDM-Site Forsmark model. This method gives a more stable numerical solution. With this method, the inflow to SFR was calculated to approximately 3.9 L/s. The observed inflow to SFR is approximately 6 L/s.

The nuclear power plant was disregarded, as this pumping well was inactive throughout the whole simulation period in the SDM-Site Forsmark model. The observed inflow to the nuclear power plant is approximately 1.5 L/s. The effects of these discrepancies related to the inflows to the nuclear power plant and SFR have been evaluated in the Forsmark EIA modelling activities and will be reported in connection with the EIA.

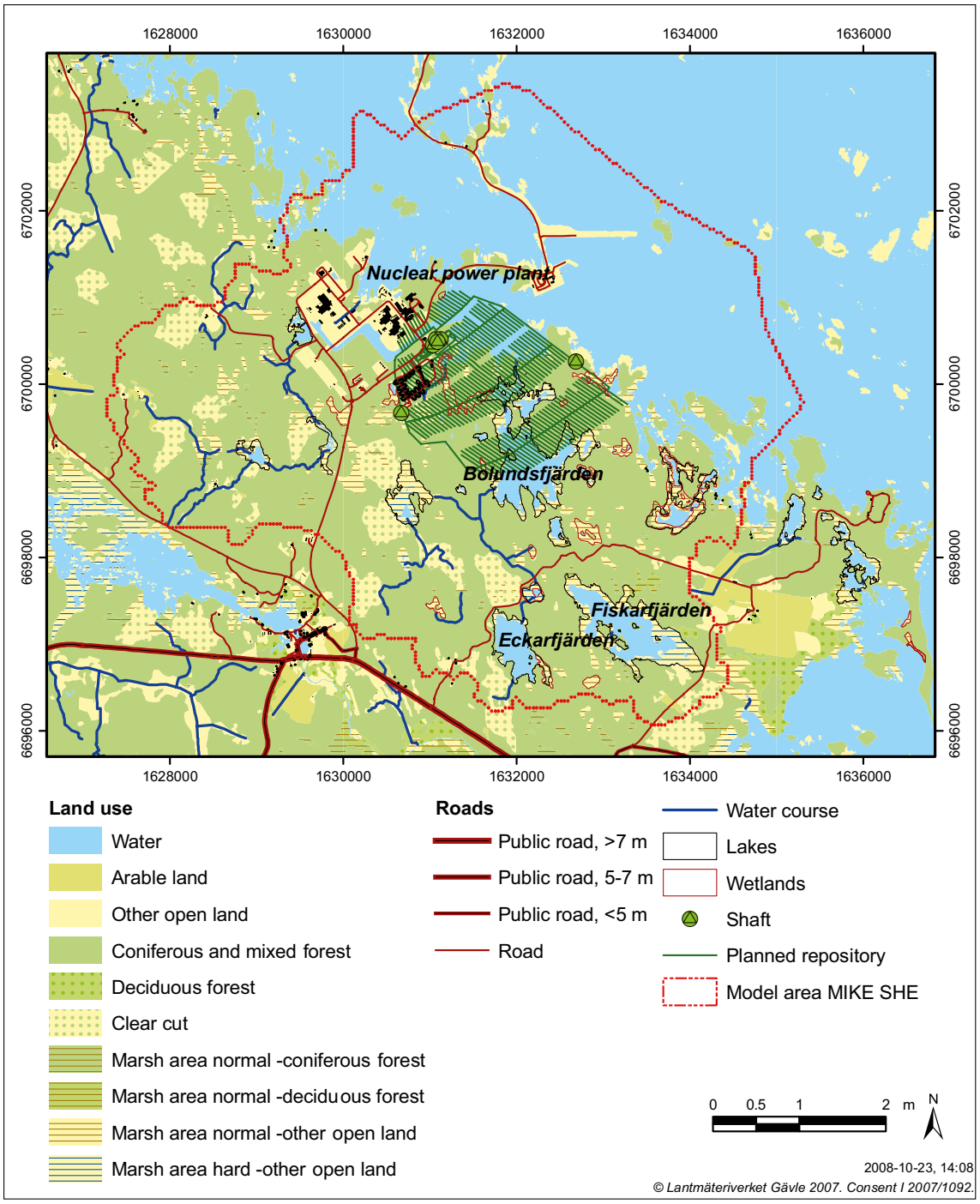

Figure 3-1. *Map showing the MIKE SHE model area and the planned repository (layout D2, version 1.0).*

3.1.2 Simulation period and initial conditions

The simulation period covers two years, from the 5th of January 2005 to the 15th of January 2007. All of the simulations in the present open repository modelling work have been performed using meteorological site data for these two years /Bosson et al. 2008/.

The year of 2005 was used as an initialization phase and results presented in this report are derived from 2006 only. The year 2006 contains both very dry conditions during the dry summer of 2006 and a wet period during the distinct snowmelt event that took place in the spring of that year.

3.2 Results for undisturbed conditions

This section gives a short presentation of the results for undisturbed conditions. The natural conditions are needed as a reference to the simulations where the tunnels, shafts and rock caverns have been implemented in the model. The presentation includes calculated water balances, surface water discharges and groundwater levels. For detailed results of undisturbed conditions, see /Bosson et al. 2008/. The updates made to the reference simulation as described earlier in this Chapter are considered to give very small changes to the results described in /Bosson et al. 2008/.

3.2.1 Water balance

The water balance presented here represents a sub-volume within the total model volume. Since the sea is represented as a highly conductive geological layer with a prescribed (time-varying) head, the sea and the model volume covered by the sea are not included in the water balance calculations. Thus, the water balance is calculated for the land part of the model area, including the littoral zone.

The calculated water balance for the year 2006 for undisturbed conditions is presented in Figure 3-2 and Table 3-1. All water balance components are expressed as area-normalised total volumetric discharges in mm, which is equivalent to mm/year in this case. The accumulated precipitation during the modelled period is 539 mm. The total evapotranspiration is calculated to 421 mm. The total storage change is –28 mm (3 mm overland storage, 2 mm groundwater storage and –33 mm snow storage). This water balance gives an estimated runoff of 146 mm (539 – 421 + 28).

The total evapotranspiration of 421 mm is a sum of the different evaporation components. The transpiration from plants is 199 mm, the evaporation from soil is 57 mm, the evaporation from snow is 33 mm and the evaporation from flooded areas is 26 mm. The amount of water intercepted by plant leaves is calculated to 76 mm and the evaporation from the saturated zone is 31 mm. The total runoff is calculated to 146 mm, with 66 mm from overland flow to rivers, 32 mm from groundwater flow to rivers (24 mm drain flow from the upper soil layer and 8 mm by leakage from the aquifer), and 48 mm (30 + 18) through net boundary outflow to the sea.

The infiltration from the overland compartment to the unsaturated zone is 397 mm and the groundwater recharge from the unsaturated to the saturated zone, is 141 mm. The water balance for the saturated zone comprises the following components: 141 mm groundwater recharge from the unsaturated zone, 31 mm evaporation, 32 mm flow to rivers, 81 mm net discharge to overland water, a net inflow from the sea of 4 mm, and a storage of 2 mm.

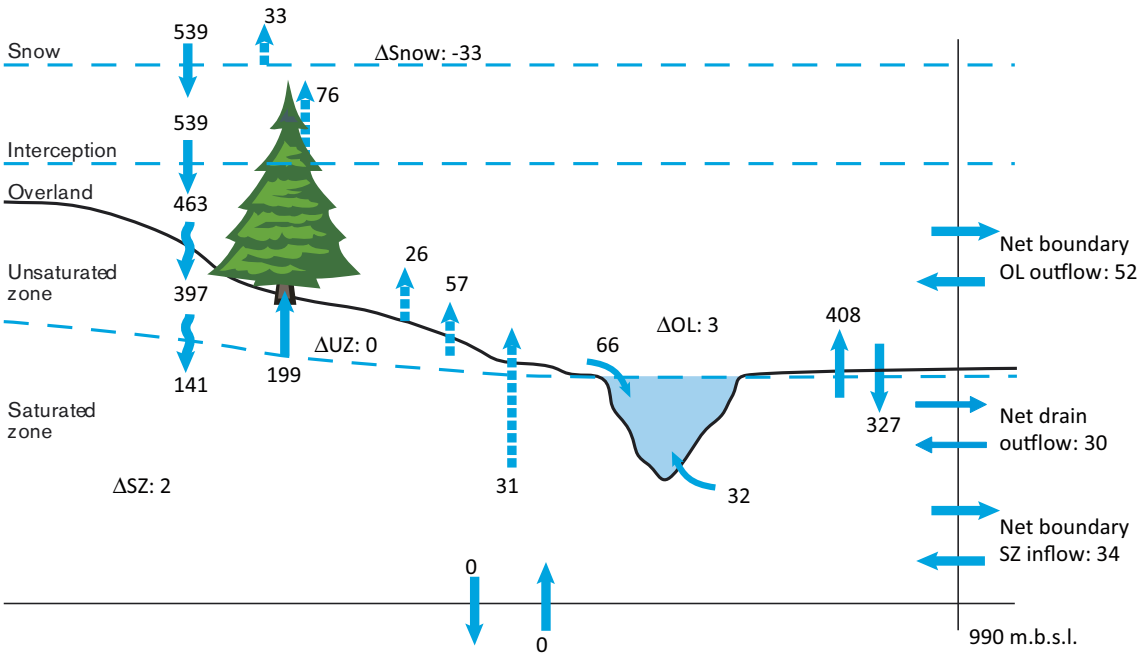

Figure 3-2. Calculated water balance 2006 for the Forsmark area during undisturbed conditions (mm).

Table 3-1. Total annual accumulated water balance (mm) for the land part of the model area in the reference simulation for undisturbed conditions.

Date	Precipitation	Canopy Storage Change	Evapo-transpiration	Snow Storage Change	Overland Storage Change	Overland Boundary Inflow	Overland Boundary Outflow	Overland to River/MOUSE	SubSurface Storage Change	SubSurface Boundary Inflow	SubSurface Boundary Outflow	Drain to River	Drain Outflow
2006-01-02	0.0	0.0	0.0	0.0	0.0	0.0	0.0	0.0	0.0	0.0	0.0	0.0	0.0
2006-02-01	-16.8	0.0	0.0	-8.9	1.3	-1.0	2.1	6.0	10.9	-1.2	3.1	1.8	1.5
2006-03-03	-69.9	-0.1	0.6	36.6	-0.8	-3.2	6.8	14.4	0.1	-2.4	6.1	5.1	4.3
2006-04-02	-119.0	-0.2	6.8	84.0	-4.5	-3.9	7.7	18.4	-8.7	-3.6	8.8	6.3	5.1
2006-05-02	-148.0	-0.2	47.2	-32.8	18.8	-10.1	24.0	37.6	23.8	-4.9	12.1	14.7	13.2
2006-06-01	-165.7	-0.2	104.1	-32.8	-1.7	-11.3	25.5	50.5	-12.0	-6.5	14.8	16.7	14.3
2006-07-01	-196.5	-0.2	206.5	-32.8	-18.8	-11.7	25.7	53.4	-64.0	-9.1	16.5	17.2	14.8
2006-08-05	-207.6	-0.2	326.1	-32.8	-34.6	-11.7	25.7	53.3	-134.6	-12.3	18.2	17.6	15.0
2006-09-04	-281.7	1.4	385.6	-32.8	-34.7	-12.6	26.2	53.4	-128.3	-15.0	19.6	17.8	15.2
2006-10-04	-333.9	2.0	419.9	-32.8	-34.4	-16.9	31.4	53.6	-114.7	-18.1	21.5	18.1	16.3
2006-11-03	-462.8	1.9	421.3	-32.0	-13.1	-58.5	77.9	55.4	-33.8	-24.7	24.6	19.1	19.5
2006-12-03	-512.0	0.1	421.3	-32.8	-1.1	-132.4	166.5	60.1	-8.6	-42.5	28.2	21.6	25.1
2007-01-02	-539.4	0.1	421.3	-32.8	2.7	-228.0	280.0	66.3	1.4	-65.9	32.3	23.9	29.9

The quite large snow storage change is an effect of the chosen period for the water balance calculation, which is set to 2006. This comes from precipitation storage through snow during December 2005, while no snow was present in the end of December 2006. The large amount of evaporation from snow comes from the relatively late snow cover during spring 2006. The snow cover did not melt until the beginning of April 2006, and was consequently accessible for evaporation during more than three months, with a rather high PET in March and April.

3.2.2 Discharge and water levels in water courses

As described above, the runoff is calculated as the net flow of water to the MIKE 11 model plus the water that leaves the model area as overland flow and groundwater flow. MIKE 11 calculates the discharges and water levels in the water courses. The calculated discharge and water levels in a water course vary during the year. Figure 3-3 shows the locations of the surface water monitoring points.

Figure 3-4 shows the calculated and measured discharges at the station upstream Lake Bolundsfjärden during 2006. In April 2006, a distinct snowmelt resulted in high peak discharges. The summer of 2006 was very dry, including a dry beginning of the autumn, followed by a sudden switch to a rather wet last part of 2006. The model captures the overall runoff dynamics during spring and summer, but underestimates the wet ending of 2006 after the long dry period. Figure 3-5 shows the measured and calculated water levels at Lake Bolundsfjärden during 2006. The calculated water levels are generally well described in the model.

3.2.3 Groundwater table

Figure 3-6 shows the calculated elevation (in m.a.s.l.) of the groundwater table in the model area as an average for the year 2006. Due to the topographical low-altitude conditions in large parts of the area, the groundwater table elevation is only up to a few meters above the sea level in large parts of the area, and consequently affected by the sea level variation. About 40% of the land area has a groundwater elevation lower than 2 m.a.s.l, as an average for 2006.

Figure 3-7 shows the calculated depth to the groundwater table in the model area as an average for 2006. As can be seen in Figure 3-7, the groundwater table is shallow and located less than 1.5 m below ground in most of the model area, with a mean depth of 1.1 m below ground surface (the sea area excluded). The deeper groundwater levels are mainly found in high-altitude areas, associated with groundwater recharge near the groundwater divides. There are also areas with a groundwater pressure head above the ground surface for which the calculated overland water level is presented. These areas are (local) low-altitude areas according to the topography, with groundwater discharge conditions, and coincide with lakes and areas in the vicinity of the main water courses.

Figure 3-8 shows the depth to the groundwater table during a period of wet conditions (2006-05-17), as calculated in the reference simulation for undisturbed conditions. In this case, the groundwater table has a mean depth of 0.8 m below ground surface (excluding the sea area).

Figure 3-9 shows the calculated depth to the groundwater table in the model area under dry summer conditions (2006-08-15), as calculated for undisturbed conditions. As can be seen in the figure, the groundwater table is considerably deeper and located more than 1.5 m below ground in most of the model area, with a mean depth of 1.8 m below ground surface (the sea area excluded). The areas with overland water are also much smaller.

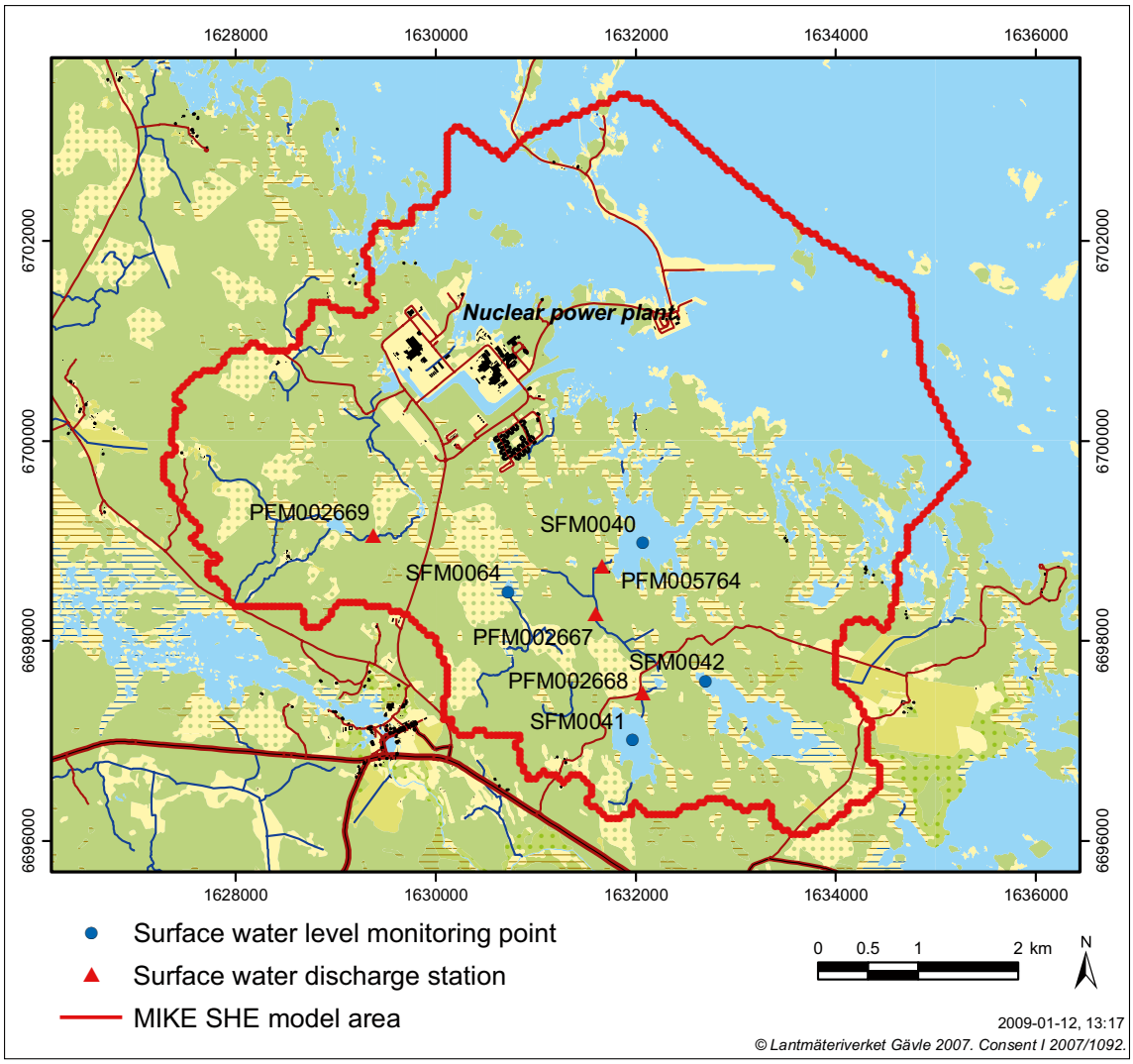

Figure 3-3. *Positions of the surface water discharge stations PFM002668 (downstream Lake Eckarfjärden), PFM002667 (downstream Lake Stocksjön), PFM002669 (downstream Lake Gunnarsboträsket) and PFM005764 (upstream Lake Bolundsfjärden) and the surface water level stations SFM0041 (Lake Eckarfjärden), SFM0042 (Lake Fiskarfjärden), SFM0064 (Lake Gällsboträsket) and SFM0040 (Lake Bolundsfjärden).*

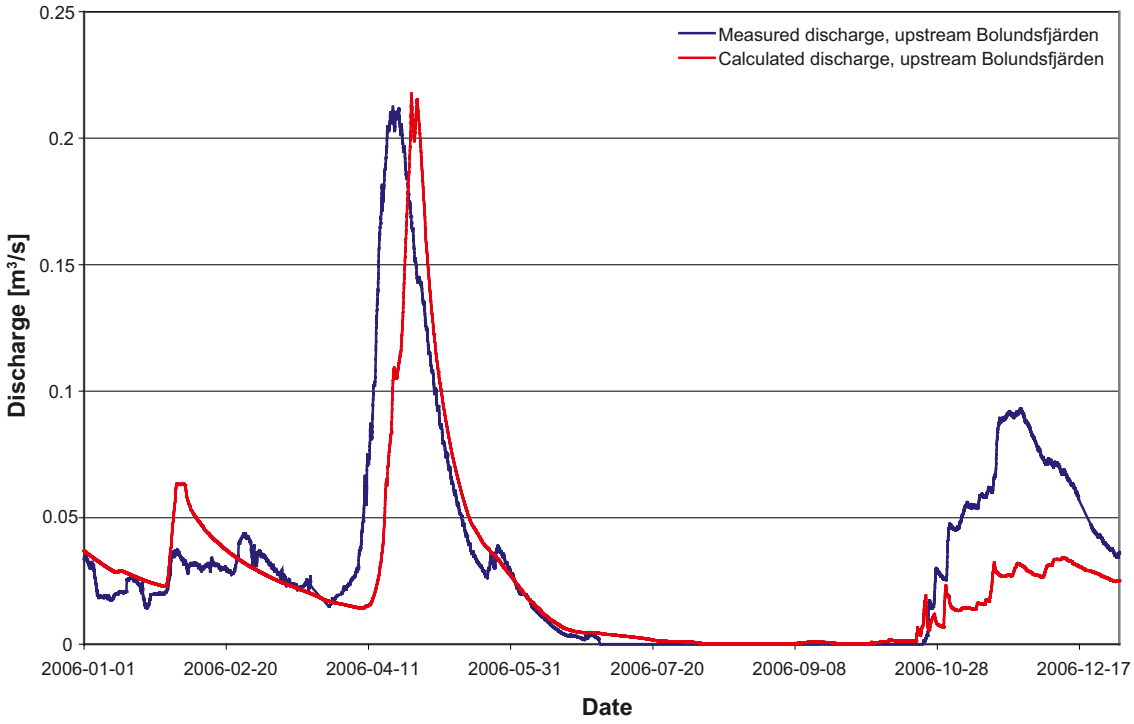

Figure 3-4. *Measured and calculated discharges upstream Lake Bolundsfjärden (reference simulation, undisturbed conditions).*

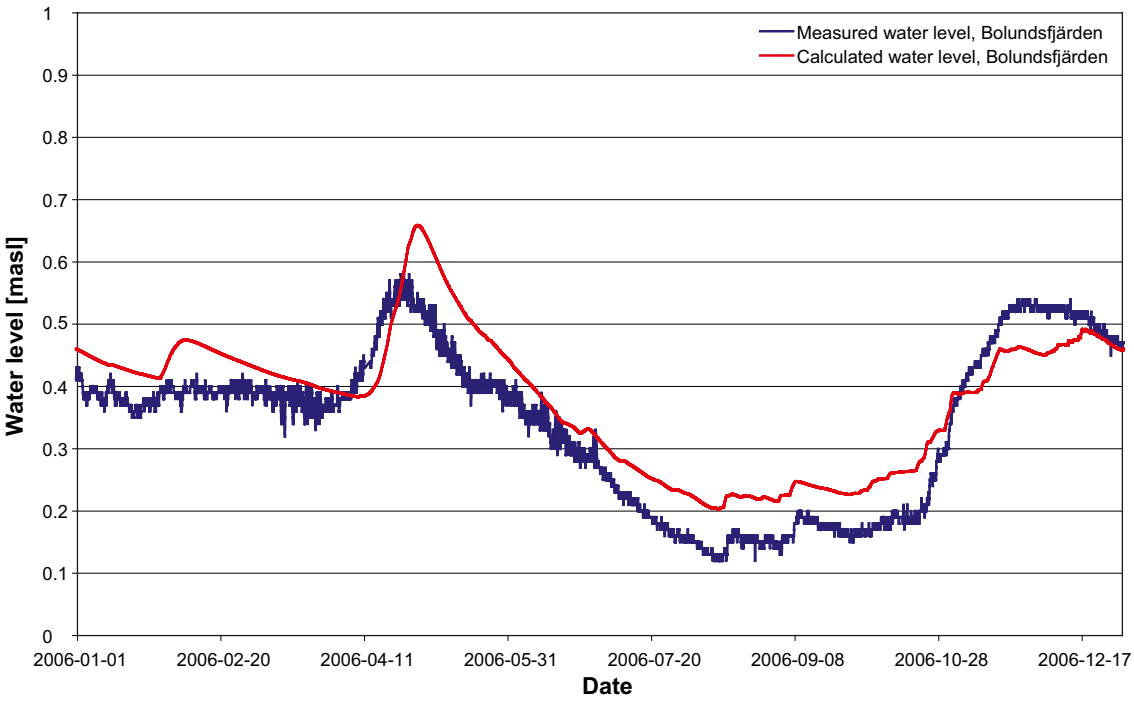

Figure 3-5. *Measured and calculated water levels in Lake Bolundsfjärden (reference simulation, undisturbed conditions).*

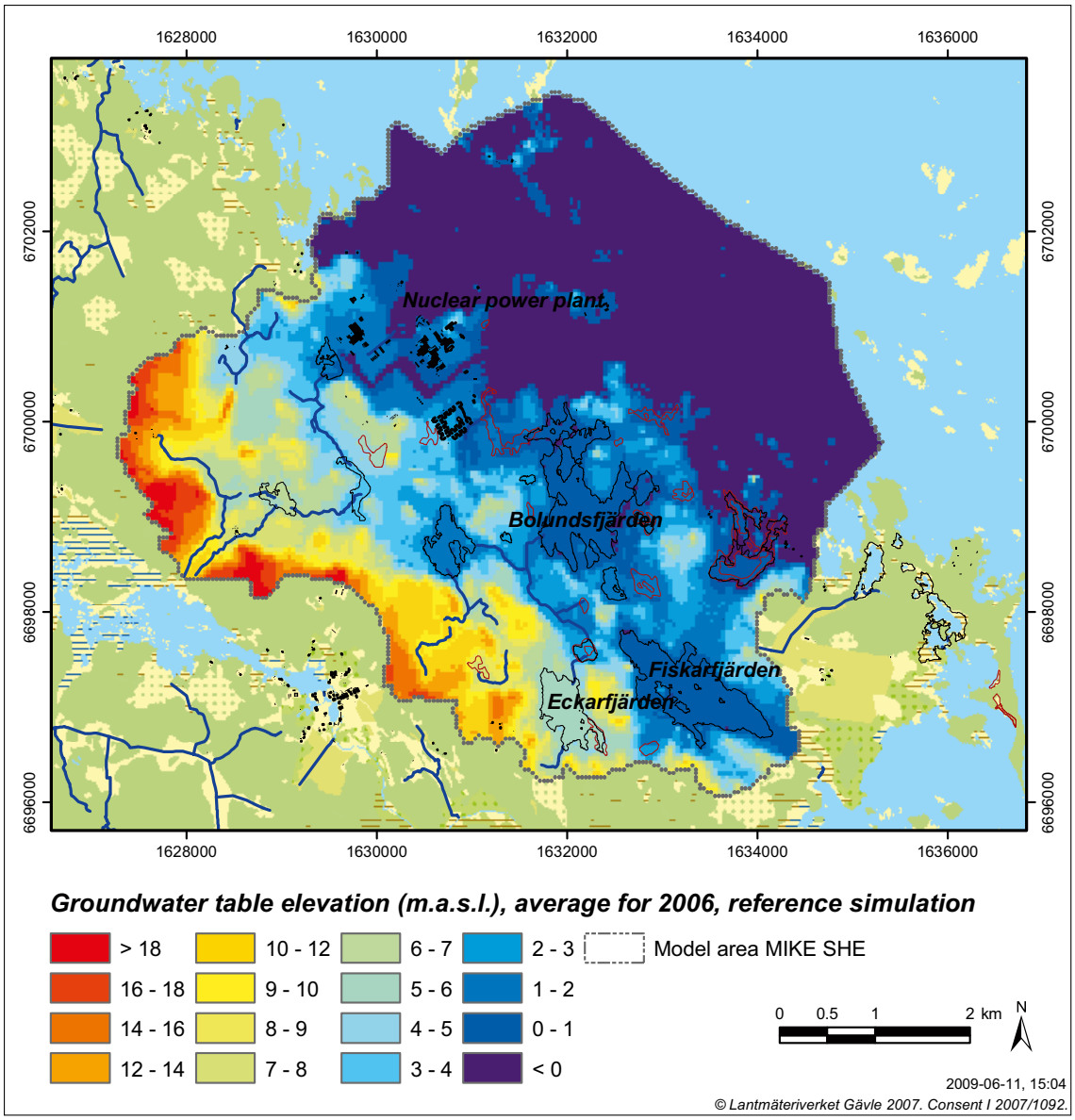

Figure 3-6. *Calculated elevation (in m.a.s.l.) of the groundwater table as an average for the year 2006 (reference simulation, undisturbed conditions).*

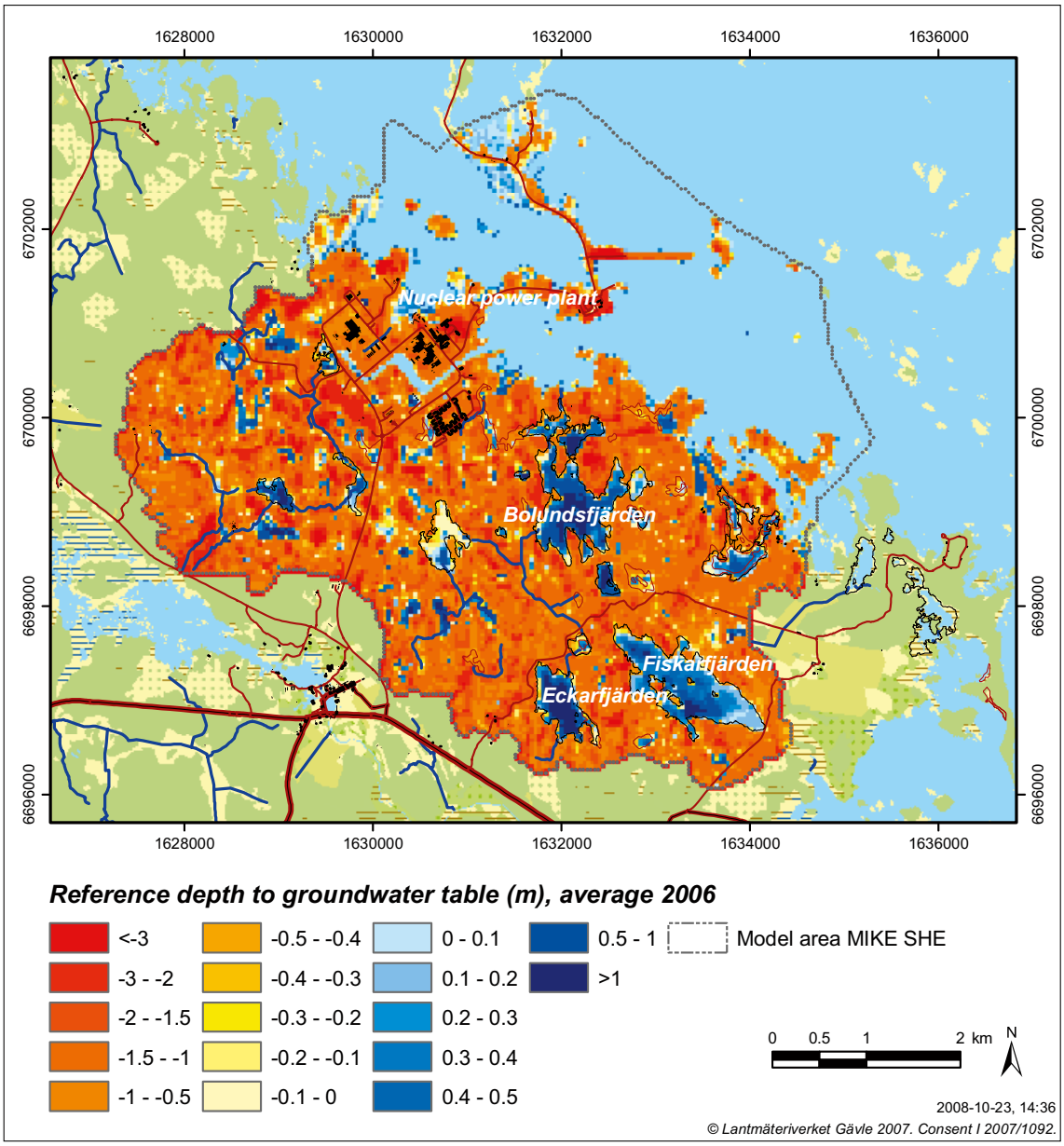

Figure 3-7. *Calculated depth to the groundwater table as an average for 2006 (reference simulation, undisturbed conditions). Positive depths indicate areas with water above the ground surface.*

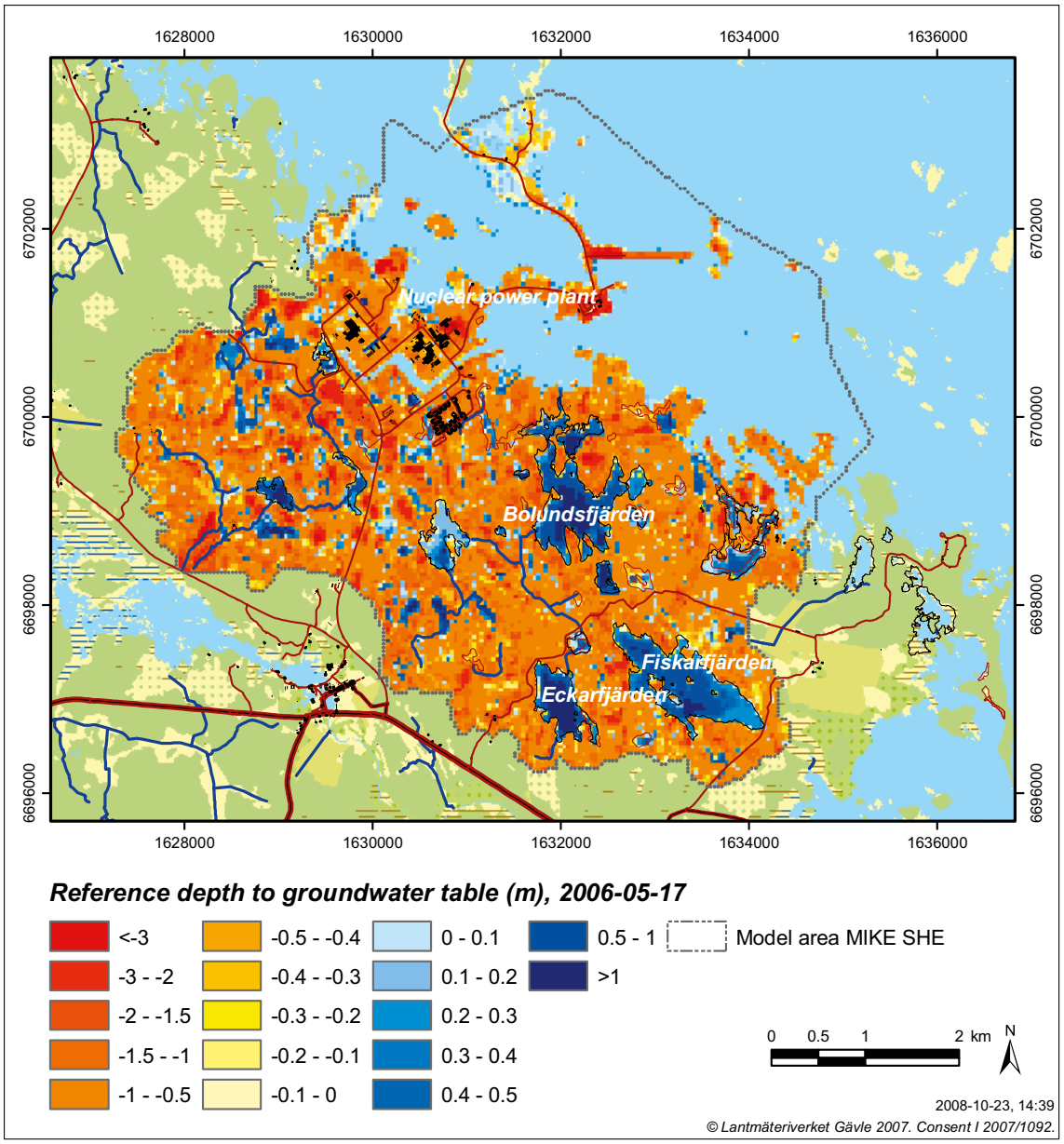

Figure 3-8. *Calculated depth to the groundwater table during a wet period (2006-05-17; reference simulation, undisturbed conditions). Positive depths indicate areas with water above the ground surface.*

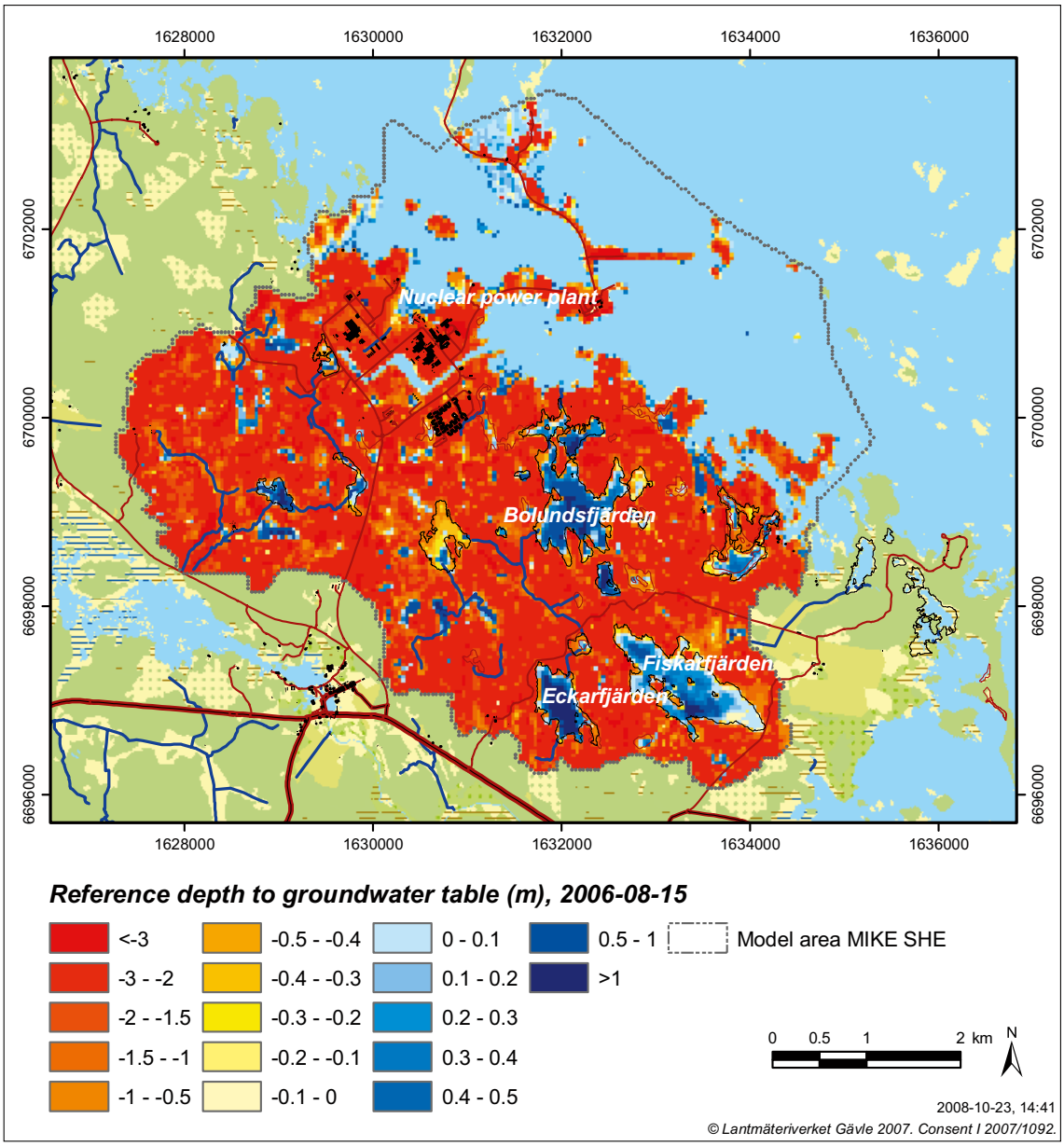

Figure 3-9. *Calculated depth to the groundwater table during a dry period (2006-08-15; reference simulation, undisturbed conditions). Positive depths indicate areas with water above the ground surface.*

4 Input to simulations of open repository conditions

The second step in the modelling process was to describe the conditions for the open repository by implementing the access tunnel, the repository tunnels and the shafts into the model, and to simulate the consequences on the surface hydrology caused by an open repository during different conditions. This Chapter describes input data and simulation cases in the open repository modelling.

4.1 Geometry of the tunnels and the shafts

The layout version of the repository from April 2008 (Forsmark layout D2, version 1.0), including 27% loss of deposition holes, has been used in the present modelling. The position of the tunnels and shafts is shown in Figure 4-1. The layout of the access tunnel from the ground surface down to the repository, the tunnels and rock caverns in the central area, the transport tunnels, and the deposition tunnels are shown in Figure 4-2.

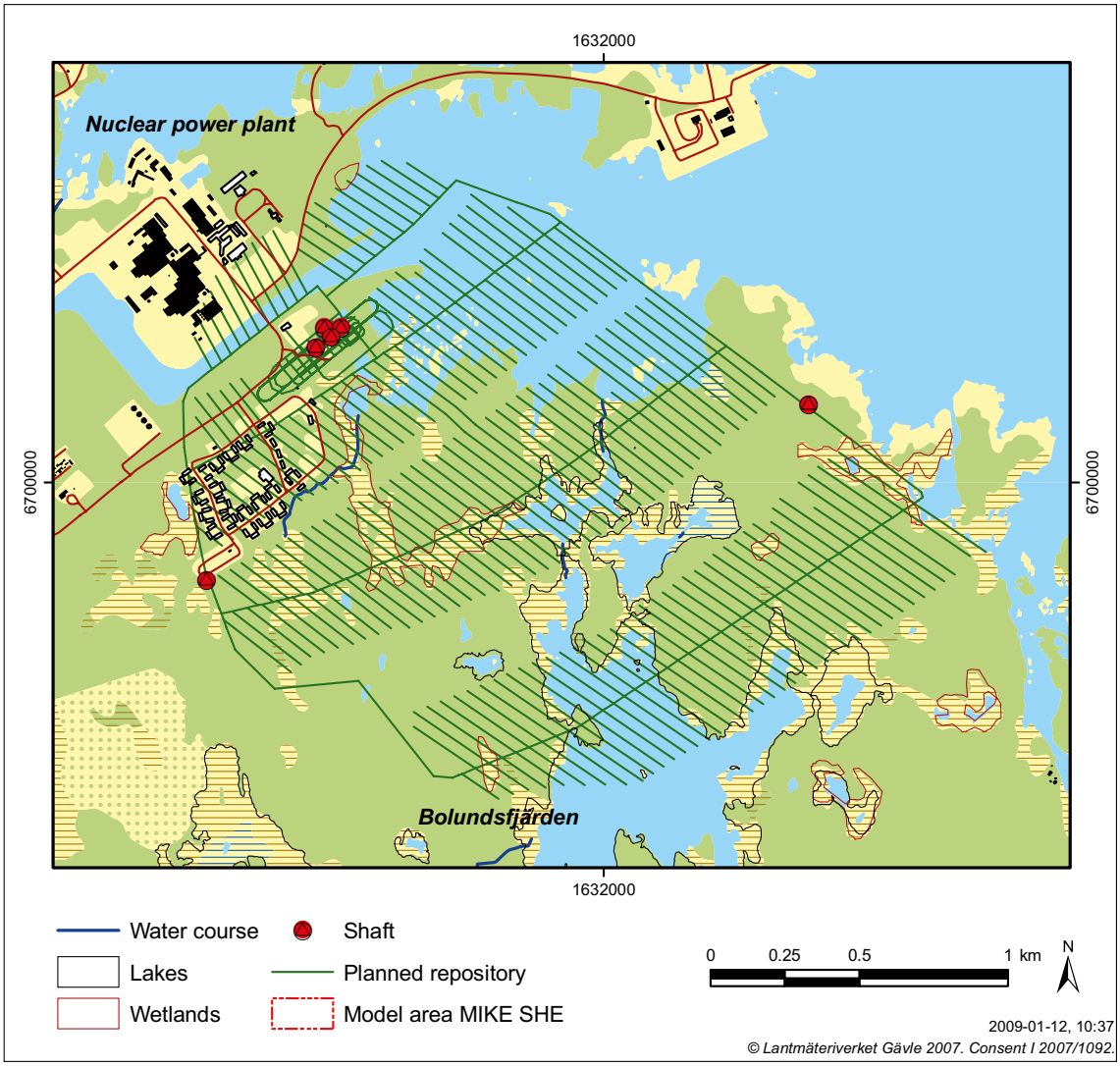

Figure 4-1. *Positions of tunnels and shafts in the open repository (layout D2, version 1.0, April 2008).*

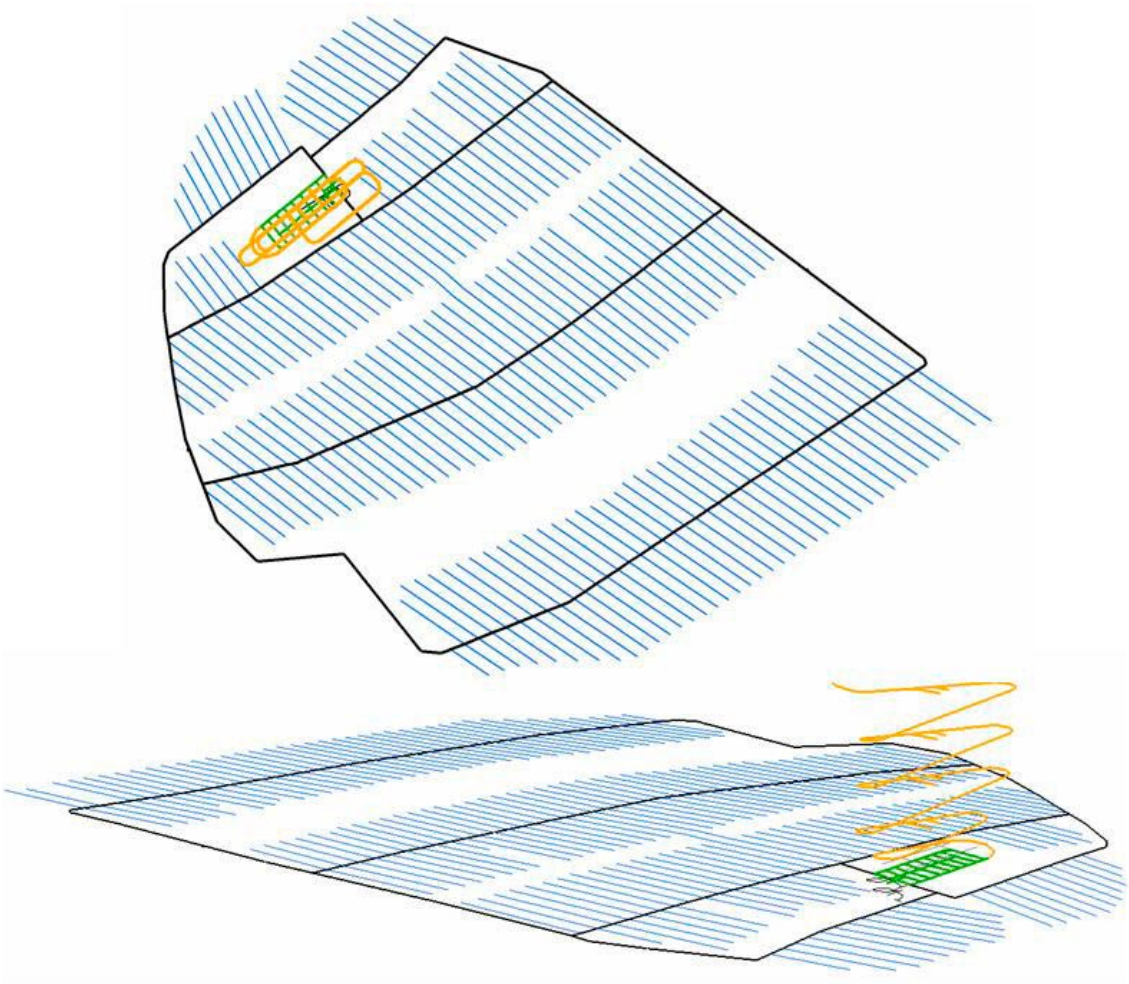

Figure 4-2. *Layout of the access tunnel from the ground down to the repository (yellow line), the tunnels and rock caverns in the central area (green lines), the transport tunnels (black lines), and the deposition tunnels (blue lines).*

The repository is described as a number of pipe links in the modelling tool MOUSE (described in Section 2.3.1). Table 4-1 shows the geometry of the tunnels included in the model, including the rock caverns in the central area. The total length of tunnels is approximately 84 km, with the majority located at approximately 450 m.b.s.l.

There are totally six shafts. These are described as cells with atmospheric pressure in MIKE SHE (as described in Section 2.3.2). Table 4-2 gives the bottom level, location, diameter and circumference of the shafts. Two of the shafts (SF00 and ST00) are very close to each other, and are positioned in the same grid cell in the model. They are consequently modelled as one unit.

Table 4-1. Geometry of tunnels in the open repository described in the model (layout D2, version 1.0, April 2008).

Calculation layer	Lower level (m.b.s.l.)	Tunnel segment length (m)	Tunnel casing area (m²)
Layer 1–3	–10	134	3,205
Layer 4	–30	213	5,108
Layer 5	–50	204	4,899
Layer 6	–70	330	6,350
Layer 7	–90	214	3,534
Layer 8	–110	212	5,094
Layer 9	–130	218	5,228
Layer 10	–150	206	4,952
Layer 11	–190	544	10,210
Layer 12	–250	636	13,678
Layer 13	–360	1,284	27,985
Layer 14	–420	760	15,916
Layer 15	–480	78,529	1,476,681
Layer 16	–540	511	9,078
Layer 17	–600		
Layer 18	–690		
Layer 19	–810		
Layer 20	–990		
Sum		83,995	1,591,916

Table 4-2. Geometry of shafts in the open repository described in the model (layout D2, version 1.0, April 2008).

Shaft	Lower level (m.b.s.l.)	X-coordinate (m)	Y-coordinate (m)	Diameter (m)	Circumference (m)
SA01	467.08	1630669	6699672	3.00	9.42
SA02	467.36	1632686	6700261	3.00	9.42
SB00	490.00	1631036	6700450	6.00	18.85
SC00	520.00	1631122	6700519	5.00	18.85
SF00	442.20	1631088	6700489	2.50	7.85
ST00	442.20	1631064	6700518	3.50	11.00

4.2 Simulation cases

Three different cases have been defined based on three different levels of grouting, which are described in terms of different hydraulic conductivities, K_{grout}, of the grouted zone surrounding the tunnels and the shafts. The thickness of the grouted zone in the bedrock, d_{grout}, is set to 5 m (Sten Palmer, personal communication), which means that the grouting leakage coefficient $LC_{grout} = K/5$ (Equation 2-7, Section 2.3.1). The three grouting levels are:

$K_{grout} = 1 \cdot 10^{-7}$ m/s $\rightarrow LC_{grout} = 2 \cdot 10^{-8}$ s^{-1}

$K_{grout} = 1 \cdot 10^{-8}$ m/s $\rightarrow LC_{grout} = 2 \cdot 10^{-9}$ s^{-1}

$K_{grout} = 1 \cdot 10^{-9}$ m/s $\rightarrow LC_{grout} = 2 \cdot 10^{-10}$ s^{-1}

It should be noted that the inflow to the repository is calculated based on both the grouting leakage coefficient and the conductivities in the surrounding bedrock (see Section 2.3.1 for details). This means that when the bedrock has a lower conductivity than the assigned grouting level, the bedrock conductivity controls the inflow, whereas the grouted zone otherwise controls the inflow.

The different grouting levels have been applied in simulation cases where full construction has been modelled as an open repository, i.e. with all the deposition tunnels open at the same time. The results presented in Chapter 5 are based on this assumption, unless otherwise stated (i.e. the results in Section 5.4.4 and selected parts of Section 5.2). This is, however, a hypothetical worst case scenario. The repository will be constructed and taken into operation in three development phases (Sten Palmer, personal communication), here denoted as phase 1, phase 2 and phase 3.

Figure 4-3 shows the three phases of the construction. It is assumed that the shafts, the access tunnel, the tunnels and rock caverns in the central area and all of the transport tunnels will be open in all of the phases, i.e. they will all be constructed in phase 1. In the three different phases, one section with deposition tunnels will be open at a time, according to Figure 4-3, except in phase 3, when two separate sections will be open. In addition to simulations with a full construction, the three different development phases have also been simulated individually, but only with a grouting level of $K = 1 \cdot 10^{-8}$ m/s. The different simulation cases are summarised in Table 4-3.

The same initial conditions and meteorological data as described for the reference simulation (Section 3.1.2) are applied in the simulation cases with an open repository. The meteorological data covers observed daily values from the years 2005 to 2006, which means that seasonal variations are included in all simulation cases.

Two longer simulations were carried out, where data from this two-year period were repeated 4 times to represent a period of totally 8 years. These simulations considered the reference case (undisturbed conditions) and an open repository case based on a grouting level of $K = 1 \cdot 10^{-8}$ m/s (Table 4-3). This was done in order to evaluate the development of the groundwater table drawdown over a longer period; the results are presented in Section 5.4.5.

Finally, a simulation was carried out to evaluate the recovery of the drawdown of the groundwater table, after the operational phase of the open repository is finished and the repository is closed. The simulation was done without tunnels and shafts, but initialised from the conditions with an open repository. The initial conditions were taken from simulations with a grouting level of $K=1 \cdot 10^{-8}$ m/s, after the third two-year cycle. The simulation was done for a two-year period (using data from 2005–2006), and compared with the fourth two-year cycle from the reference simulation with undisturbed conditions, when calculating the drawdown of the groundwater table, see Table 4-3 (results are presented in Section 5.4.6).

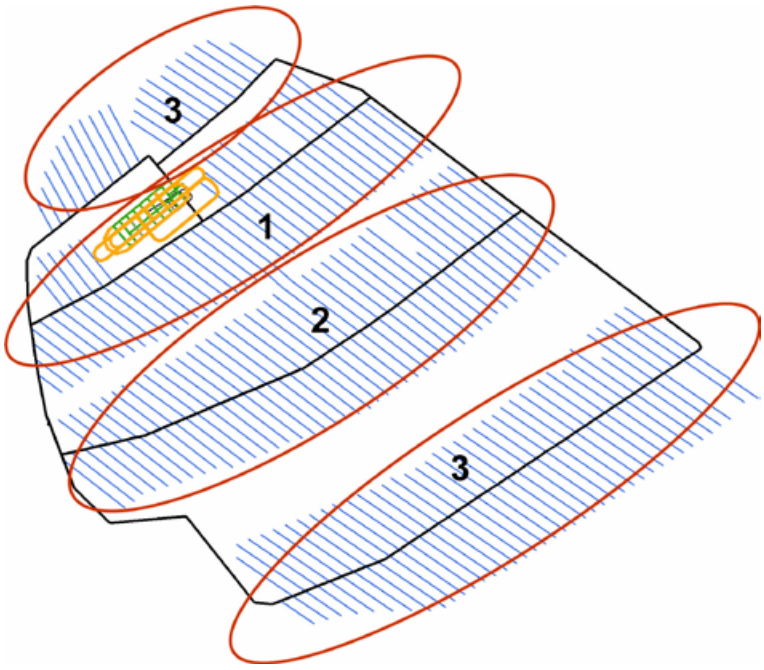

Figure 4-3. *Development phases in the construction and operation of the open repository.*

Table 4-3. Summary of the different simulation cases. Results for the highlighted years only are presented and evaluated.

Simulation case	Grouting level	Meteorological data							
Development phase 1	K=1·10^{-8} m/s	2005	2006						
Development phase 2	K=1·10^{-8} m/s	2005	2006						
Development phase 3	K=1·10^{-8} m/s	2005	2006						
Full construction	K=1·10^{-7} m/s	2005	2006						
Full construction	K=1·10^{-8} m/s	2005	2006	2005	2006	2005	2006	2005	2006
Full construction	K=1·10^{-9} m/s	2005	2006						
Recovery after closing the repository (initial conditions from K=1·10^{-8} m/s)	no repository							2005	2006
Reference simulation	no repository	2005	2006	2005	2006	2005	2006	2005	2006
Simulation cycle		1st		2nd		3rd		4th	

5 Results for open repository conditions

Most results from the open repository simulations concern the case of the whole construction being open, i.e. with all the deposition tunnels open at the same time. As explained above, this is a hypothetical worst case scenario. In reality, the open repository will be constructed and operated in three phases (Section 4.2). Results from simulations with the three individual phases are also presented. All open repository results are compared to the corresponding reference simulation without tunnels and shafts, i.e. with the results for undisturbed conditions.

Water balances are presented for the entire model area, as well as for different parts of the model area including detailed results for the saturated zone. Inflows to the tunnels and shafts are presented for each level of grouting for the full open construction as well as for the different development phases of the construction (one grouting level only). The effects of the full construction on the surface water system are presented in terms of the changes in water levels in lakes in the area and in the accumulated discharges at selected discharge stations.

The drawdown of the groundwater table is shown for each level of grouting as well as for the different development phases of the construction. The temporal and spatial variation of the groundwater table drawdown and the head changes are analysed through horizontal cross sections (for different periods and different depths) and as vertical profiles through the model area and the open repository. Finally, the long term development of groundwater table drawdown is studied.

5.1 Water balance

The inflow of water to the open repository construction affects the total turnover of water in the model area. Table 5-1 shows a summary of the total accumulated water balances for the land part of the model area during 2006 for undisturbed conditions and with the open repository for the three different levels of grouting. Observe that parts of the tunnel system are located under the sea part of the model area, see Figure 4-1, and are consequently not included in the water balance in Table 5-1.

With a grouting level of $K=1\cdot10^{-7}$ m/s the total runoff sums up to 115 mm, compared to 146 mm for undisturbed conditions, i.e. a reduction of the total runoff with 31 mm. The inflow to tunnels and shafts in this case is 37 mm, which means that the remaining difference in the water balance of 6 mm can be explained by a slightly changed evapotranspiration and changes in subsurface storage. This means that the inflow to the open repository in this case (37 mm) is 25% of the total runoff for undisturbed conditions (146 mm). The corresponding relations between inflow to tunnels, with a grouting level of $K=1\cdot10^{-8}$ m/s and $K=1\cdot10^{-9}$ m/s, and undisturbed total runoff are 15% and 7%, respectively.

Going further into the detailed results, the open repository construction affects the runoff to the streams, which is reduced by 11 mm (–11%) from 98 mm to 87 mm in the case with a grouting level of $K=1\cdot10^{-7}$ m/s. Here, the largest effect is found in the overland flow to streams, which is reduced with 9 mm (–14%) in the case with a grouting level of $K=1\cdot10^{-7}$ m/s. The effect is however mostly seen in the downstream parts of the area, especially downstream Lake Bolundsfjärden, where the groundwater depth is small during undisturbed conditions and a larger drawdown of the groundwater table is seen during disturbed conditions (see Section 5.4).

In all cases, undisturbed conditions as well as disturbed conditions with an open repository, there is a net subsurface inflow from the sea, and a net overland outflow to the sea. The reason for this is mainly a circulation of sea water in the upper soil layers along the shore line due to water level variations of the sea. The net overland outflow to the sea is more or less the same in all of the cases, while the net subsurface inflow from the sea is changed when the open repository is introduced. Actually, this is the runoff component that changes the most in relative terms, with an increase of 16 mm (+49%) from 34 mm to 50 mm in the case with a grouting level of $K=1\cdot10^{-7}$ m/s.

The increased inflow from the sea mainly occurs in the bedrock layers (14 mm out of the 16 mm above), which is seen in Table 5-2 where the water balance for the saturated zone is presented layer by layer in the bedrock for the land part of the model area. This water balance shows the amount of water going into respectively out from the different layers as accumulated annual volumes according to definitions in Figure 5-1. The most interesting numbers in Table 5-2, with the highest values or the largest differences between the cases, are highlighted.

As can be seen in Table 5-2, the total horizontal inflow in the bedrock from the sea area increases with 14 mm, from an outflow of 4 mm to an inflow of 10 mm, in the case with a grouting level of $K=1\cdot10^{-7}$ m/s. More than half of this change is found in the two lower sheet joint layers, at approximately 70 and 110 m.b.s.l, but also the horizontal flow in the uppermost bedrock layer changes considerably.

The vertical flow is, however, generally much larger than the horizontal, and changes considerably when the open repository is introduced. The net vertical inflow from the Quaternary deposits (QD) to the bedrock (layer 3) changes with 22 mm, from 4 mm for undisturbed conditions to 26 mm in the case with a grouting level of $K=1\cdot10^{-7}$ m/s.

All in all, this means that out of the 37 mm of inflow to the open repository (grouting level of $K=1\cdot10^{-7}$ m/s), 14 mm (38%) can be explained by increased horizontal net inflow from the sea and 22 mm (60%) by increased vertical net inflow from the QD. The remaining 1 mm comes from reduced storage in the bedrock, because steady state conditions were not reached during the limited simulation period. Observe that the above only holds for the parts of the open repository that is located under the land part of the model area (see Figure 4-1).

Table 5-1. Total accumulated water balances for 2006 (mm) for the land part of the model area, for the reference simulation without open repository and with open repository for three levels of grouting.

	Reference simulation, without open repository	With open repository, grouting level $K=1\cdot10^{-7}$ m/s	With open repository, grouting level $K=1\cdot10^{-8}$ m/s	With open repository, grouting level $K=1\cdot10^{-9}$ m/s
Precipitation	539.4	539.4	539.4	539.4
Evapotranspiration	421.3	418.9	420.8	422.5
Canopy storage change	0.1	0.1	0.1	0.1
Snow storage change	–32.8	–32.8	–32.8	–32.8
Overland storage change	2.7	2.4	2.4	2.7
Subsurface storage change	1.4	–2.2	–0.7	0.6
Net overland outflow to sea	51.9	50.6	50.2	50.9
Net subsurface inflow from sea	33.6	50.1	40.9	36.4
Drainflow to sea	29.9	27.2	27.8	28.7
Overland flow to river	66.3	57.0	59.1	62.1
Drainflow to river	23.9	22.8	23.2	23.5
Net baseflow to river	7.8	7.6	7.7	7.6
Inflow to the open repository	–	37.3	22.1	9.7

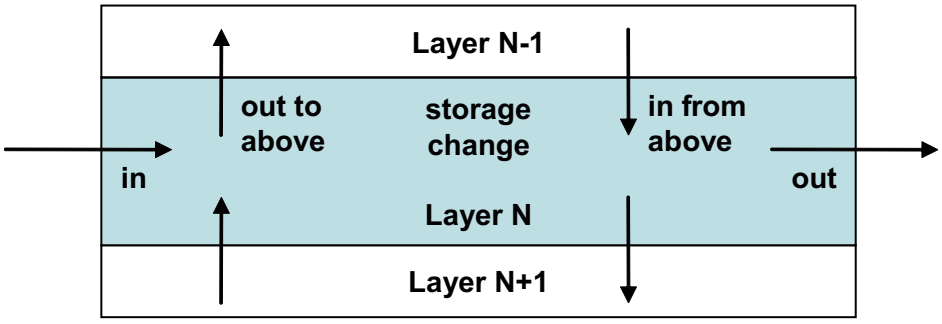

Figure 5-1. *Water balance components for the saturated zone (see Table 5-2). In- and outflow arrows in the figure are labelled for layer N only (because the values for the lower arrows are presented for the layer below in Table 5-2).*

Table 5-2. Water balances for 2006 (mm) in the saturated zone for the land part of the model area and for each bedrock calculation layer. Numbers are presented for undisturbed conditions and for open repository cases with the three levels of grouting. The water balance components in the table are defined in Figure 5-1.

		Undisturbed conditions				Grouting K= $1 \cdot 10^{-7}$ m/s				Grouting K= $1 \cdot 10^{-8}$ m/s				Grouting K= $1 \cdot 10^{-9}$ m/s			
Layer	Lower level (m.b.s.l)	Net horizontal outflow	Vertical out to above	Vertical in from above	To open reposi-tory	Net horizontal outflow	Vertical out to above	Vertical in from above	To open reposi-tory	Net horizontal outflow	Vertical out to above	Vertical in from above	To open reposi-tory	Net horizontal outflow	Vertical out to above	Vertical in from above	To open reposi-tory
L3	10	0.14	8.42	12.32		–1.52	5.66	31.75	0.02	–0.81	6.06	25.01	0.04	–0.15	6.75	18.03	0.01
L4	30	1.01	3.40	7.13		0.84	2.08	30.33	1.18	0.76	2.25	22.17	0.19	0.93	2.54	13.95	0.02
L5	50	0.06	1.15	3.88		–0.40	0.49	26.96	0.20	–0.12	0.56	19.54	0.18	0.01	0.68	11.14	0.05
L6	70	1.04	0.68	3.35		–1.68	0.26	26.92	3.71	0.08	0.29	19.21	0.82	0.84	0.35	10.76	0.13
L7	90	0.05	0.51	2.15		–0.35	0.25	24.88	0.30	–0.12	0.20	18.22	0.22	–0.01	0.24	9.68	0.06
L8	110	1.22	0.34	1.93		–3.70	0.12	24.79	9.90	–0.21	0.11	18.03	2.34	0.96	0.14	9.53	0.32
L9	130	0.22	0.38	0.75		–0.04	0.10	18.57	0.59	0.08	0.06	15.86	0.20	0.16	0.08	8.20	0.04
L10	150	0.04	0.33	0.49		–0.56	0.11	18.04	0.64	–0.39	0.09	15.60	0.53	–0.14	0.11	8.02	0.13
L11	190	0.03	0.27	0.38		–0.72	0.07	17.92	0.96	–0.52	0.07	15.44	0.78	–0.18	0.08	8.00	0.26
L12	250	0.01	0.17	0.25		–0.76	0.04	17.65	1.25	–0.62	0.04	15.15	0.97	–0.31	0.05	7.89	0.40
L13	360	0.04	0.12	0.19		–1.09	0.16	17.27	0.26	–0.84	0.08	14.85	0.30	–0.41	0.05	7.81	0.33
L14	420	0.01	0.08	0.11		–0.05	0.78	18.73	0.03	0.01	0.59	15.90	0.04	0.03	0.29	8.13	0.04
L15	480	0.00	0.07	0.09		0.10	0.45	18.42	18.21	0.07	0.34	15.60	15.45	–0.04	0.18	7.96	7.96
L16	540	0.01	0.05	0.06		–0.07	1.21	0.87	0.00	–0.05	1.02	0.76	0.00	–0.02	0.64	0.50	0.00
L17	600	0.00	0.04	0.04		–0.05	0.77	0.51	0.00	–0.04	0.66	0.45	0.00	–0.01	0.41	0.29	0.00
L18	690	0.00	0.03	0.04		–0.03	0.56	0.36	0.00	–0.02	0.47	0.32	0.00	–0.01	0.31	0.21	0.00
L19	810	0.00	0.02	0.03		–0.03	0.35	0.21	0.00	–0.02	0.29	0.18	0.00	–0.01	0.18	0.12	0.00
L20	990	0.00	0.01	0.01		–0.04	0.18	0.10	0.00	–0.03	0.15	0.08	0.00	–0.01	0.09	0.06	0.00
Sum		3.88			0.00	–10.14			37.26	–2.79			22.06	1.62			9.74

In order to include the whole open repository construction in the water balance, water balances are also made for the whole model area. In Table 5-3, the water balance for the saturated zone is presented layer by layer in the bedrock, similarly to Table 5-2 but now for the whole model area. Consequently, both the land and the sea parts of the model area are covered, including the whole open repository construction. In Table 5-3, however, the average flow during 2006 is expressed in units of L/s, in order to allow a comparison of contribution to the open repository inflow from different parts of the area, e.g. the land area and the sea area (i.e. Table 5-6).

The calculated changes of vertical net inflow from the QD over the land part due to the open repository (found in Table 5-2, layer 3, but expressed as average flow changes in L/s) are 18, 12 and 6 L/s for the three grouting levels of $K=1\cdot10^{-7}$ m/s, $K=1\cdot10^{-8}$ m/s and $K=1\cdot10^{-9}$ m/s, respectively. The corresponding changes of vertical inflow to the bedrock from both the land and the sea area (found in Table 5-3, layer 3) are 33, 20 and 9 L/s.

Moreover, according to the results in Table 5-3, the total horizontal inflow in the bedrock from the sea boundary increases with 1.4 L/s, from an outflow of 0.4 L/s to an inflow of 1.0 L/s, in the case with a grouting level of $K=1\cdot10^{-7}$ m/s. More than half of this change is found in the deep bedrock above the repository, between approximately 250 and 420 m.b.s.l.

The inflow to tunnels and shafts are further discussed in Section 5.2, but is also presented in Table 5-3. The total inflow is 36 L/s with a grouting level of $K=1\cdot10^{-7}$ m/s, 22 L/s with $K=1\cdot10^{-8}$ m/s, and 10 L/s with $K=1\cdot10^{-9}$ m/s.

Table 5-3 also includes the calculated inflows to SFR. As mentioned earlier in Section 3.1.1, SFR has been described with a simplified approach in the MIKE SHE SDM-Site Forsmark model. With this method, the inflow to SFR was calculated to approximately 3.9 L/s during undisturbed conditions. The observed inflow to SFR is approximately 6 L/s. The calculated inflow to SFR is slightly reduced when the open repository is introduced.

Even though some changes can be seen in the overall water balances discussed above when introducing the open repository, these changes are not major, neither when the whole model area is considered, nor when only the land part is considered. On the other hand, large areas of the model area are not influenced when the groundwater table drawdown is being mapped (see Section 5.4). In order to visualise the magnitude of the open repository influence in areas where the groundwater table is affected, water balances for only these areas have been calculated.

Table 5-4 shows a summary of the total accumulated water balances in mm during 2006, for undisturbed and disturbed conditions, for those areas where the groundwater table drawdown exceeds 0.3 m with a grouting level of $K=1\cdot10^{-7}$ m/s. Inside this influence area, the open repository construction creates a major change in the water balance. With a grouting level of $K=1\cdot10^{-7}$ m/s the inflow to the open repository is 212 mm, which is approximately 40% of the precipitation over the area. The change in the evapotranspiration is small. The changes are instead found on the different runoff components. The total runoff decreases with 163 mm, from an outflow of 142 mm to an inflow of 21 mm, in the case with a grouting level of $K=1\cdot10^{-7}$ m/s. The rest of the changes are mainly found in subsurface storage changes.

In Table 5-5, the water balance for the saturated zone is presented layer by layer in the bedrock, similarly to Table 5-3, but now only for the influence area (the same area as in Table 5-4). In Table 5-5, however, the unit is average flow in L/s during 2006, to allow a comparison with the water balances for the whole model area in Table 5-3.

The calculated changes of vertical net inflow from the QD inside the influence area due to the open repository (found in Table 5-5, layer 3) are 11, 8 and 4 L/s for the three grouting levels of $K=1\cdot10^{-7}$ m/s, $K=1\cdot10^{-8}$ m/s and $K=1\cdot10^{-9}$ m/s, respectively. The corresponding changes of vertical inflow to the bedrock from the whole model area (found in Table 5-3, layer 3) are 33, 20 and 9 L/s.

Moreover, according to the results in Table 5-5 the total horizontal outflow in the bedrock from the influence area to neighbouring areas increases with 0.8 L/s in the case with a grouting level of $K=1\cdot10^{-7}$ m/s. On the other hand, in some layers an increased inflow is found, especially in the top bedrock layer (layer 3) and in the middle sheet joint layer (layer 6). In these two layers together, the net inflow increases with 3.2 L/s. This is then further re-distributed as increased outflow, mainly in the upper and lower sheet joint layers (layer 4 and 8).

Table 5-3. Water balances for 2006 (L/s) in the saturated zone for the whole model area and for each bedrock calculation layer. Numbers are presented for undisturbed conditions and for open repository cases with the three levels of grouting. The water balance components in the table are defined in Figure 5-1.

		Undisturbed conditions					Grouting level K= $1 \cdot 10^{-7}$ m/s					Grouting level K= $1 \cdot 10^{-8}$ m/s					Grouting level K= $1 \cdot 10^{-9}$ m/s				
Layer	Lower level (m.b.s.l)	Net hori-zontal out-flow	Verti-cal out to above	Verti-cal in from above	To SFR	To open reposi-tory	Net hori-zontal out-flow	Verti-cal out to above	Verti-cal in from above	To SFR	To open reposi-tory	Net hori-zontal out-flow	Verti-cal out to above	Verti-cal in from above	To SFR	To open reposi-tory	Net hori-zontal out-flow	Verti-cal out to above	Verti-cal in from above	To SFR	To open reposi-tory
L3	10	0.01	7.43	11.70	0.00		0.01	4.73	41.98	0.00	0.02	0.01	5.07	29.74	0.00	0.03	0.01	5.69	19.28	0.00	0.01
L4	30	0.48	3.10	7.34	0.00		0.47	1.72	39.49	0.00	2.12	0.48	1.87	26.66	0.00	0.32	0.48	2.13	15.69	0.00	0.04
L5	50	0.00	1.04	4.80	0.00		–0.01	0.40	35.76	0.00	0.24	0.00	0.46	24.45	0.00	0.20	0.00	0.55	13.61	0.00	0.05
L6	70	0.00	0.63	4.39	0.51		–0.02	0.22	35.35	0.42	3.01	–0.01	0.24	24.04	0.45	0.68	–0.01	0.29	13.29	0.47	0.12
L7	90	0.00	0.47	3.72	0.58		–0.03	0.20	31.92	0.48	0.26	–0.02	0.17	22.85	0.52	0.19	–0.01	0.19	12.61	0.55	0.06
L8	110	0.00	0.32	2.99	0.74		–0.04	0.10	31.10	0.62	8.02	–0.03	0.09	22.08	0.67	1.90	–0.02	0.11	11.93	0.70	0.27
L9	130	–0.01	0.37	2.29	2.03		–0.03	0.18	22.59	1.74	0.55	–0.03	0.08	19.53	1.84	0.24	–0.02	0.08	10.94	1.91	0.10
L10	150	–0.01	0.81	0.72	0.00		–0.04	0.56	20.71	0.00	0.66	–0.03	0.52	17.92	0.00	0.55	–0.02	0.56	9.44	0.00	0.14
L11	190	–0.02	0.56	0.48	0.00		–0.08	0.33	19.87	0.00	0.78	–0.06	0.31	17.19	0.00	0.63	–0.04	0.35	9.11	0.00	0.21
L12	250	–0.01	0.39	0.34	0.00		–0.11	0.21	19.05	0.00	1.08	–0.08	0.20	16.50	0.00	0.88	–0.05	0.23	8.82	0.00	0.37
L13	360	0.00	0.28	0.23	0.00		–0.56	0.26	18.12	0.00	0.28	–0.43	0.19	15.70	0.00	0.32	–0.21	0.17	8.44	0.00	0.31
L14	420	0.00	0.17	0.13	0.00		–0.26	0.85	18.99	0.00	0.03	–0.20	0.66	16.28	0.00	0.03	–0.10	0.36	8.53	0.00	0.03
L15	480	–0.01	0.14	0.10	0.00		–0.08	0.51	18.88	0.00	18.80	–0.07	0.39	16.19	0.00	16.13	–0.04	0.23	8.47	0.00	8.45
L16	540	0.00	0.10	0.07	0.00		–0.06	1.53	1.19	0.00	0.00	–0.05	1.32	1.05	0.00	0.00	–0.02	0.83	0.66	0.00	0.00
L17	600	–0.01	0.08	0.05	0.00		–0.06	1.01	0.74	0.00	0.00	–0.05	0.88	0.66	0.00	0.00	–0.03	0.56	0.41	0.00	0.00
L18	690	–0.02	0.06	0.04	0.00		–0.10	0.73	0.54	0.00	0.00	–0.07	0.64	0.48	0.00	0.00	–0.05	0.41	0.30	0.00	0.00
L19	810	0.00	0.04	0.04	0.00		0.00	0.45	0.38	0.00	0.00	0.00	0.39	0.33	0.00	0.00	0.00	0.25	0.21	0.00	0.00
L20	990	0.00	0.02	0.02	0.00		0.00	0.24	0.20	0.00	0.00	0.00	0.20	0.17	0.00	0.00	0.00	0.13	0.11	0.00	0.00
Sum		0.38			3.86	0.00	–1.00			3.26	35.85	–0.65			3.48	22.10	–0.13			3.63	10.16

Table 5-4. Total accumulated water balances during 2006 (mm) for the influence area, which here is defined as the area where the groundwater table drawdown exceeds 0.3 m in a simulation with a grouting level of $K=1\cdot10^{-7}$ m/s. Numbers are presented for undisturbed conditions and for open repository cases with the three studied levels of grouting. Observe that the same area definition, i.e. based on the influence area for a grouting level of $K=1\cdot10^{-7}$ m/s, is applied on all of the four cases below when extracting the water balances.

	Reference simulation, without open repository	With open repository, grouting level $K=1\cdot10^{-7}$ m/s	With open repository, grouting level $K=1\cdot10^{-8}$ m/s	With open repository, grouting level $K=1\cdot10^{-9}$ m/s
Precipitation	539.4	539.4	539.4	539.4
Evapotranspiration	429.3	423.7	428.1	430.1
Canopy storage change	0.1	0.1	0.1	0.1
Snow storage change	–32.8	–32.8	–32.8	–32.8
Overland storage change	2.2	–4.6	–7.2	–1.4
Subsurface storage change	–0.7	–39.4	–25.2	–6.6
Net overland outflow	17.1	–39.2	–38.8	–20.2
Net subsurface outflow	51.3	2.8	30.0	46.4
Drain outflow	72.7	15.9	37.3	52.8
Overland flow to river	–0.6	–0.4	–0.5	–0.5
Drainflow to river	1.2	0.2	0.6	0.9
Net baseflow to river	0.2	–0.1	0.0	0.1
Inflow to the open repository	–	211.9	147.2	71.5

Table 5-5. Water balances for 2006 (L/s) for each bedrock calculation layer for the influence area where the groundwater table drawdown exceeds 0.3 m in a simulation with a grouting level of K=1·10^{-7} m/s (the same subarea is applied on all water balances). Numbers are presented for undisturbed conditions and for open repository cases with three levels of grouting. The water balance components are defined in Figure 5-1.

		Undisturbed conditions				Grouting K= 1·10^{-7} m/s				Grouting K= 1·10^{-8} m/s				Grouting K= 1·10^{-9} m/s			
Layer	Lower level (m.b.s.l)	Net horizontal outflow	Vertical out to above	Vertical in from above	To open reposi-tory	Net horizontal outflow	Vertical out to above	Vertical in from above	To open reposi-tory	Net horizontal outflow	Vertical out to above	Vertical in from above	To open reposi-tory	Net horizontal outflow	Vertical out to above	Vertical in from above	To open reposi-tory
L3	10	0.13	0.95	3.02		–1.47	0.02	12.76	0.00	–0.69	0.07	10.15	0.00	–0.12	0.26	6.47	0.00
L4	30	0.55	0.18	2.12		2.24	0.00	14.64	0.00	1.75	0.00	10.92	0.00	1.14	0.01	6.36	0.00
L5	50	0.18	0.04	1.43		1.26	0.00	12.51	0.00	1.01	0.01	9.18	0.00	0.61	0.00	5.21	0.00
L6	70	0.56	0.01	1.23		–1.02	0.00	11.25	2.32	0.23	0.00	8.16	0.34	0.57	0.00	4.60	0.04
L7	90	0.02	0.04	0.69		0.15	0.07	10.02	0.10	0.10	0.03	7.63	0.10	0.06	0.02	4.01	0.03
L8	110	0.62	0.03	0.65		1.45	0.02	9.72	0.58	0.64	0.01	7.40	0.19	0.66	0.01	3.90	0.03
L9	130	0.01	0.07	0.08		0.11	0.01	7.68	0.00	0.08	0.00	6.56	0.00	0.04	0.00	3.21	0.00
L10	150	0.01	0.06	0.06		–0.01	0.00	7.56	0.00	–0.02	0.00	6.48	0.00	–0.02	0.00	3.17	0.00
L11	190	–0.01	0.05	0.04		0.03	0.00	7.57	0.13	0.07	0.00	6.50	0.13	0.06	0.00	3.19	0.05
L12	250	0.00	0.02	0.02		–0.09	0.00	7.41	0.00	–0.09	0.00	6.30	0.00	–0.04	0.00	3.08	0.00
L13	360	0.00	0.02	0.01		0.01	0.03	7.53	0.00	–0.09	0.02	6.40	0.00	–0.09	0.01	3.13	0.01
L14	420	0.00	0.01	0.00		0.30	0.03	7.53	0.00	0.16	0.02	6.49	0.00	–0.01	0.01	3.21	0.00
L15	480	0.00	0.01	0.00		0.03	0.02	7.22	7.34	–0.06	0.01	6.32	6.51	–0.10	0.01	3.21	3.38
L16	540	0.00	0.01	0.00		–0.05	0.28	0.10	0.00	–0.04	0.24	0.09	0.00	–0.02	0.15	0.07	0.00
L17	600	0.00	0.00	0.00		–0.03	0.17	0.05	0.00	–0.03	0.15	0.05	0.00	–0.01	0.09	0.03	0.00
L18	690	0.00	0.00	0.00		–0.01	0.12	0.03	0.00	–0.01	0.11	0.03	0.00	–0.01	0.07	0.02	0.00
L19	810	0.00	0.00	0.00		–0.02	0.08	0.01	0.00	–0.02	0.07	0.01	0.00	–0.01	0.04	0.01	0.00
L20	990	0.00	0.00	0.00		–0.03	0.04	0.00	0.00	–0.02	0.03	0.00	0.00	–0.01	0.02	0.00	0.00
Sum		2.07			0.00	2.84			10.47	2.97			7.28	2.71			3.54

The inflow to the open repository is also presented in Table 5-5. Note that the presented inflows in Table 5-5 only concern the parts of the open repository that are located inside the influence area (defined as above). Large parts of the open repository are located outside this area, which is the reason why the numbers are much less than in Table 5-3, where the results from the whole model area are presented.

In Table 5-6, a summary is presented of the changes in vertical net inflow, as well as changes in the horizontal net inflow from the sea boundary, when the open repository is introduced. The vertical net inflow is separated between the influence area, the rest of the land area and the sea area. As can be seen from Table 5-6, the changed vertical inflow from the land area contributes to the open repository inflow with 50–60%, depending on the grouting level, with a higher relative contribution at the higher grouting level. Approximately 60–70% of the changed vertical inflow from land can be attributed to the influence areas, coinciding with the vertical fracture zones. In total, the influence area contributes to the open repository inflow with 30–40%. The changed inflow from the sea gives most of the remaining contribution, with the majority coming from vertical inflow from the sea area covered by the model. Very little comes from changed horizontal inflow over the model boundary in the sea.

5.2 Inflow to tunnels and shafts

The inflow to tunnels and shafts increases with an increased hydraulic conductivity of the grouting and varies between the different calculation layers. A grouting conductivity of $1 \cdot 10^{-7}$ m/s results in a mean inflow over the evaluated simulation period (year 2006) of c 33 L/s to tunnels and 3.1 L/s to shafts. The lowest inflow of c 10 L/s for tunnels and 0.6 L/s for shafts is reached with a grouting conductivity of $1 \cdot 10^{-9}$ m/s. The inflows in the three simulation cases are listed in Table 5-7 for each layer. It should be noted that the inflow to the repository is calculated based on both the grouting conductivity and the conductivities in the surrounding bedrock (see Section 2.3.1 for details). This means that when the bedrock has a lower conductivity than the grouting the bedrock mainly controls the inflow, whereas the situation is at hand when the grouting has the lower conductivity.

The major part of the inflow comes from layer 15 at approximately 450 m.b.s.l. where the open repository is located. The inflow to the tunnel is however also dependent on the properties of the surrounding bedrock. Thus, the inflows are higher in layers 4, 6 and 8, where the horizontally highly conductive zones (the so-called sheet joints) are located.

In Table 5-8 the inflows to the tunnels are presented similarly as in Table 5-7, but now expressed as specific inflow in L/s/km tunnel length in each layer. This gives a somewhat different picture of the flow distribution among the layers. Now the sheet joint layers appear as the most important ones, especially the lower sheet joint layer (layer 8). At repository depth (layer 15) the specific inflow is not remarkable, but still the majority of the total inflow comes from this layer.

In Figure 5-2 the inflow from the rock at repository depth has been resolved in the horizontal plane, by showing the discharge to the repository from each grid cell in layer 15. The results show what could be termed a cage effect with the largest inflows along the boundaries of the repository, i.e. the outer transport tunnels, especially along the boundary towards the sea. The pattern from the fracture zones is also clear, with higher inflows along high-conductive zones (see also Section 5.4.4).

The meteorological conditions are hardly reflected in the calculated inflows. The inflows are somewhat higher after wet periods with large rain volumes, but the variation is small. In Figure 5-3 the relative variations in inflow for some selected layers are presented, as well as the total inflow, for a grouting level of $K=1 \cdot 10^{-8}$ m/s. The amplitude of the total inflow is less than 0.5 L/s. The relative variation is largest in the upper layers, above the sheet joint layers, where the variations are reduced to ± 3%. Below 200 m.b.s.l. the variations are negligible.

The open repository will be constructed and taken into operation in three development phases, called phase 1, phase 2 and phase 3. In all development phases, the access tunnel and all of the transport tunnels will be open, but only one section with deposition tunnels will be open at a time (see Section 4.2 for details). In Table 5-9, the inflows to tunnels and shafts are presented for the three different phases, based on results from a simulation with a grouting level of $K = 1 \cdot 10^{-8}$ m/s.

Table 5-6. Summary water balance for 2006 (L/s) showing the changes in flow components in the bedrock when introducing the open repository for different levels of grouting.

Changes in flow components due to the open repository:	With open repository, grouting level $K=1\cdot10^{-7}$ m/s		With open repository, grouting level $K=1\cdot10^{-8}$ m/s		With open repository, grouting level $K=1\cdot10^{-9}$ m/s	
	(L/s)	relative contribution	(L/s)	relative contribution	(L/s)	relative contribution
Vertical net inflow to bedrock in the influence area (fracture zones)	10.67	30%	8.02	36%	4.15	41%
Vertical net inflow to bedrock in the land area, excl influence area	7.26	20%	4.15	19%	1.82	18%
Vertical net inflow to bedrock from the sea area	15.05	42%	8.23	37%	3.36	33%
Horizontal net inflow to bedrock from the sea boundary	1.38	4%	1.03	5%	0.51	5%
Storage change in bedrock	–0.89	2%	–0.29	1%	–0.10	1%
Reduced inflow to SFR	–0.60	2%	–0.40	2%	–0.20	2%
Inflow to the open repository	35.85		22.10		10.16	

Table 5-7. Calculated mean inflow (L/s) to tunnels and shafts during 2006 for each calculation layer and for the three studied levels of grouting.

Calculation layer	Lower level (m.b.s.l.)	Inflow to tunnels, grouting level $K=1\cdot10^{-7}$ m/s	Inflow to tunnels, grouting level $K=1\cdot10^{-8}$ m/s	Inflow to tunnels, grouting level $K=1\cdot10^{-9}$ m/s	Inflow to shafts, grouting level $K=1\cdot10^{-7}$ m/s	Inflow to shafts, grouting level $K=1\cdot10^{-8}$ m/s	Inflow to shafts, grouting level $K=1\cdot10^{-9}$ m/s
Layer 1–3	–10	0.0	0.0	0.0	0.0	0.0	0.0
Layer 4	–30	1.7	0.2	0.0	0.5	0.1	0.0
Layer 5	–50	0.2	0.2	0.0	0.0	0.0	0.0
Layer 6	–70	2.7	0.6	0.1	0.3	0.1	0.0
Layer 7	–90	0.2	0.1	0.0	0.0	0.1	0.0
Layer 8	–110	7.5	1.7	0.2	0.5	0.2	0.0
Layer 9	–130	0.1	0.1	0.0	0.4	0.2	0.1
Layer 10	–150	0.6	0.5	0.1	0.1	0.1	0.0
Layer 11	–190	0.3	0.4	0.1	0.5	0.3	0.1
Layer 12	–250	0.4	0.6	0.3	0.7	0.3	0.1
Layer 13	–360	0.2	0.2	0.2	0.1	0.1	0.1
Layer 14	–420	0.0	0.0	0.0	0.0	0.0	0.0
Layer 15	–480	18.8	16.1	8.4	0.0	0.0	0.0
Layer 16	–540	0.0	0.0	0.0	0.0	0.0	0.0
Layer 17	–600	0.0	0.0	0.0	0.0	0.0	0.0
Layer 18	–690	0.0	0.0	0.0	0.0	0.0	0.0
Layer 19	–810	0.0	0.0	0.0	0.0	0.0	0.0
Layer 20	–990	0.0	0.0	0.0	0.0	0.0	0.0
Sum		32.7	20.7	9.6	3.1	1.4	0.6

Table 5-8. Calculated specific mean inflow (L/s/km tunnel) to the open repository during 2006 for each calculation layer and for the three studied levels of grouting.

Calculation layer	Lower level (m.b.s.l.)	Tunnel length (m)	Inflow to ramps and tunnels, grouting level K= $1 \cdot 10^{-7}$ m/s	Inflow to ramps and tunnels, grouting level K= $1 \cdot 10^{-8}$ m/s	Inflow to ramps and tunnels, grouting level K= $1 \cdot 10^{-9}$ m/s
Layer 1–3	10	134	0.12	0.20	0.08
Layer 4	30	213	7.78	1.14	0.13
Layer 5	50	204	1.03	0.80	0.19
Layer 6	70	330	8.22	1.72	0.25
Layer 7	90	214	1.02	0.67	0.16
Layer 8	110	212	35.21	8.11	1.07
Layer 9	130	218	0.63	0.28	0.05
Layer 10	150	206	2.70	2.21	0.56
Layer 11	190	544	0.52	0.67	0.24
Layer 12	250	636	0.67	0.88	0.41
Layer 13	360	1,284	0.16	0.18	0.16
Layer 14	420	2,222	0.01	0.01	0.01
Layer 15	480	77,067	0.24	0.21	0.11
Layer 16	540	511	0.00	0.00	0.00
Layer 17	600		0.00	0.00	0.00
Layer 18	690		0.00	0.00	0.00
Layer 19	810		0.00	0.00	0.00
Layer 20	990		0.00	0.00	0.00
Sum		83,995	0.39	0.25	0.11

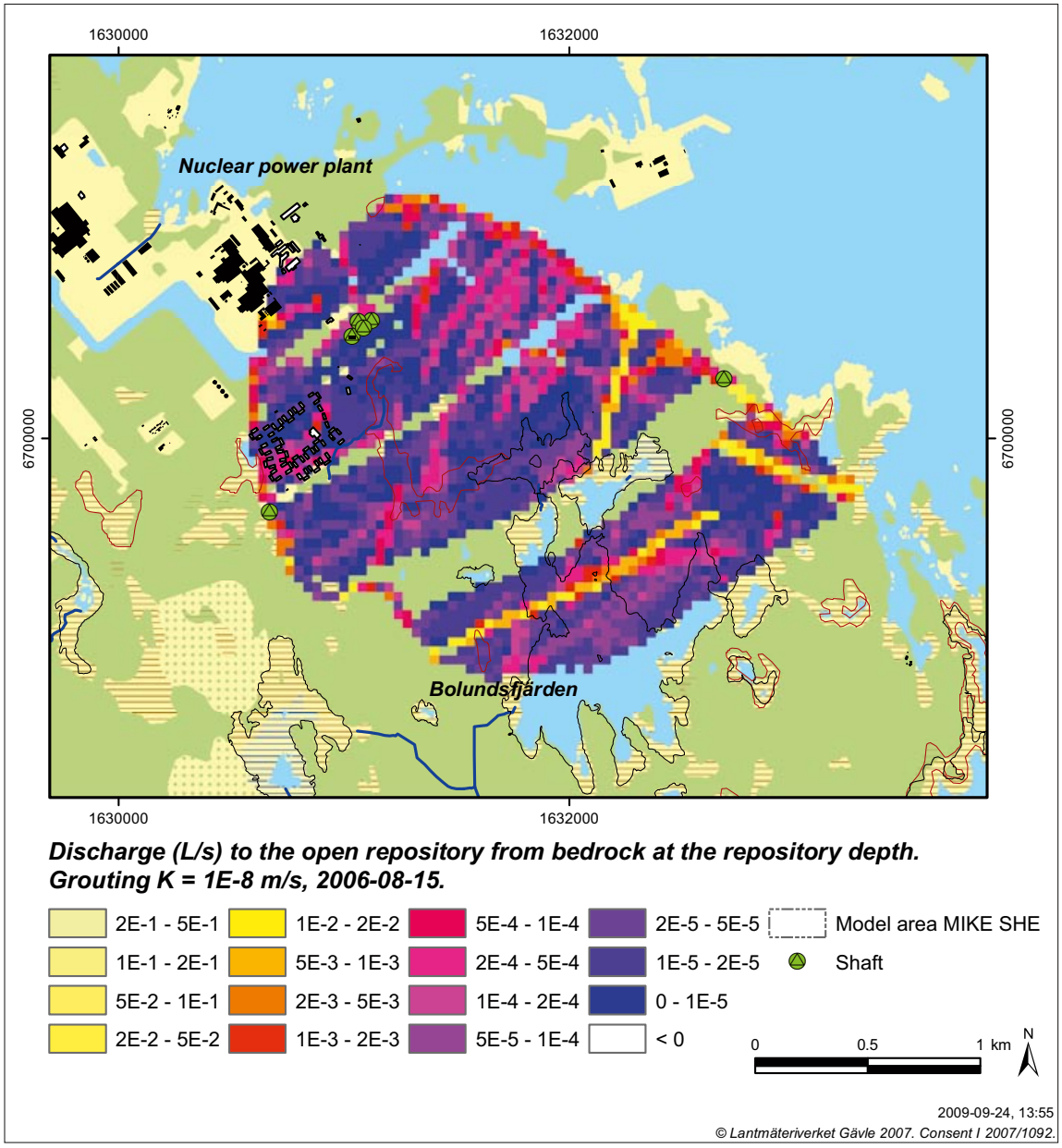

Figure 5-2. *Calculated discharge (L/s) to the open repository from each grid cell in the layer where the repository is located (layer 15). The discharges represent the date 2006-08-15 in a simulation with a grouting level of $K=1{\cdot}10^{-8}$ m/s.*

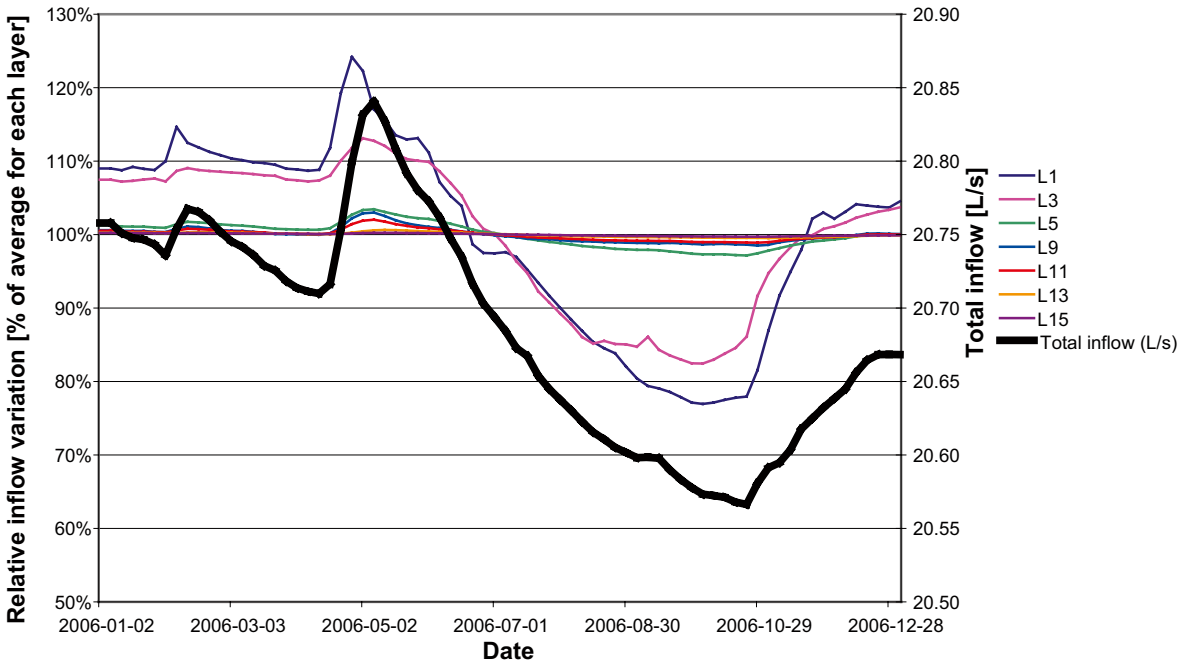

Figure 5-3. *Temporal variations in the calculated inflow for the year 2006 (for a grouting level of $K=1{\cdot}10^{-8}$ m/s), expressed as total inflow (black line, right vertical axis) and relative variations for selected layers (all other lines, left vertical axis).*

Table 5-9. Calculated mean inflow (L/s) to tunnels and shafts during 2006 for each calculation layer and for the three development phases. The results are from a simulation with a grouting level of $K=1{\cdot}10^{-8}$ m/s.

Calculation layer	Lower level (m.b.s.l.)	Inflow to tunnels, phase 1	Inflow to tunnels, phase 2	Inflow to tunnels, phase 3	Inflow to shafts, phase 1	Inflow to shafts, phase 2	Inflow to shafts, phase 3
Layer 1–3	–10	0.0	0.0	0.0	0.0	0.0	0.0
Layer 4	–30	0.3	0.3	0.2	0.1	0.1	0.1
Layer 5	–50	0.2	0.2	0.2	0.0	0.0	0.0
Layer 6	–70	0.6	0.6	0.6	0.1	0.1	0.1
Layer 7	–90	0.1	0.1	0.1	0.0	0.1	0.0
Layer 8	–110	1.8	1.8	1.8	0.2	0.2	0.2
Layer 9	–130	0.1	0.1	0.1	0.2	0.2	0.2
Layer 10	–150	0.5	0.5	0.5	0.1	0.1	0.1
Layer 11	–190	0.4	0.4	0.4	0.3	0.3	0.3
Layer 12	–250	0.6	0.6	0.6	0.3	0.3	0.3
Layer 13	–360	0.3	0.3	0.3	0.1	0.1	0.1
Layer 14	–420	0.0	0.0	0.0	0.0	0.0	0.0
Layer 15	–480	7.9	10.0	13.3	0.0	0.0	0.0
Layer 16	–540	0.0	0.0	0.0	0.0	0.0	0.0
Layer 17	–600	0.0	0.0	0.0	0.0	0.0	0.0
Layer 18	–690	0.0	0.0	0.0	0.0	0.0	0.0
Layer 19	–810	0.0	0.0	0.0	0.0	0.0	0.0
Layer 20	–990	0.0	0.0	0.0	0.0	0.0	0.0
Sum		12.6	14.7	18.0	1.5	1.5	1.5

Compared to the full open repository construction, the inflows for the different phases are smaller. Phase 1 has only an inflow of approximately 61% of the inflow to the full construction. The corresponding inflow for phase 2 is 71% and for phase 3 it is 87% of the inflow for the full construction. The difference is however only seen at the repository level. The inflow to the shafts is more or less unchanged compared to the full construction, only slightly higher.

5.3 Surface water levels and discharges in water courses

The mean water levels in the studied lakes in the area are hardly affected by the repository and tunnel constructions. The low-permeable sediment layers under the lakes are assumed to have a strong influence on the lake water levels and prevent a lowering of the water level in the lakes. Whether this assumption about the importance of the lake sediments is correct is further elaborated in Chapter 6, where a number of sensitivity analyses are presented.

For Lake Eckarfjärden and Lake Fiskarfjärden, the effects of the repository on the water levels are negligible. The average difference over 2006 is less than 0.3 cm in all studied grouting cases, with a maximum difference of less than 1 cm.

For Lake Bolundsfjärden and Lake Gällsboträsket, which are located closer to the repository in the downstream part of the model area, some difference between the different levels of grouting can be noted, see Figures 5-4 to 5-7, with the largest drawdown of the water level for the highest grouting conductivity ($K=1\cdot10^{-7}$ m/s). The average drawdown over 2006 in Lake Gällsboträsket varies between 0.8 and 1.5 cm, depending on the grouting level, with a maximum drawdown between 2.7 and 5.5 cm, see Figure 5-5. The average drawdown during 2006 in Lake Bolundsfjärden varies between 0.5 and 1.5 cm, depending on the grouting level, with a maximum drawdown between 2.0 and 4.0 cm, see Figure 5-7. The maximum drawdown is found during the highest peak in the end of April 2006.

The water level drawdown in Lake Bolundsfjärden and Lake Gällsboträsket is a consequence of the groundwater table drawdown around and the head change under these lakes; such head changes are not present at the other lakes (see Figure 5-15, Section 5.4.2). The drawdown of the groundwater table around these lakes reduces the inflow to the lakes from surrounding areas, which in turn lowers the lake water levels. This is further discussed in the end of this section.

The discharges in the water courses are only affected to a very small extent by the tunnels and shafts. Table 5-10 shows a comparison of the accumulated discharges between the reference model (undisturbed conditions) and the open repository models with different levels of grouting for the four monitoring stations. Actually, the calculated difference at Lake Eckarfjärden, Lake Stocksjön and Lake Gunnarsboträsket are so small that the changes can not be resolved by the model due to small numerical anomalies.

The effect is notable at Lake Bolundsfjärden in the downstream part of the catchment, close to the repository, where a level of grouting of $K= 1\cdot10^{-7}$ m/s results in a decrease in the accumulated discharge by 8%. The calculated accumulated change in discharge upstream Lake Bolundsfjärden is shown in Figure 5-8. The reduced inflow to Lake Bolundsfjärden is a consequence of the groundwater table drawdown in the upstream area, which is not present upstream the other monitoring stations in Table 5-10 (see Figure 5-15, Section 5.4.2).

The previous discussion raises the question weather it is a reduced inflow from the upstream water course or an increased recharge through the bottom of the lakes that causes the drawdown of the lakes. This is in particular of interest for Lake Bolundsfjärden, being located in the centre of the influence area. The overland water balance for Lake Bolundsfjärden is presented in Table 5-11, both for undisturbed conditions and with an open repository using a grouting level of $K=1\cdot10^{-8}$ m/s.

The overland inflow is slightly reduced (–0.2 L/s), but the major change for the lake is found in a reduced subsurface discharge to the lake through the bottom (–1.4 L/s). Altogether, this reduces the net outflow from the lake with 1.7 L/s, which should be compared with the reduction of inflow from the upstream water course of 1.8 L/s. This means that the increased recharge from the lake (or reduced discharge to the lake) is more or less equivalent to the reduced inflow from the upstream water course, and consequently of the same importance for the drawdown of the lake.

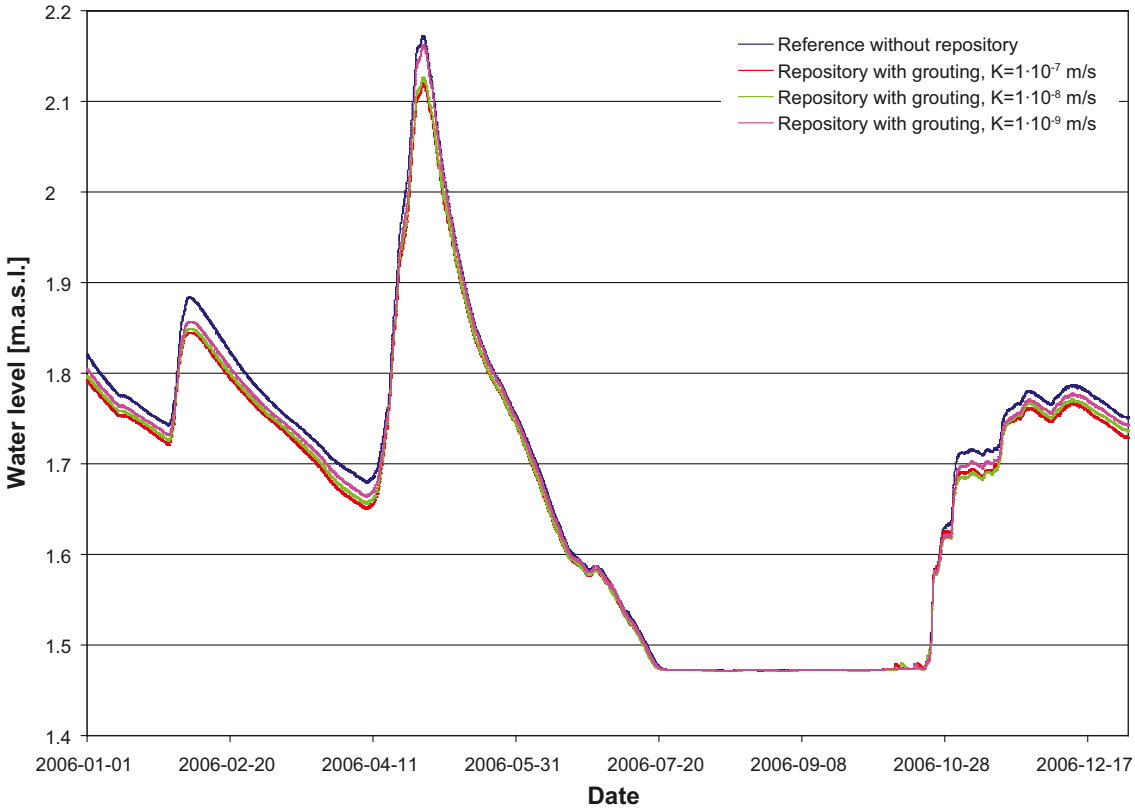

Figure 5-4. *Calculated water levels in Lake Gällsboträsket for different levels of grouting.*

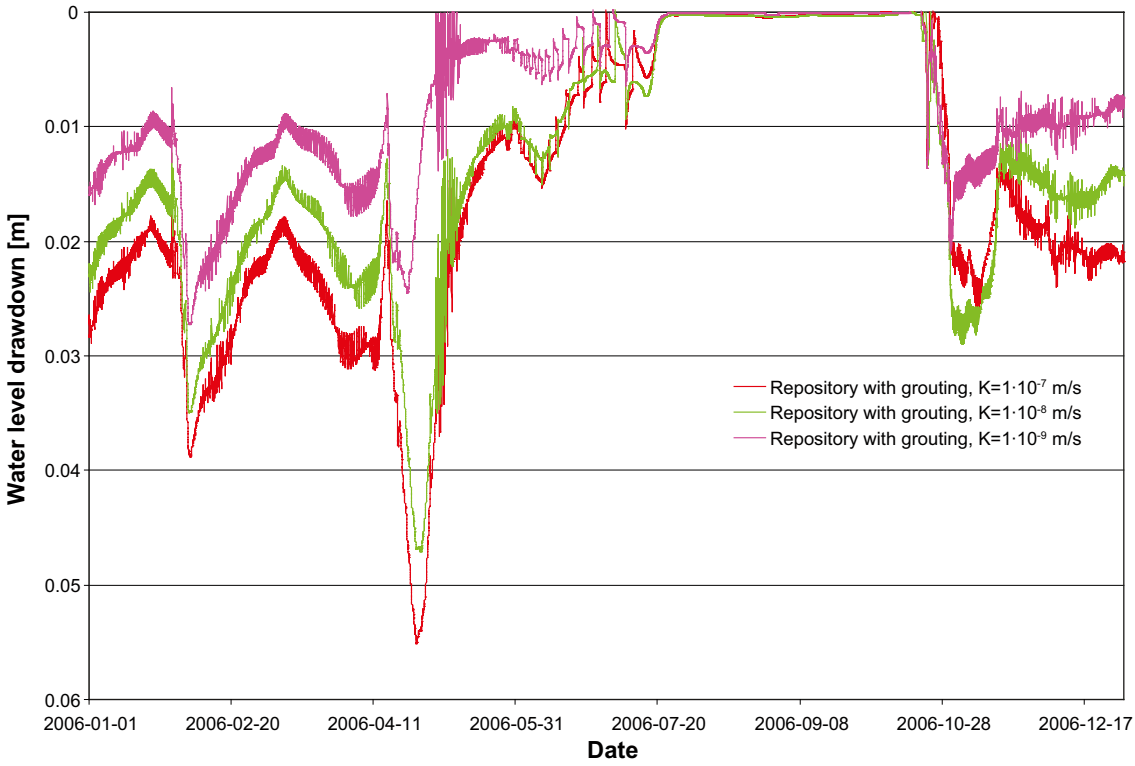

Figure 5-5. *Calculated water level drawdowns in Lake Gällsboträsket for different levels of grouting.*

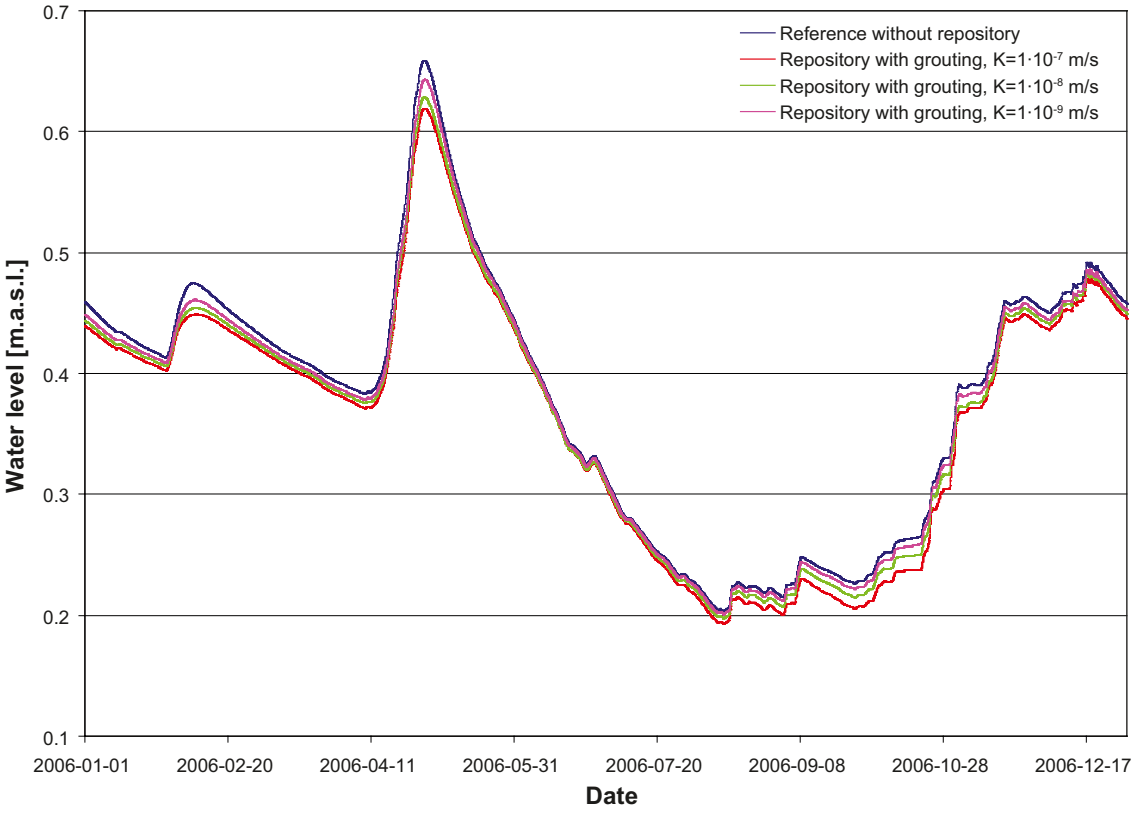

Figure 5-6. *Calculated water levels in Lake Bolundsfjärden for different levels of grouting.*

Figure 5-7. *Calculated water level drawdowns in Lake Bolundsfjärden for different levels of grouting.*

Table 5-10. Relative changes (reductions) in calculated average discharges in water courses (during 2006) when introducing an open repository with different levels of grouting.

	$K=1\cdot10^{-7}$ m/s	$K=1\cdot10^{-8}$ m/s	$K=1\cdot10^{-9}$ m/s
Downstream Lake Eckarfjärden	< 1%	< 1%	< 1%
Downstream Lake Stocksjön	< 1%	< 1%	< 1%
Downstream Lake Gunnarsboträsket	< 1%	< 1%	< 1%
Upstream Lake Bolundsfjärden	8%	7%	4%

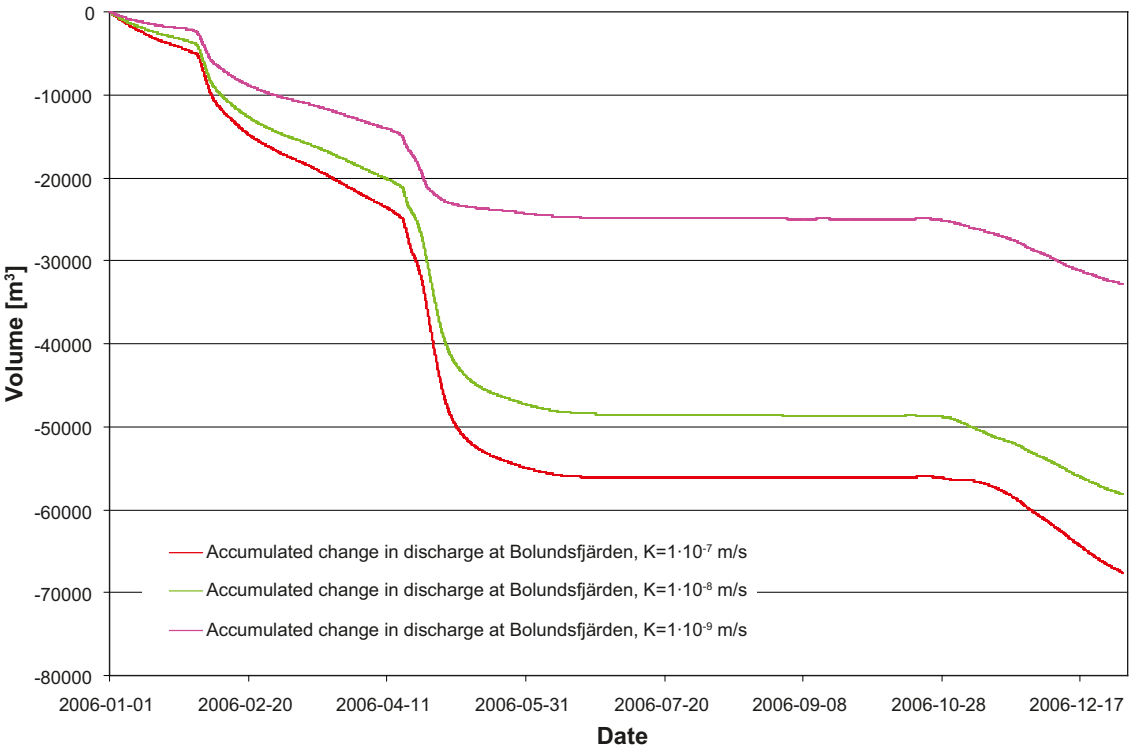

Figure 5-8. *Calculated accumulated change in discharge upstream Lake Bolundsfjärden for the three different levels of grouting.*

Table 5-11. Overland-water balance during 2006 (L/s) for Lake Bolundsfjärden, for undisturbed conditions and with an open repository with the grouting level $K=1\cdot10^{-8}$ m/s.

	Reference simulation, without open repository	With open repository, grouting level $K=1\cdot10^{-8}$ m/s	Difference
Net precipitation (incl evaporation and storage)	4.8	4.7	–0.1
Net overland inflow to lake	4.5	4.3	–0.2
Net subsurface discharge to lake	3.1	1.7	–1.4
Infiltration	2.0	2.0	0.1
Net river outflow from lake (excl inflow from the upstream water course)	10.4	8.7	–1.7
Inflow from the upstream water course	25.5	23.6	–1.8

5.4 Groundwater table drawdown and head changes

The influence area is here defined as the area where the groundwater table is lowered more than 0.3 m due to the repository. Figure 5-9 shows the drawdown of the groundwater table, as an average for 2006, for a grouting level of $K=1\cdot10^{-8}$ m/s. Figure 5-10 shows the same groundwater table drawdown in an enlarged view around the open repository. The size and the form of the influence area and the drawdown depend on a number of factors. These are discussed in this Chapter. An overview, with references to specific sections, is given below.

The groundwater table drawdown varies in time due to different meteorological and hydrological conditions, which is illustrated in Section 5.4.1. The influence area and the groundwater head changes increases with depth, and are generally affected by the horizontal and vertical conductivity in the upper bedrock and the Quaternary deposits, and more specifically by the pattern of the vertical fracture zones reaching the upper bedrock.

The influence area, shown in Figure 5-10, covers a number of bands north and west of Lake Bolundsfjärden, and one band north-west, and partly south-east of Lake Stocksjön. All of these bands coincide with vertical fracture zones. In addition, the influence area covers a number of smaller areas south of the nuclear power plant, and a larger area rather close to, and north-east of the power plant. Also these areas coincide with vertical fracture zones. The largest drawdown of the groundwater table is found in the area north-east of the power plant. The drawdown of the groundwater table is here up to approximately 15 meter. All this, is further elaborated in Section 5.4.2.

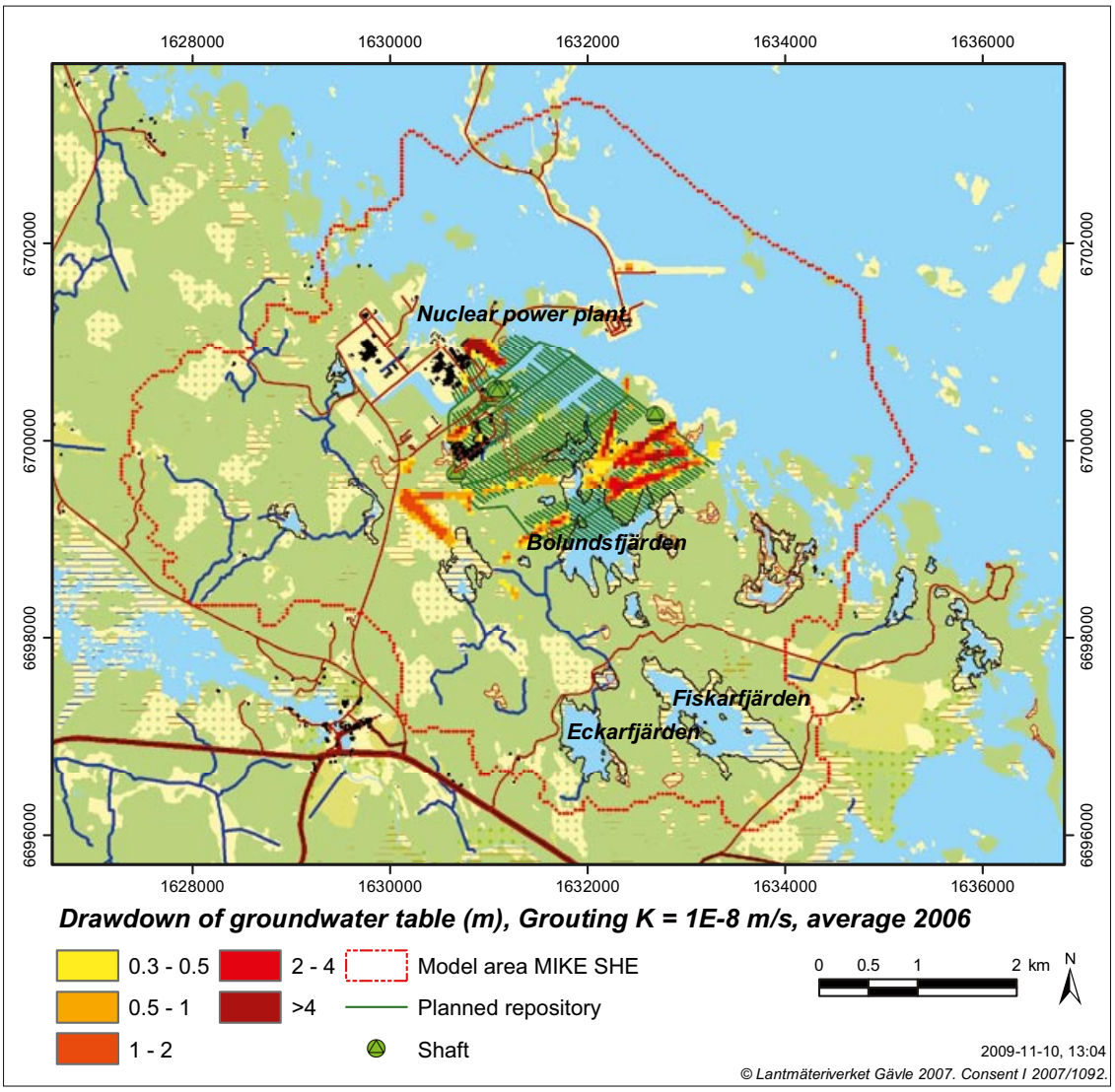

Figure 5-9. *Drawdown of the groundwater table as an average for 2006 for a case with $K=1\cdot10^{-8}$ m/s in the grouted zone.*

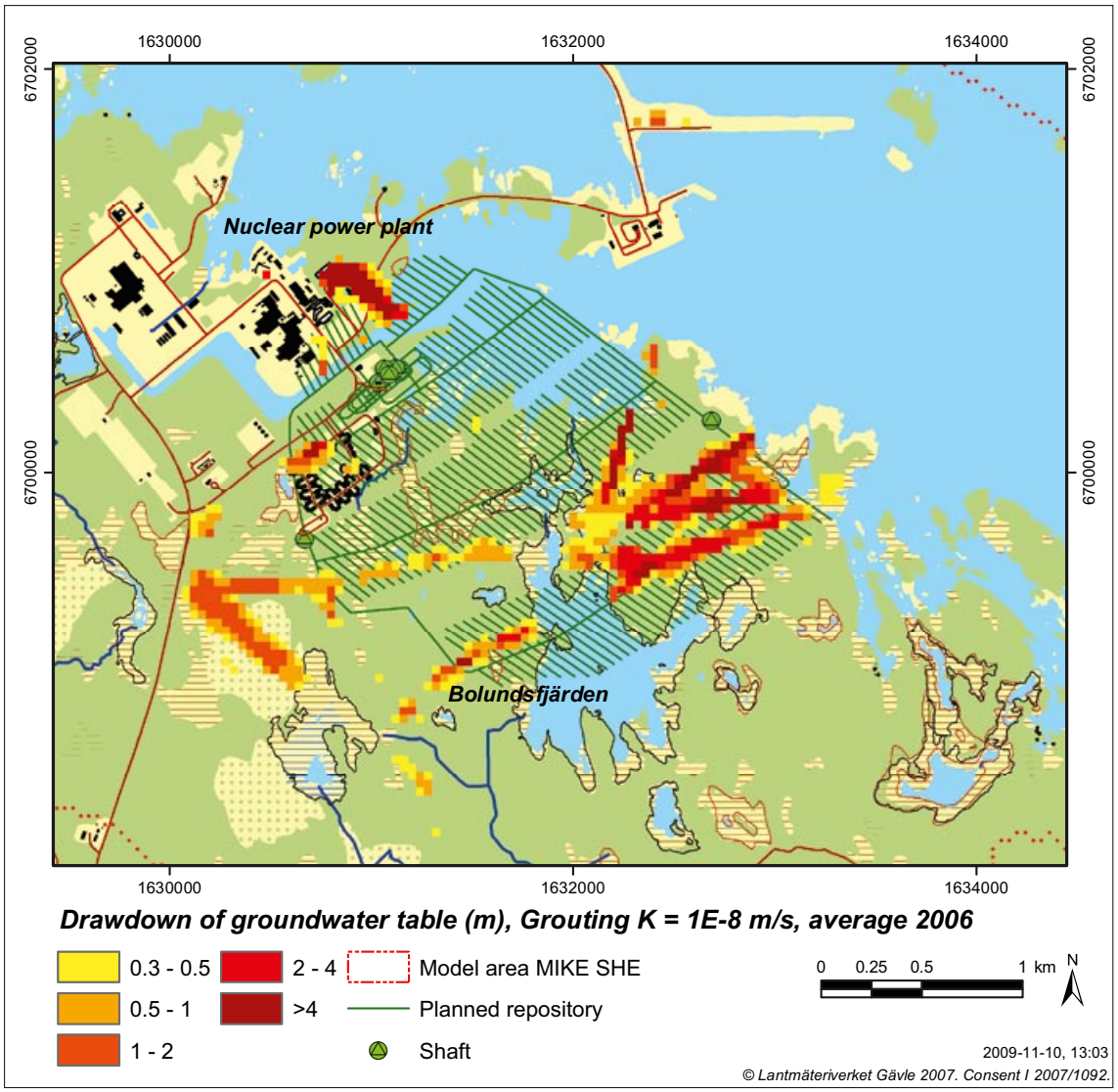

Figure 5-10. *Detailed view over the drawdown of the groundwater table as an average for 2006 for a case with $K=1{\cdot}10^{-8}$ m/s.*

Notable is however that the influence area in the uppermost bedrock (Figure 5-15) covers the eastern part of the nuclear power plant. Depending on the local groundwater head conditions around the nuclear power plant, this means a potential risk for mass transport by groundwater flow from the nuclear power plant to the open repository, as well as a theoretical risk of settlings.

The level of grouting in tunnels and shafts is also, of course, an important factor influencing the size of the groundwater table drawdown and the head changes. This is presented in Section 5.4.3 for three different levels of grouting: $K=1{\cdot}10^{-7}$, $1{\cdot}10^{-8}$ and $1{\cdot}10^{-9}$ m/s. The groundwater table drawdown for the three different development phases of the open repository are presented in Section 5.4.4 for a grouting level of $K=1{\cdot}10^{-8}$ m/s.

In reality, the repository will be open for many decades, and the groundwater table drawdown will have time to be fully developed to steady state conditions (or semi-steady, due to the influence of the temporal variations in the meteorological and hydrological conditions). In practice, it would take too long time to simulate the full period, so in order to save simulation time a rather short simulation period has been applied, only two years, where the first year is used as an initialisation period. The drawback of this approach is however the risk that the influence area and the groundwater table drawdown is underestimated. This is further investigated in Section 5.4.5.

5.4.1 Temporal variations in the groundwater table drawdown

In Table 5-12, the influence areas for different drawdown limits for the groundwater table are presented for each month during 2006. The results are based on a grouting level of $K=1\cdot10^{-8}$ m/s. The results show that the size of the influence area is clearly affected by the meteorological and hydrological variations during the year.

In Figures 5-11 and 5-12, the drawdown of the groundwater table for two types of conditions are presented: (i) relatively wet conditions with a high groundwater table represented by May 17th 2006, shown in Figure 5-11, and (ii) dry conditions with a low groundwater table represented by August 15th 2006, shown in Figure 5-12. One could imagine that these two dates would appear as extremes in Table 5-12, due to the large difference in groundwater elevation, but this is not the case. Conversely, it can be seen that both dates are rather representing the lower end. One could also imagine that the influence area would be less during wet periods, because during wet periods, with lots of precipitation, the groundwater table is recharged anyway, but neither this is the case.

However, the drawdown of the groundwater table is an effect from an increased downward flow, controlled by the gradient between the groundwater table and the groundwater head deeper in the bedrock. This gradient increases during wet periods, with an increased downward flow as a result, and it seems like this overrides the effect from an increased recharge during wet periods.

The summer months during 2006 (May–August) have the smallest influence areas. This period is characterised by a decreasing groundwater table elevation, due to increasing evapotranspiration and during 2006 in addition low amounts of precipitation. These meteorological conditions affect the groundwater conditions in the upper layers more than in the deeper bedrock, meaning that the downward gradient due to the open repository is reduced in these periods, with less influence from the repository as a result.

The opposite situation holds during the rest of the year, resulting in larger influence areas. Especially the periods with an increasing groundwater table elevation give larger influence areas (February, April, October, and November). During these periods, larger precipitation volumes increase the groundwater table elevation rather fast, creating a larger downward gradient in the rising phase (e.g. in April), with larger influence from the repository as a result. Later, in the recession after a peak in the groundwater table (e.g. in May), the groundwater head deeper in the bedrock slowly increases with less gradient and less influence from the repository as a result. This means that both a large and a small influence area can be found during a peak in the groundwater table; the larger area during the rising part and the smaller area in the recession after the peak.

Table 5-12. Influence area (km^2) each month during 2006, calculated for a grouting level of $K=1\cdot10^{-8}$ m/s.

Date	Maximum lowering of the water table (m)	Influence area, drawdown >0.3 m	Influence area, drawdown >0.5 m	Influence area, drawdown >1 m
January 17th 2006	14.6	1.46	0.85	0.42
February 16th 2006	13.9	1.52	0.86	0.39
March 18th 2006	15.6	1.22	0.77	0.40
April 17th 2006	14.7	1.73	0.86	0.44
May 17th 2006	12.8	0.75	0.51	0.28
June 16th 2006	15.5	0.79	0.52	0.28
July 16th 2006	16.8	0.80	0.55	0.34
August 15th 2006	17.1	0.91	0.66	0.41
September 14th 2006	18.3	1.05	0.80	0.50
October 14th 2006	18.4	1.28	0.93	0.59
November 18th 2006	17.1	1.81	1.42	0.70
December 18th 2006	15.6	1.78	1.30	0.58
Average 2006	14.9	1.02	0.75	0.46

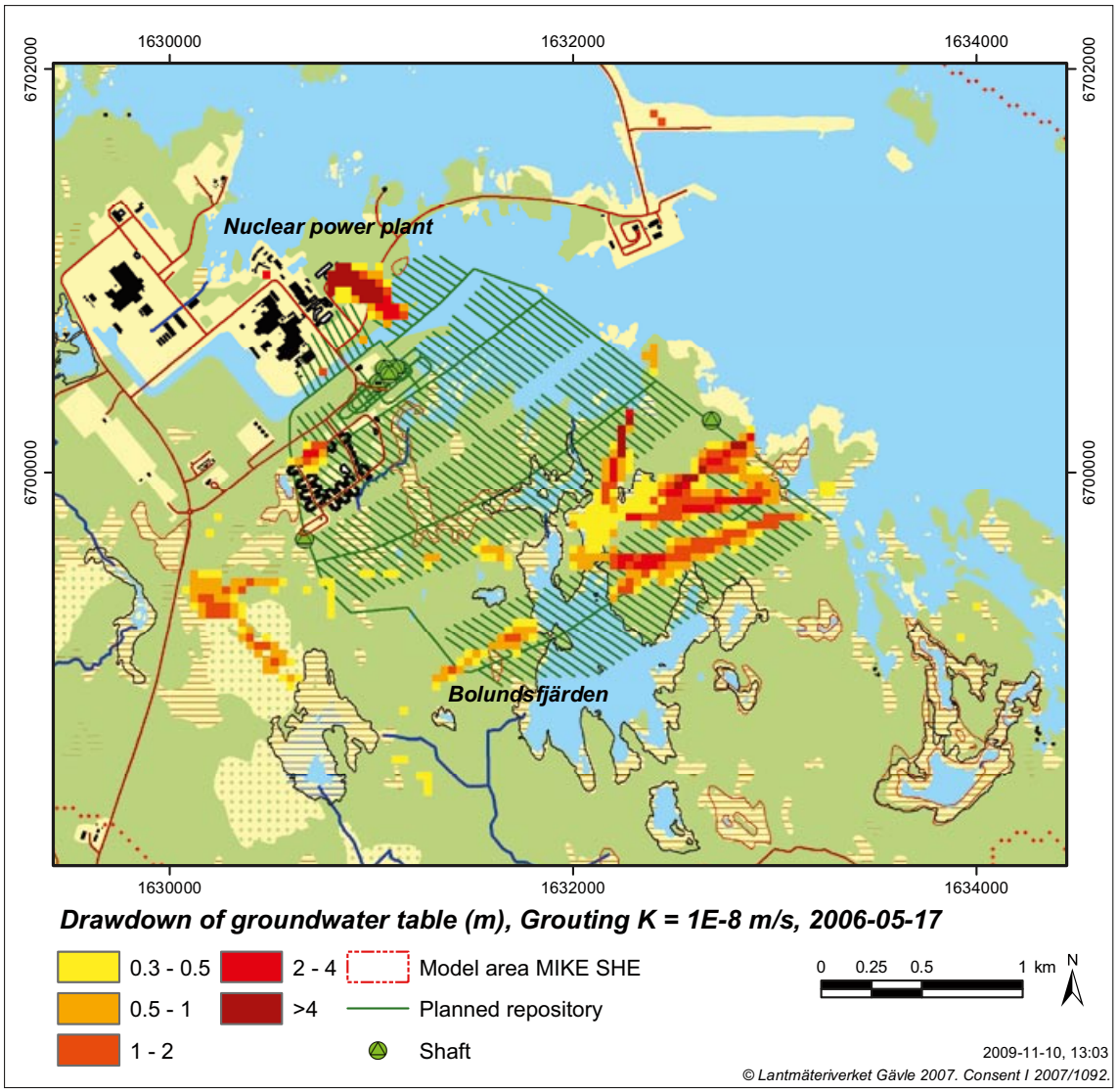

Figure 5-11. *Detailed view of the drawdown of the groundwater table under wet conditions, May 17th 2006, with a grouting level of $K=1\cdot10^{-8}$ m/s.*

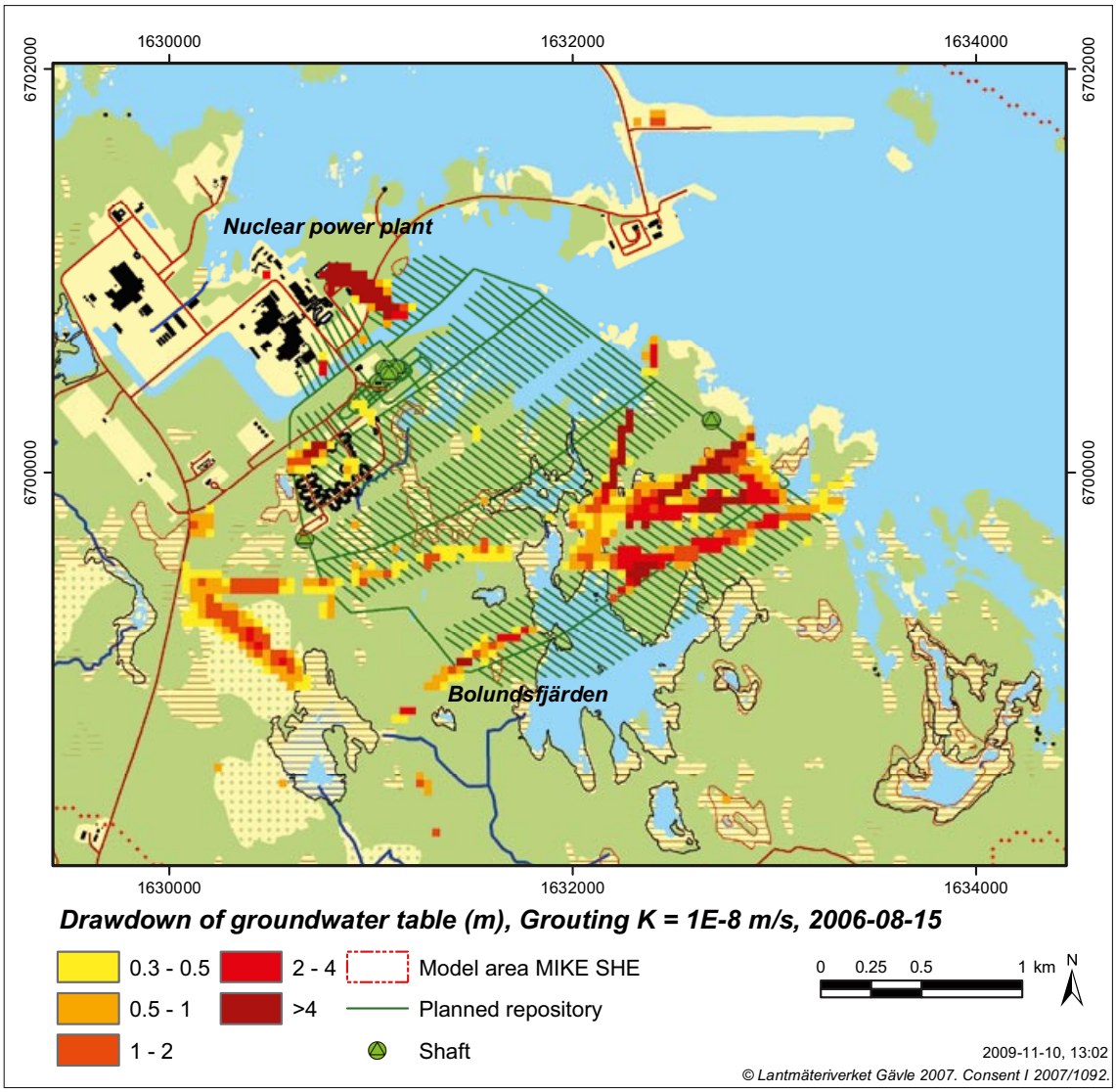

Figure 5-12. *Detailed view of the drawdown of the groundwater table under dry conditions, August 15th 2006, with a grouting level of $K=1\cdot10^{-8}$ m/s.*

The largest drawdown of the groundwater table, being approximately 15 metres according to Table 5-12, is found in the area north-east of the power plant (Figure 5-12). The explanation for this is found in Section 5.4.2. The maximum influence area in Table 5-12 is found on November 18th and the minimum influence area on May 17th . The influence areas for these two dates, with groundwater table drawdown larger than 0.3 m, are presented together in Figure 5-13. The influence areas from the two extremes show approximately the same overall banded pattern, only with differing sizes.

5.4.2 Head changes and vertical flow pattern at different depths

The results presented above refer to the drawdown of the groundwater table. The impact of the repository on the groundwater table is rather mild and concentrated to vertical fracture zones in the upper part of the bedrock. However, there are differences in the head changes of the groundwater when considering different depths in the model. In this section, results for groundwater head changes and vertical flow patterns are shown for the QD and for different depths in the shallow bedrock (down to 50 m.b.s.l.).

In all cases in this section, the level of grouting has been set to $K=1\cdot10^{-8}$ m/s and all of the results are taken from August 15th 2006. Figure 5-14 and Figure 5-15 show the head changes of the groundwater in the QD and at different depths in the bedrock (layers 2, 3, 4 and 5). Compared to the head change in the QD, the head changes in the bedrock are considerably larger and cover a much larger area.

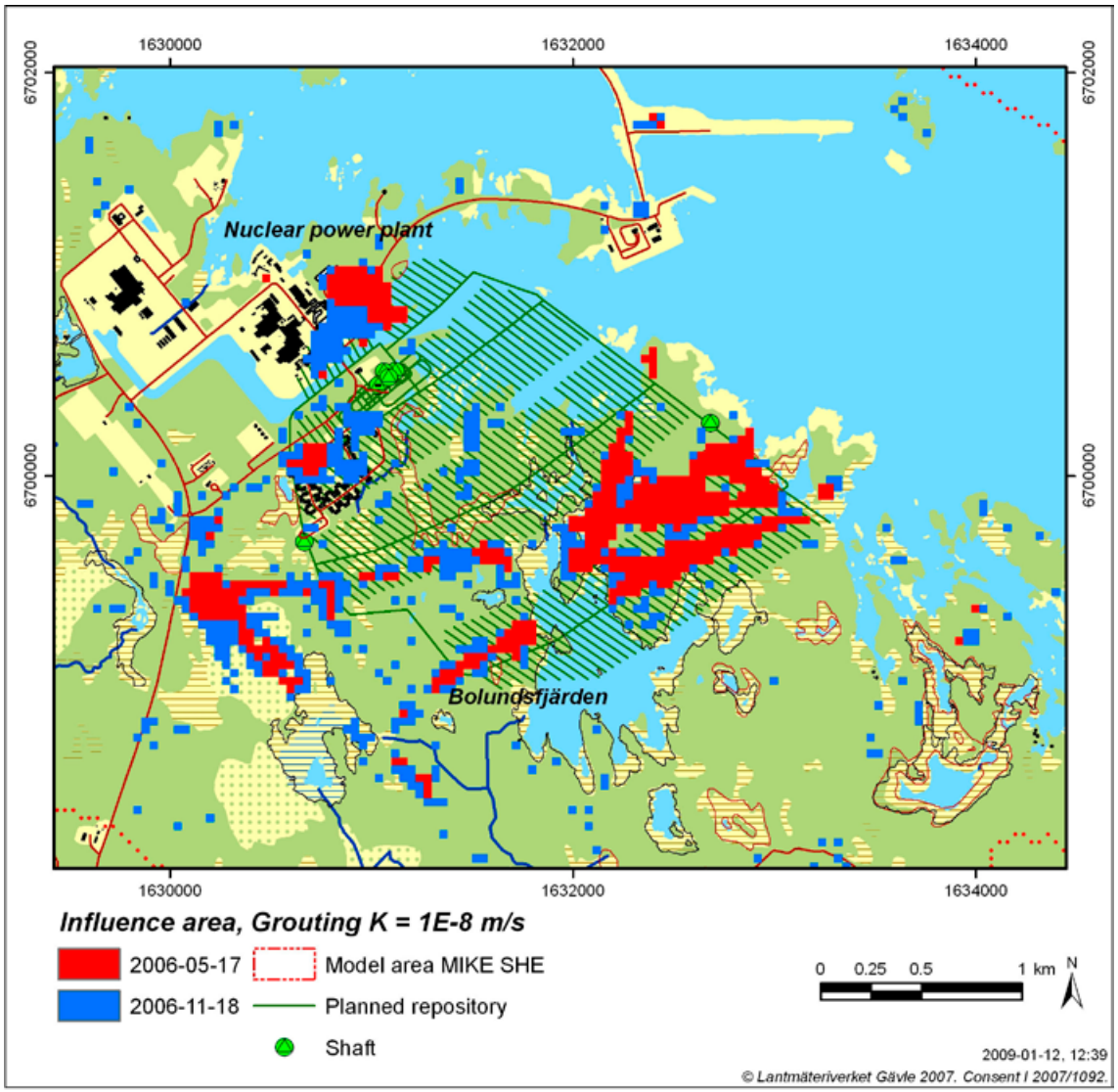

Figure 5-13. *Detailed view of the influence areas (with groundwater table drawdown larger than 0.3 m) on November 18th (red and blue areas) and May 17th (red areas), representing the maximum and minimum areas during 2006 for a grouting level of $K=1 \cdot 10^{-8}$ m/s.*

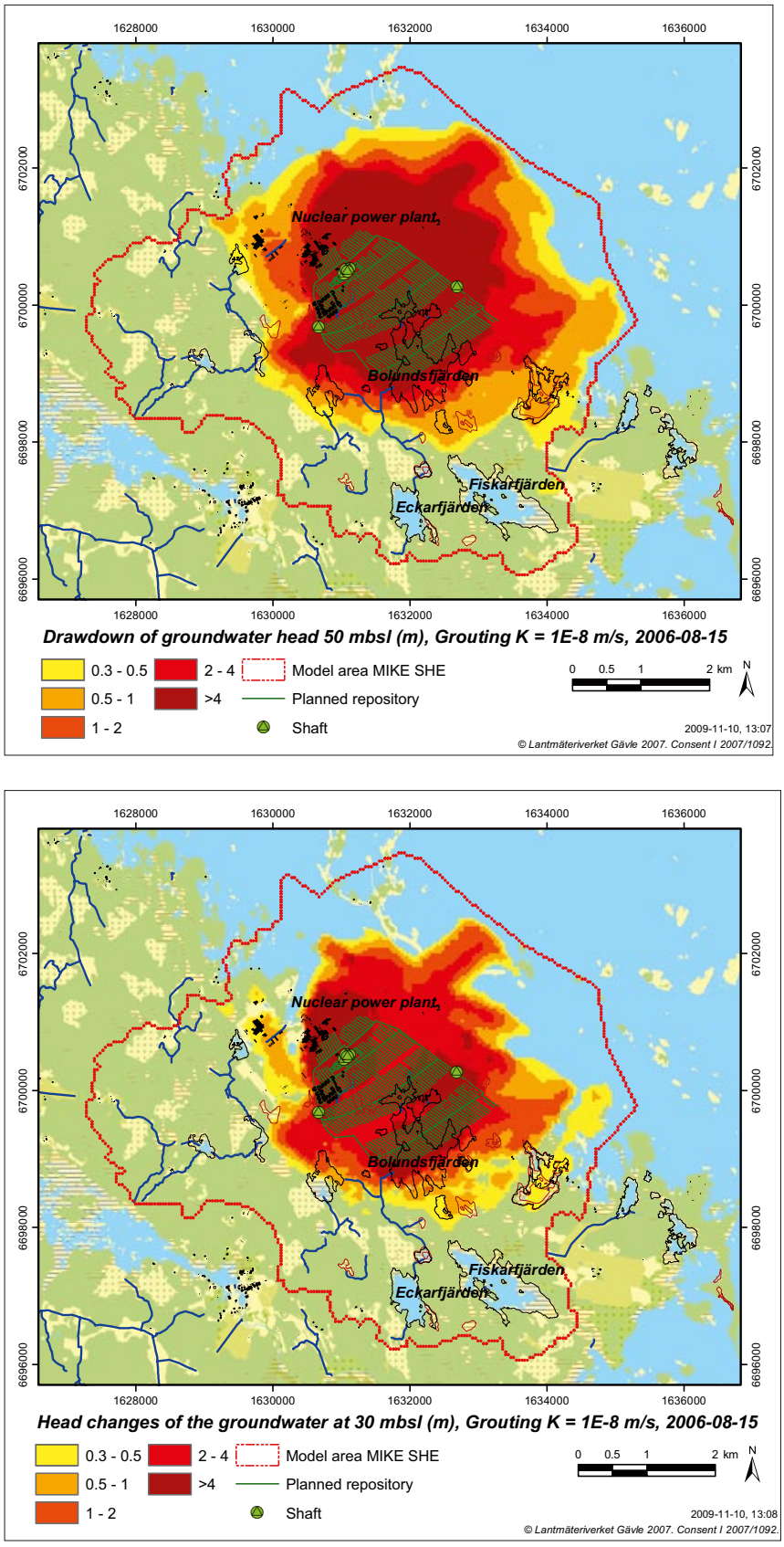

Figure 5-14. *Head changes of the groundwater at 50 m.b.s.l. (layer 5, upper map) and 30 m.b.s.l. (layer 4, lower map), on August 15th, 2006, and with a grouting level of $K=1\cdot10^{-8}$ m/s.*

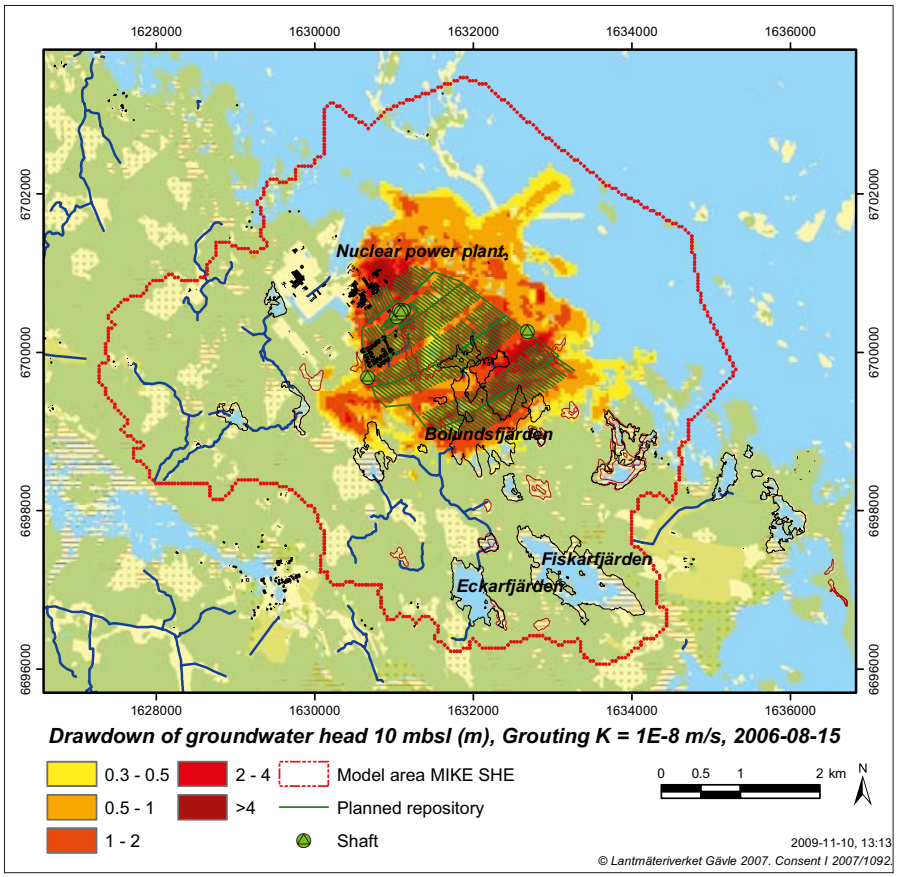

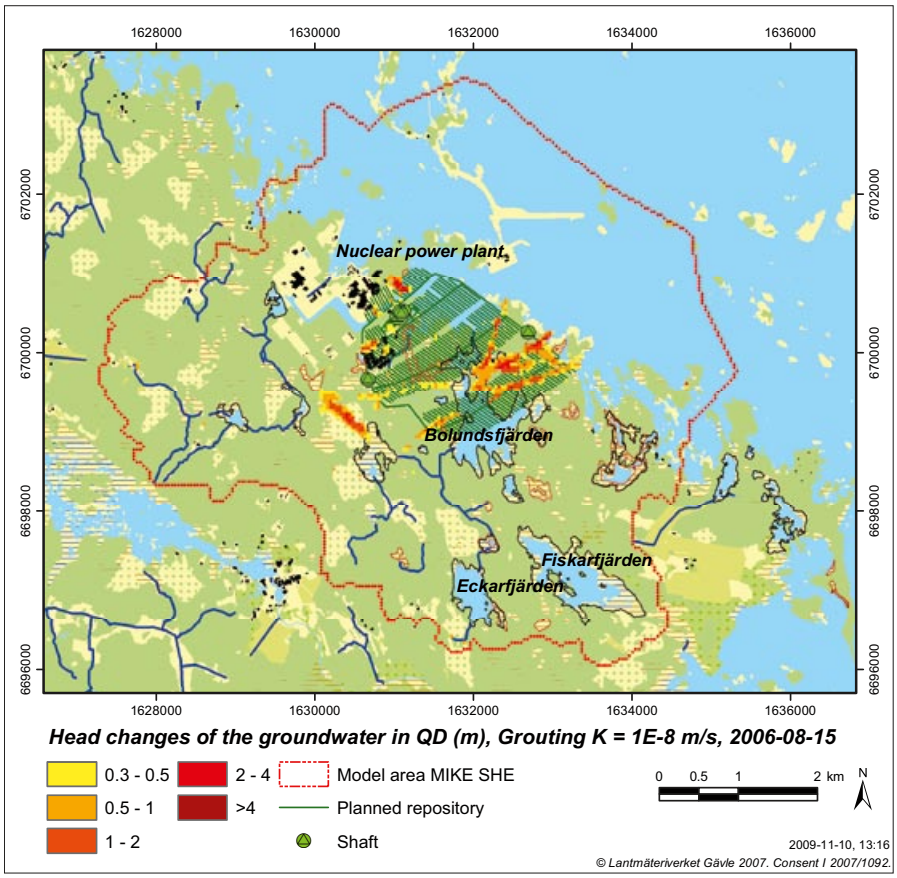

Figure 5-15. *Head changes of the groundwater at 10 m.b.s.l. (layer 3, upper map) and in the deep QD (layer 2, lower map), on August 15th, 2006, and with a grouting level of $K=1\cdot10^{-8}$ m/s.*

This is also clearly seen in Figure 5-16, where the groundwater head with an open repository is shown at different depths in two profiles through the catchment area and through the centre of the open repository; one from SW to NE and one from NW to SE.

The head changes at 50 m.b.s.l. and partly at 30 m.b.s.l. (Figure 5-14) reach the model boundary, and it seems like the open repository draws water from the sea boundary (defined as a head boundary equal to the time-varying sea level). However, the water balance including the repository shows a very small flow across the model boundary, with a small flow contribution to the repository inflow, only 4–5% of the total inflow according to Table 5-6 (Section 5.1). This can be explained by the rather low-conductive bedrock along the sea model boundary.

The influence areas at 50 m.b.s.l. and 30 m.b.s.l. are similar, with a head change of more than 1 m in most of the model area, although somewhat smaller at 30 m.b.s.l. In the uppermost bedrock at 10 m.b.s.l. however, the head change is much smaller, less than 1 m in most of the area, and the influence area has been further reduced. When reaching the QD, the influence area is completely changed, and now only appears along certain bands. The reason for this change can be found in the hydraulic conductivities of the bedrock, which are illustrated in Figure 5-17 and 5-18 where the horizontal and vertical conductivities are presented for a SW-NE profile through the area corresponding to the upper profile in Figure 5-16.

In Figure 5-17 the so-called sheet joints are clearly visible. They are horizontally high-permeable structures represented in three layers in the model, at 30 m.b.s.l. (layer 4), at 70 m.b.s.l. (layer 6) and at 110 m.b.s.l. (layer 8). These sheet joints spread the head changes efficiently over a relatively large area in the layers where the sheet joints are present. The horizontal representation of the sheet joints covers a relatively large area of the model, as illustrated in Figure 5-19, where the horizontal conductivity at 70 m.b.s.l. (layer 6) is shown. The sheet joints in layer 4 and layer 8 are located in approximately the same area, however not having exactly the same horizontal shape. For further details on the hydraulic conductivities and geological properties within the model area, see /Bosson et al. 2008/.

The horizontally high-permeable sheet joint areas are not present in the vertical conductivity distribution, see Figure 5-18. Instead, the main vertical groundwater flow occurs in the vertical fracture zones. Figure 5-20 shows the vertical conductivity at 50 m.b.s.l. (layer 5). The fracture zones appear clearly with vertical conductivities of up to $1 \cdot 10^{-6}$ m/s, compared to $1 \cdot 10^{-10}$ to $1 \cdot 10^{-9}$ m/s for the background bedrock. This has of course a strong influence on the pattern of vertical groundwater flow, as illustrated in Figure 5-21 where the vertical groundwater flow at 50 m.b.s.l. (layer 5) is shown for the reference simulation (i.e. without the repository). The high flows, both upward and downward, are found along the fracture zones.

The largest drawdown of the groundwater table is found in the area north-east of the power plant (Figure 5-12 and lower part of Figure 5-15). The drawdown of the groundwater table is here up to approximately 15 meter, which is seen in the lower profile in Figure 5-16 (at the length scale of approximately 1,900 meter). This is a consequence of the presence of a local vertical fracture zone in this area, with high vertical conductivities in the upper bedrock. This is clearly seen in Figure 5-20.

It is interesting to notice the downward flow in the centre of the area, although a discharge area would have been expected for a low-lying area close to the sea. This can be explained by the sheet joints connecting the land part with the underground offshore SFR facility. The hypothesis is that the inflow to the SFR keeps the groundwater head low in the sheet joints. This prevailing head change within the sheet joints, due to the SFR, gives a downward flow in the bedrock on the landside, even if the opposite would have been expected from the topographical conditions. The downward flow rather close to the sea model boundary, caused by the SFR, is also illustrated in Figure 5-21, which can be compared with the natural flow conditions without SFR shown in Figure 5-22. Although the effect from SFR reaches to the model boundary, the presented water balances for undisturbed conditions in Section 5.1 (e.g. Table 5-3) shows a very small flow across the model boundary. This is an effect of the rather low conductive bedrock along the sea model boundary.

The corresponding results, but with an open repository included (as well as SFR), are shown in Figure 5-23. Compared to Figure 5-21, without an open repository (but with SFR), the downward flows are now further strengthened above the repository, with most of the model area having a downward flow direction. This includes the area above the SFR, and it seems like the repository draws water from the sea boundary. However, the water balances including the repository show that this flow contribution is very small, only 4–5% of the total inflow according to Table 5-6 in Section 5.1.

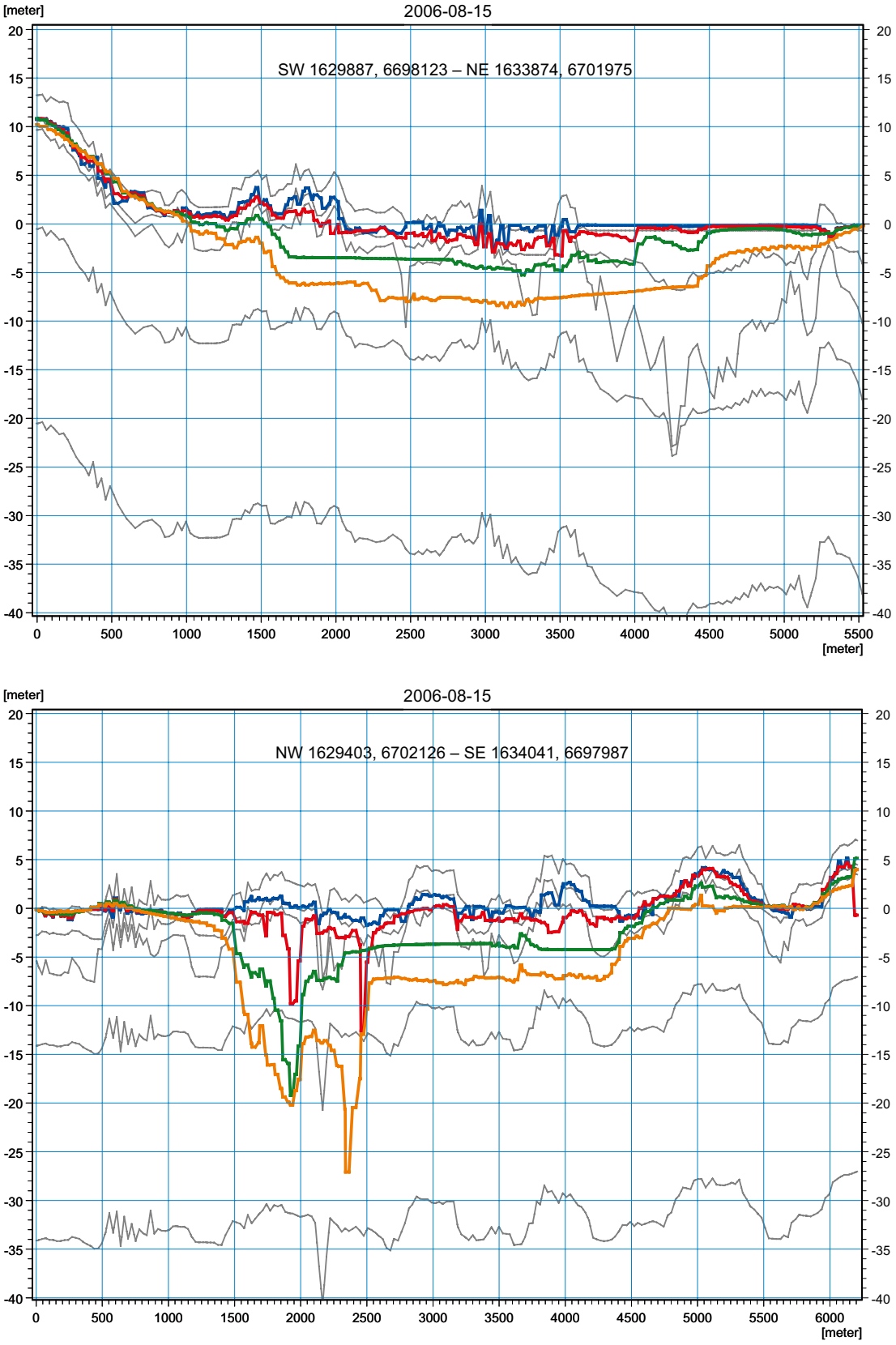

Figure 5-16. *Groundwater head elevations for different layers (coloured thick lines) in two profiles, based on an open repository with a grouting level of K=1·10^{-8} m/s; a profile SW-NE (upper) and NW-SE (lower) through the model area and the repository. The grey lines show the lower level of each calculation layer. The head elevations are from August 15th 2006. The blue line shows the head elevation in layer 2 (lower QD), the red line the head elevation in layer 3 (bedrock at 10 m.b.s.l.), the green line the head elevation in layer 4 (bedrock at 30 m.b.s.l.), and the orange line the head elevation in layer 5 (bedrock at 50 m.b.s.l.).*

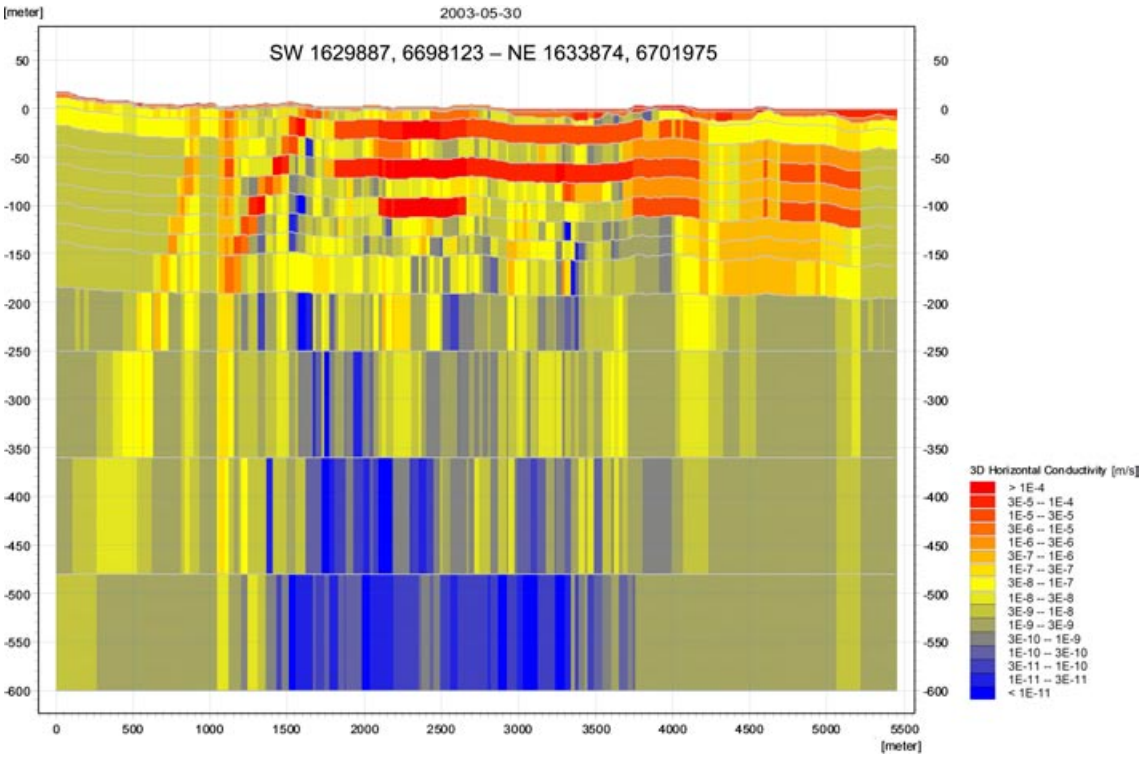

Figure 5-17. *Horizontal hydraulic conductivities (m/s) in a SW-NE section through the repository. Red colours show a high-permeable layer.*

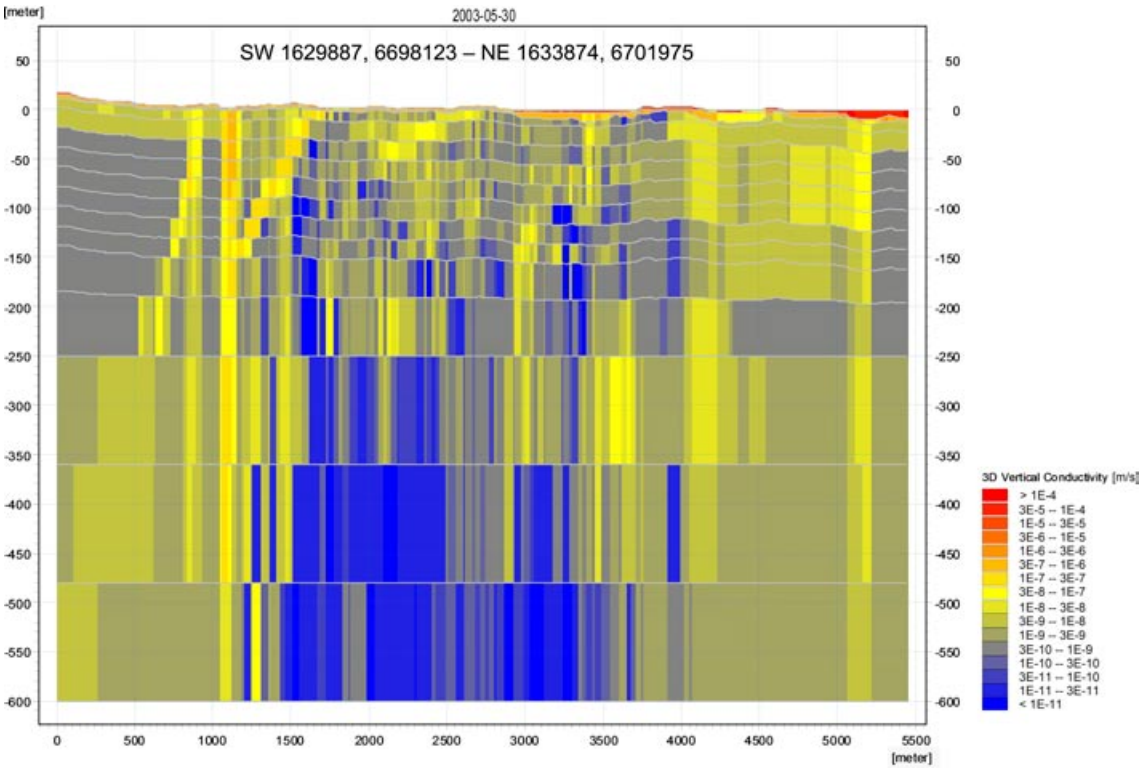

Figure 5-18. *Vertical hydraulic conductivities (m/s) in a SW-NE section through the repository. Red colours show a high-permeable layer. The sheet joints shown in the upper part of Figure 5-17 have only a minor influence in the vertical direction.*

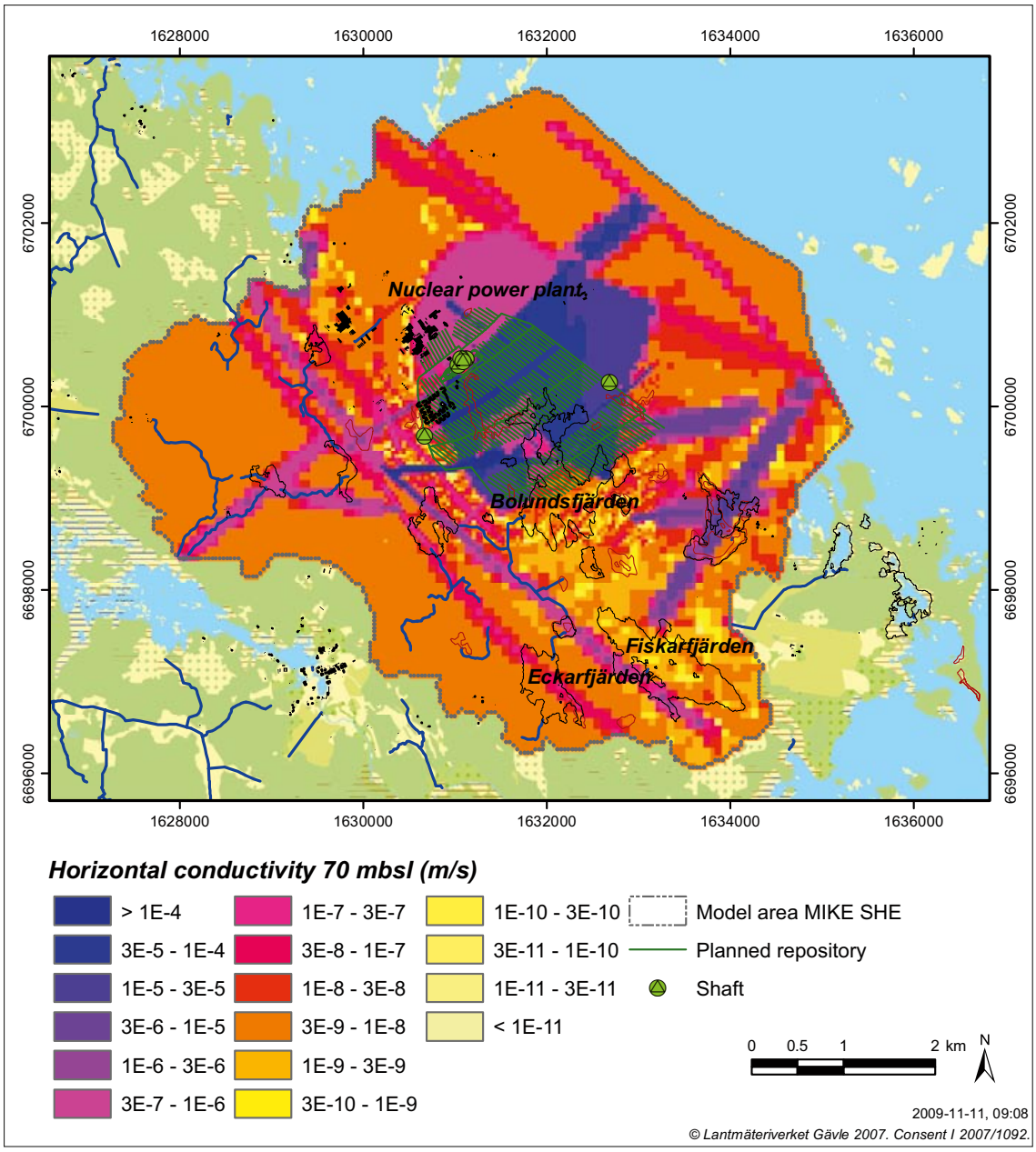

Figure 5-19. *Horizontal hydraulic conductivities (m/s) in the bedrock, calculation layer 6 (70 m.b.s.l). Blue and purple colours show high-permeable zones.*

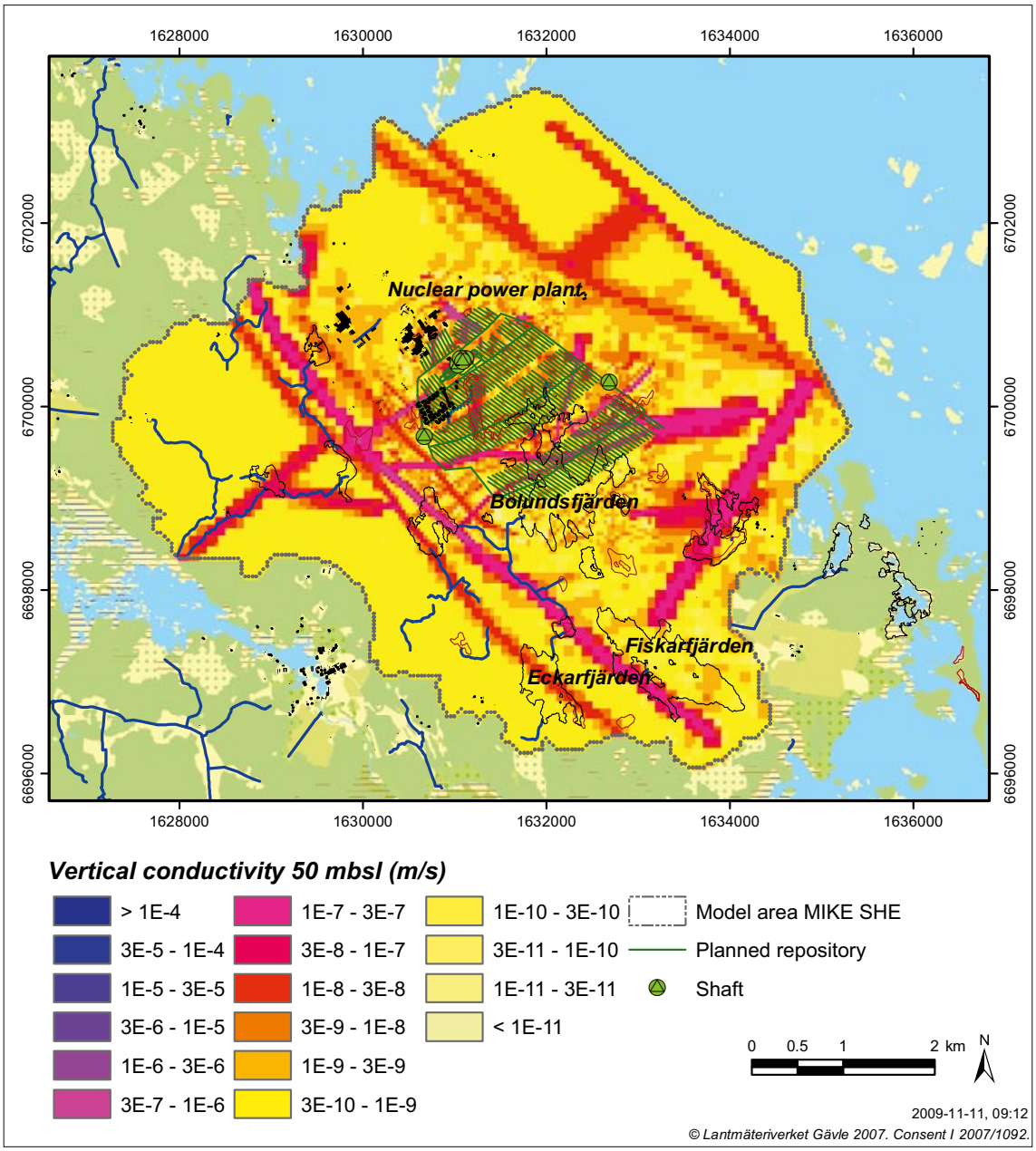

Figure 5-20. *Vertical conductivities (m/s) in the bedrock, calculation layer 5 (50 m.b.s.l.). Blue and purple colours show high-permeable zones.*

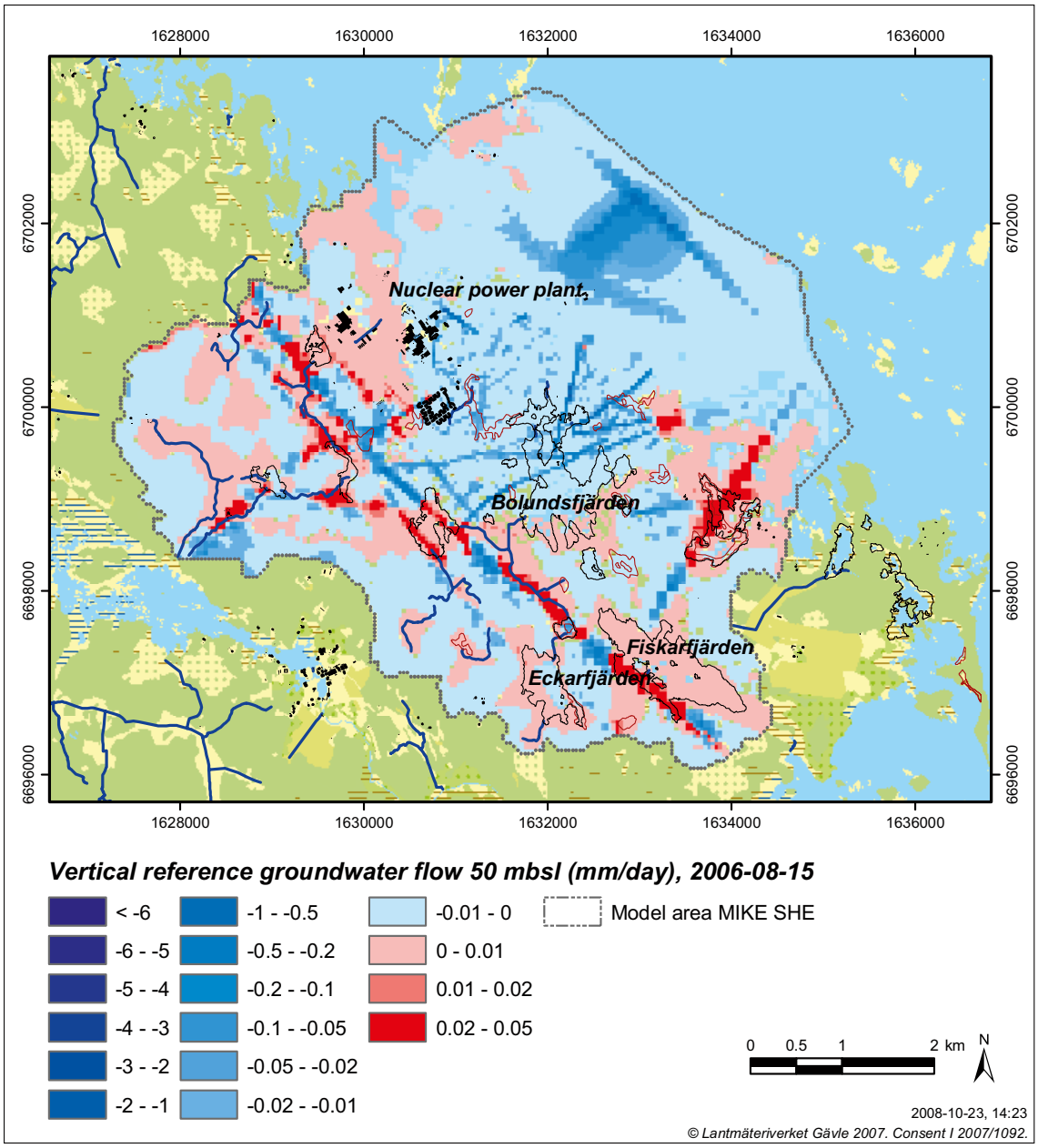

Figure 5-21. *Vertical groundwater flow (mm/day) in calculation layer 5 (50 m.b.s.l.), August 15th, 2006, based on the reference simulation without the repository but with SFR in the model. Blue colours indicate downward flow and red colours indicate upward flow.*

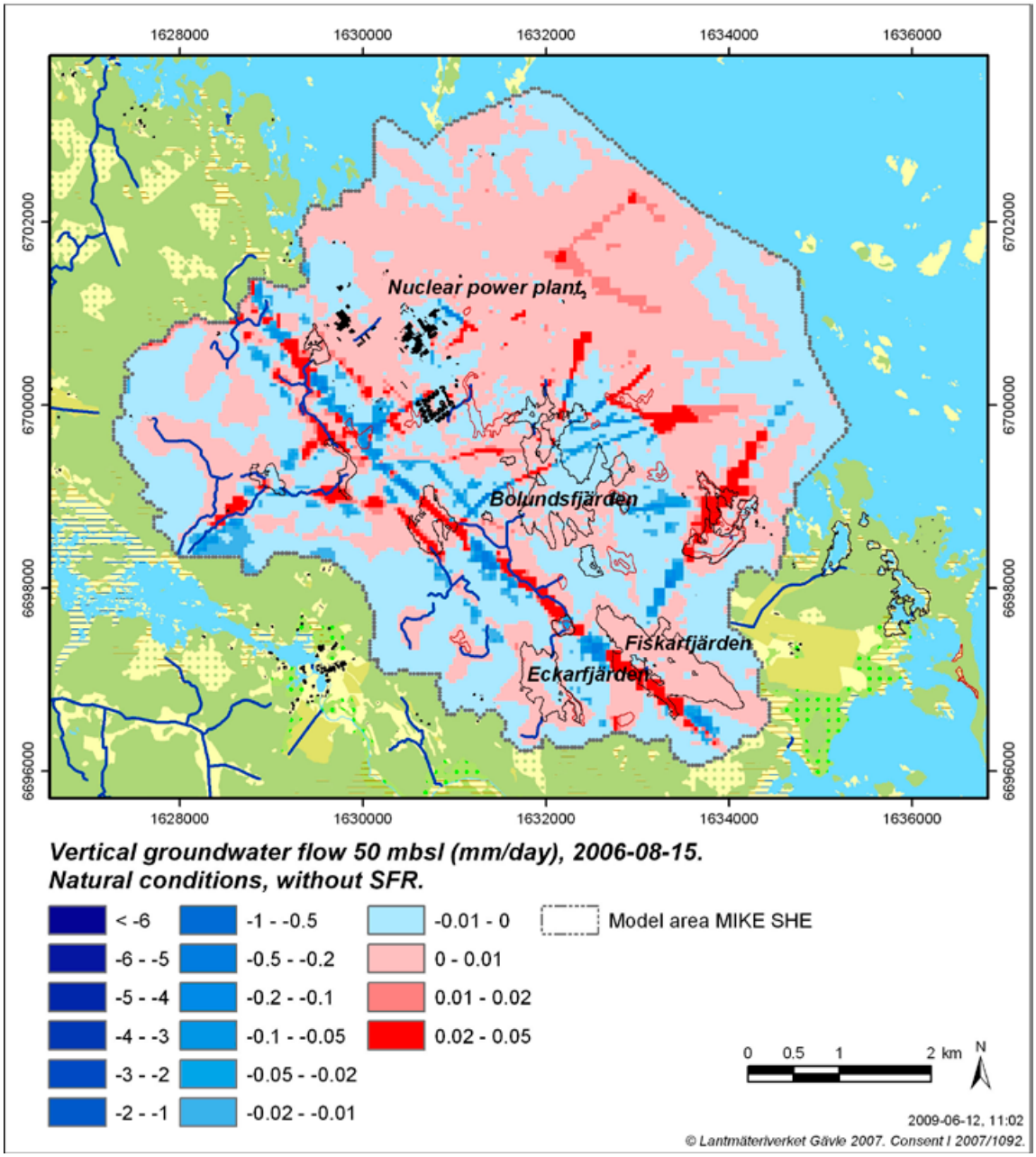

Figure 5-22. *Vertical groundwater flow (mm/day) in calculation layer 5 (50 m.b.s.l.), August 15th, 2006, based on a simulation without the repository and without SFR in the model. Blue colours indicate downward flow and red colours indicate upward flow.*

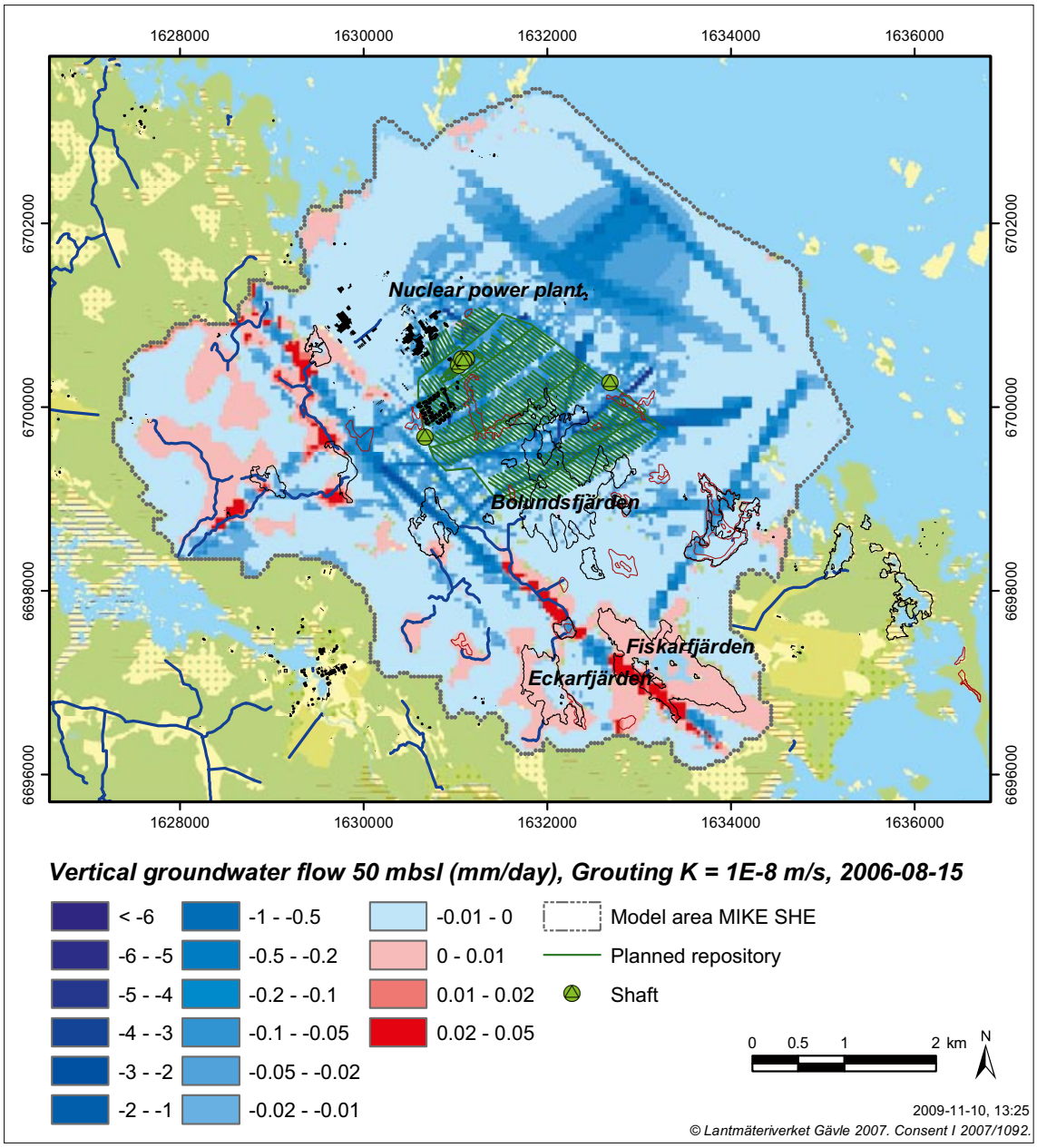

Figure 5-23. *Vertical groundwater flow (mm/day) in calculation layer 5 (50 m.b.s.l.), August 15th, 2006, based on a simulation with an open repository with a grouting level of $K=1{\cdot}10^{-8}$ m/s and with SFR in the model. Blue colours indicate downward flow and red colours indicate upward flow.*

All in all, it can be concluded that the vertical fracture zones connect the deep open repository with the upper bedrock, where the sheet joints are located. When the vertical groundwater flow in the fracture zones reaches a sheet joint, where the horizontal transmissivity is high, the head change is spread over a large area in the model. This holds up to the upper sheet joint at 30 m.b.s.l. (layer 4). The upper 20 m of the bedrock (layer 3) have according to the interpretation only vertical fracture zones /Follin et al. 2007/. This means that this layer acts as a barrier between the upper sheet joint layer and the QD, only having connectivity through the fracture zones. Because the transmissivity in the QD is relatively low, the head change in the QD is limited to the areas around the underlying vertical fracture zones.

5.4.3 Groundwater table drawdown for different levels of grouting

The level of grouting of the tunnels affects the drawdown of the groundwater table. Figures 5-24 to 5-26 show the average drawdown of the groundwater table during 2006 for the three levels of grouting that have been studied: $K=1\cdot10^{-7}$ m/s, $1\cdot10^{-8}$ m/s and $1\cdot10^{-9}$ m/s. The overall pattern of the influence area is the same for all of the three grouting levels. A grouting level of $K=1\cdot10^{-7}$ m/s obviously gives the largest influence area and drawdown around the repository and also the highest inflow to the tunnels and shafts (Section 5.2).

Table 5-13 shows a summary of the influence area and drawdown of the groundwater table for the different levels of grouting. A grouting level of $K=1\cdot10^{-7}$ m/s gives an influence area with a drawdown larger then 0.3 m that is three times larger than that for a grouting level of $K=1\cdot10^{-9}$ m/s, while it for a grouting level of $K=1\cdot10^{-8}$ m/s is two times larger. The influence areas for the three levels of grouting are shown together in Figure 5-27.

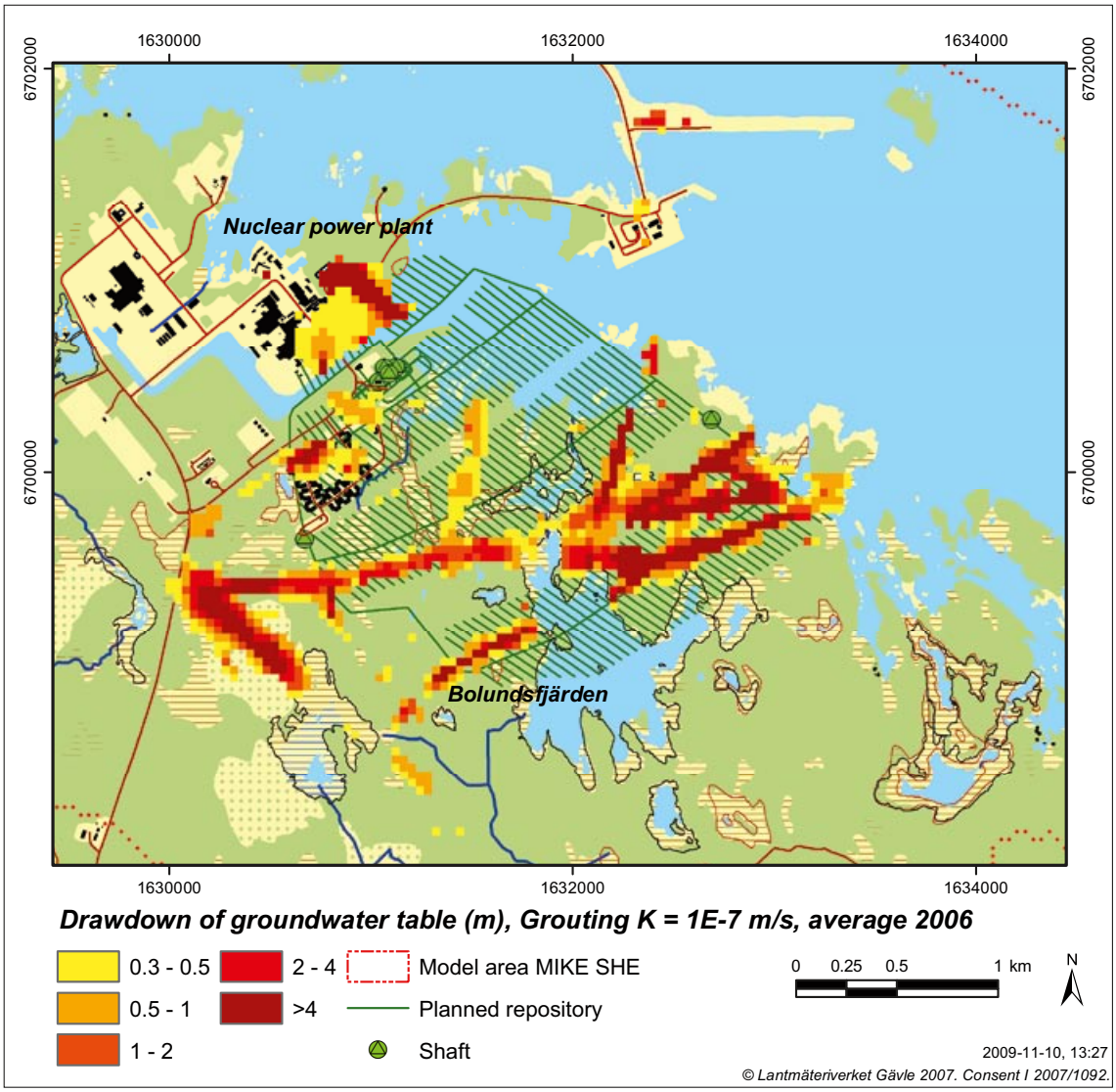

Figure 5-24. *Detailed view of the drawdown of the groundwater table calculated as an average for 2006 with a grouting level of $K=1\cdot10^{-7}$ m/s.*

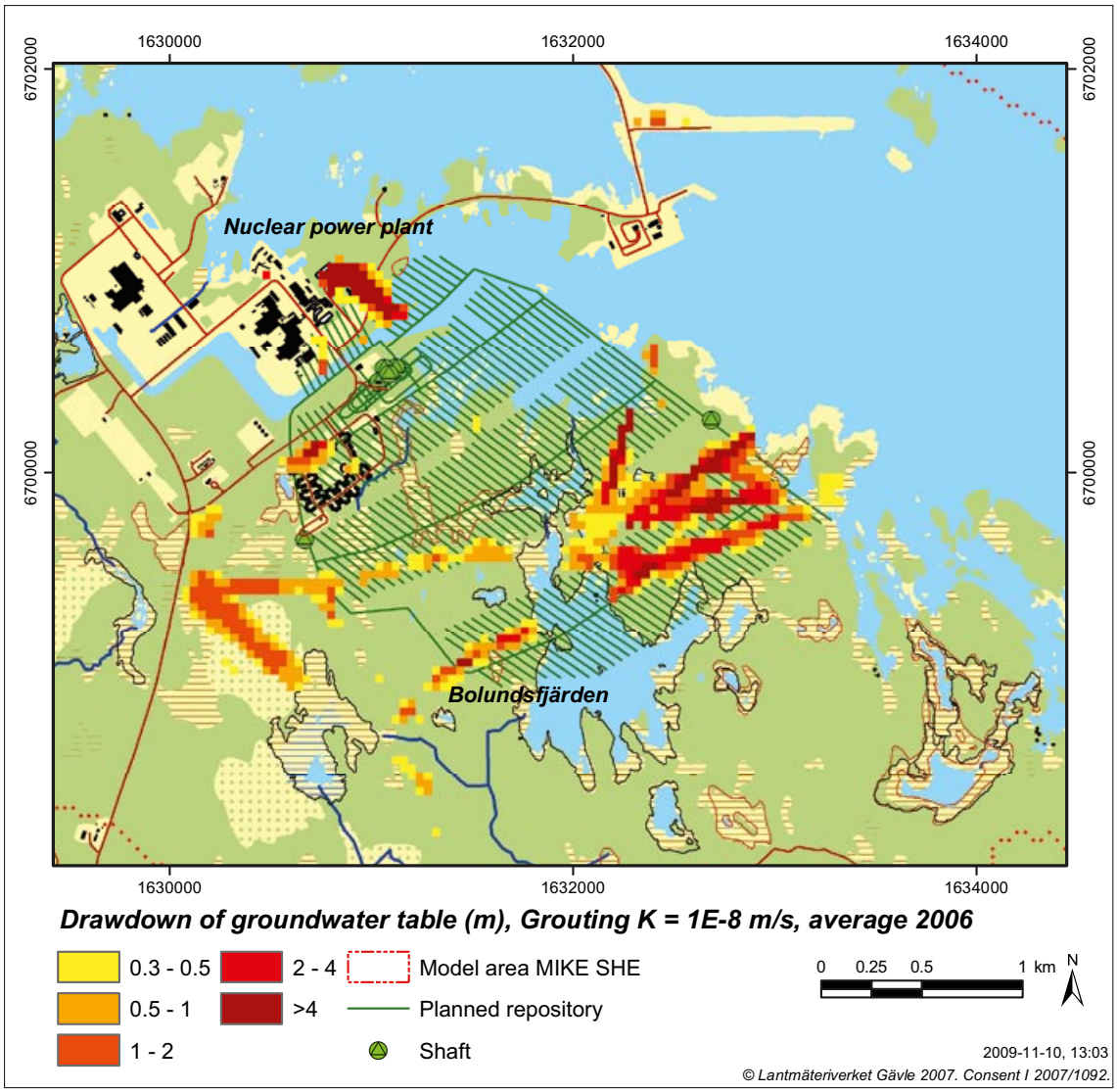

Figure 5-25. *Detailed view of the drawdown of the groundwater table calculated as an average for 2006 with a grouting level of $K=1\cdot10^{-8}$ m/s.*

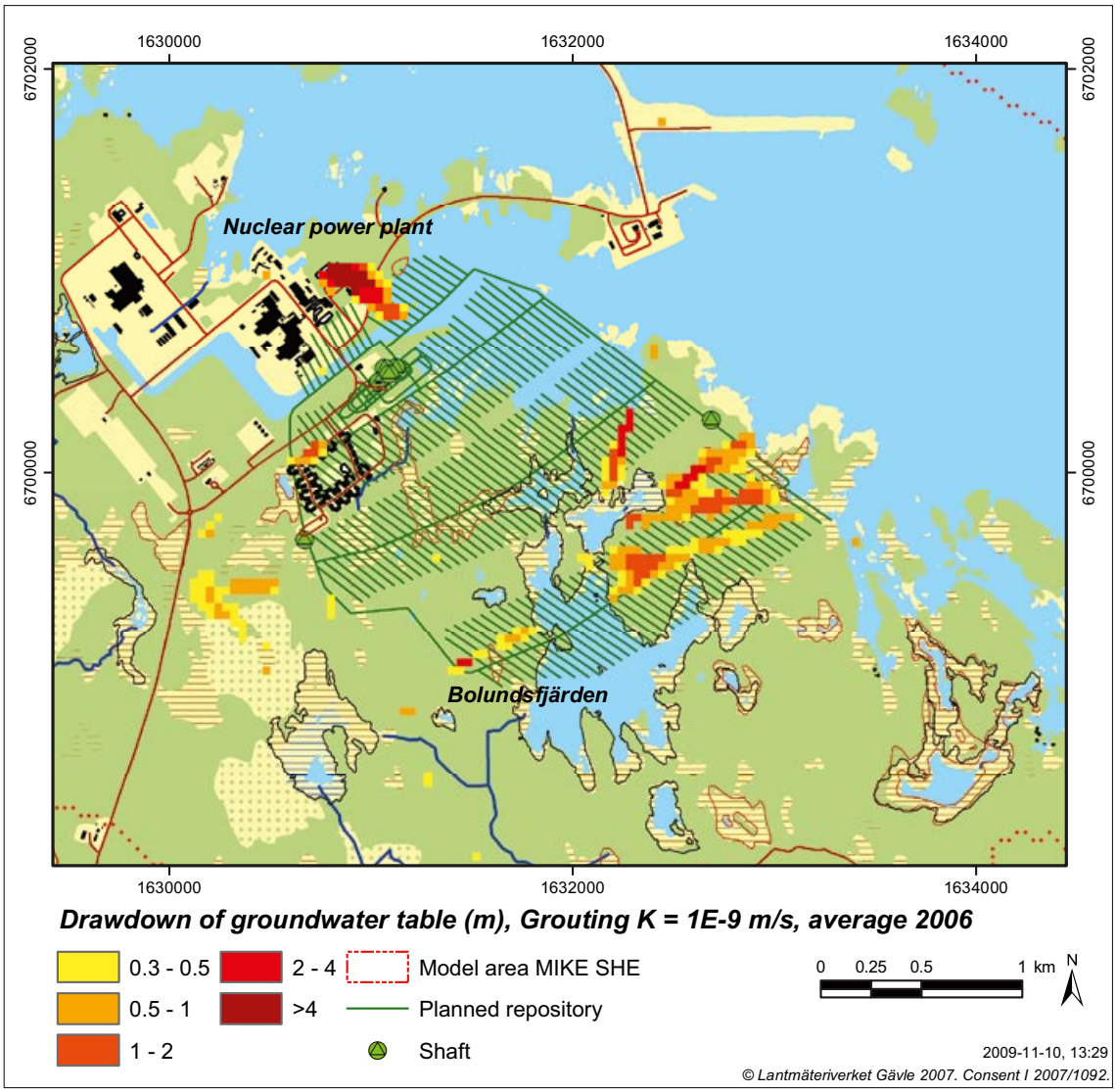

Figure 5-26. *Detailed view of the drawdown of the groundwater table calculated as an average for 2006 with a grouting level of $K=1{\cdot}10^{-9}$ m/s.*

Table 5-13. Influence areas (km²) with different limits for the groundwater table drawdown and for different levels of grouting of the full open repository. The areas are taken from the average drawdown during 2006.

Case	Maximum lowering of the water table, (m)	Influence area, drawdown >0.1 m	Influence area, drawdown >0.3 m	Influence area, drawdown >0.5 m	Influence area, drawdown >1 m	Influence area, drawdown >2m	Influence area, drawdown >4m
$K=1{\cdot}10^{-7}$ m/s,	47.6	2.96	1.57	1.13	0.75	0.56	0.39
$K=1{\cdot}10^{-8}$ m/s,	14.9	2.11	1.02	0.75	0.46	0.25	0.12
$K=1{\cdot}10^{-9}$ m/s,	4.5	1.30	0.49	0.32	0.14	0.06	0.02

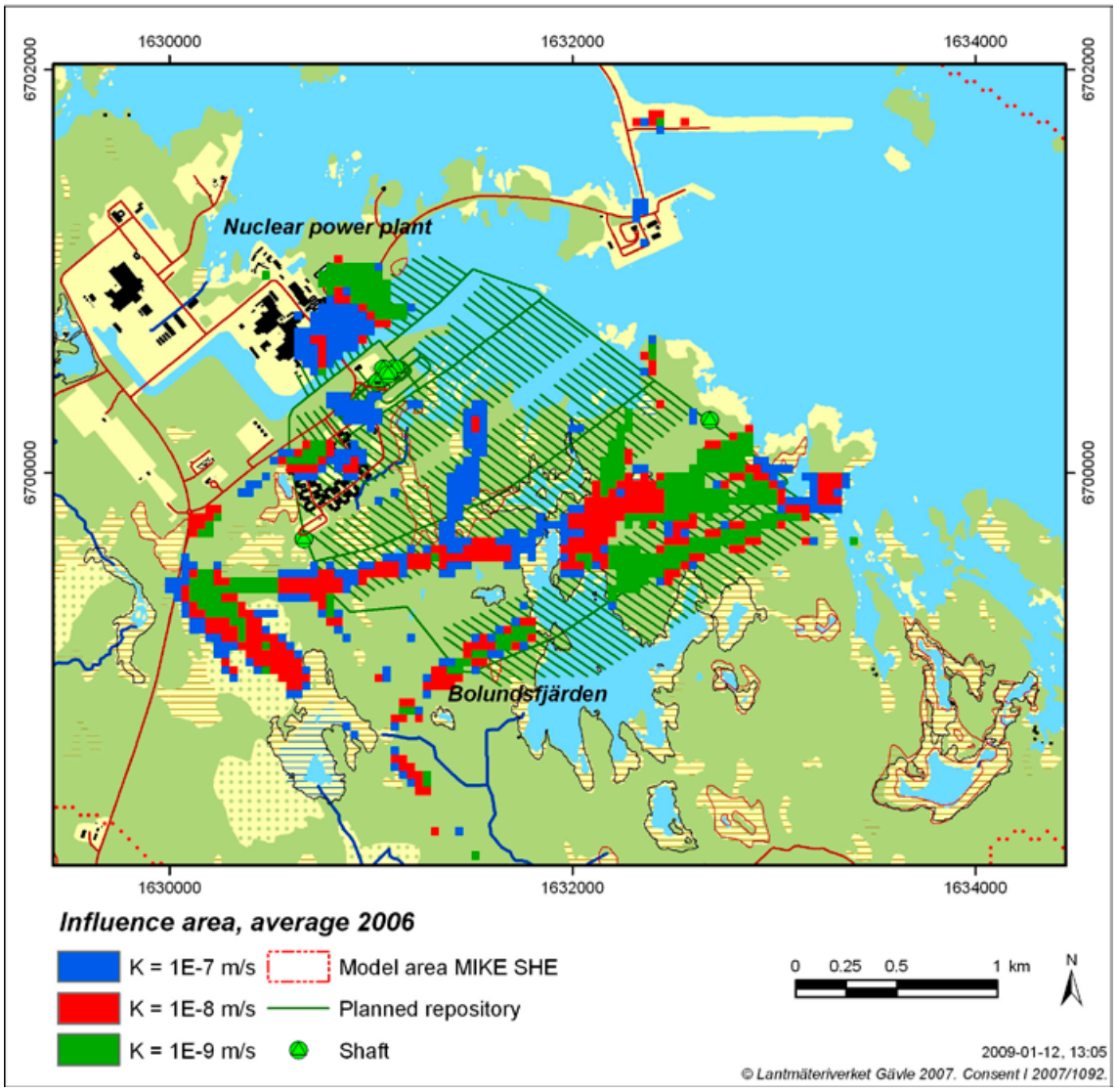

Figure 5-27. *Detailed view of the influence areas (defined as the areas with an average groundwater table drawdown larger than 0.3 m during 2006) for the three grouting levels $K=1\cdot10^{-7}$m/s (blue, red and green areas), $1\cdot10^{-8}$ m/s (red and green areas) and $1\cdot10^{-9}$m/s (green areas only).*

5.4.4 Groundwater table drawdown for different development phases

The whole open repository will not be constructed and taken in operation at once, but instead in three development phases called phase 1, phase 2 and phase 3. In all the different phases, the access tunnel and all of the transport tunnels will be open, but only one section with deposition tunnels will be open at a time (see Section 4.2 for details).

The drawdown of the groundwater table varies with the development phase of the repository construction. Figures 5-28 to 5-30 show the average drawdowns of the groundwater table during 2006 for the three development phases, all with a grouting level of $K=1\cdot10^{-8}$ m/s. The overall pattern of the influence area is the same for all three development phases. This means that it is not primarily specific parts/areas of the repository that cause the groundwater table drawdown, but rather the total length of tunnels, especially those located below or crossing high-conductive zones (see Figure 5-2, Section 5.2).

Table 5-14 shows a summary of the influence areas and groundwater table drawdowns for the different development phases compared to those for the full construction. For obvious reasons, the largest impact is reached if the whole repository is open at the same time, which is a hypothetical case that will not occur in reality. Out of the three phases, phase 3 gives the largest impact with an influence area for a drawdown larger than 0.3 m that is approximately 92% of that obtained for the full construction. Phase 1 gives the smallest impact, with approximately 68% of the influence area for the full construction.

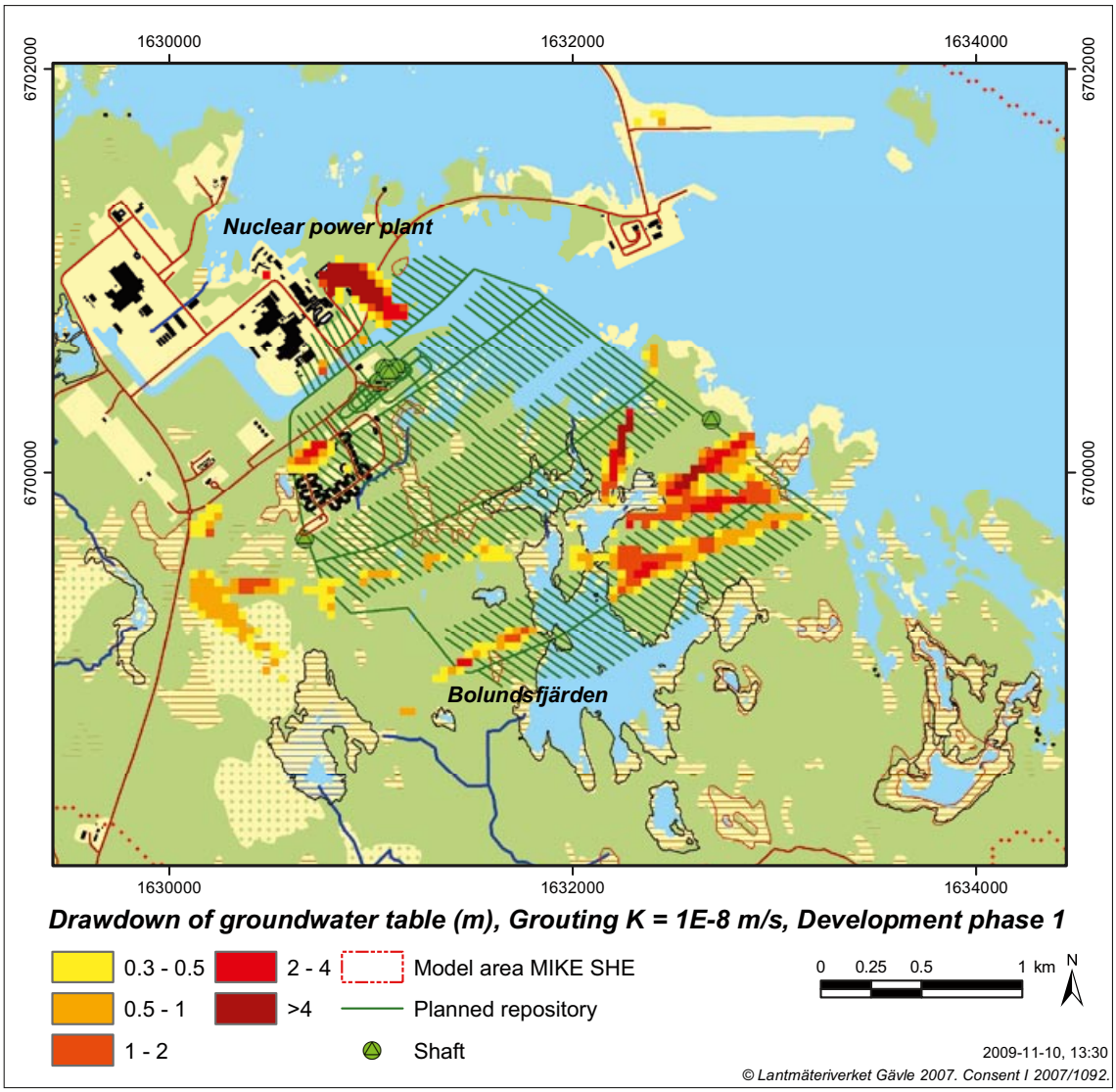

Figure 5-28. *Detailed view of the drawdown of the groundwater table during development phase 1, average for 2006, with a grouting level of $K=1{\cdot}10^{-8}$ m/s.*

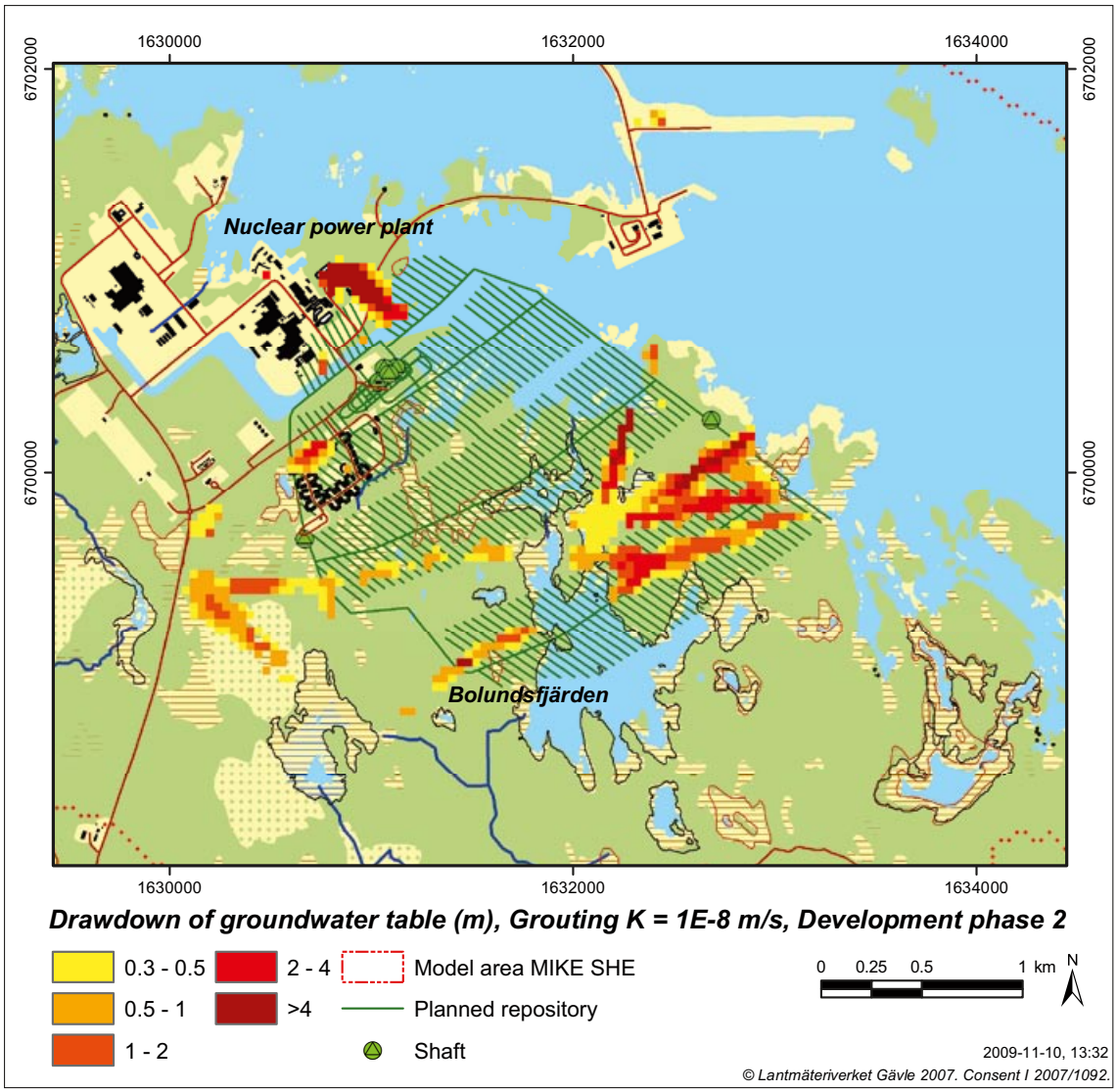

Figure 5-29. *Detailed view of the drawdown of the groundwater table during development phase 2, average for 2006, with a grouting level of $K=1{\cdot}10^{-8}$ m/s.*

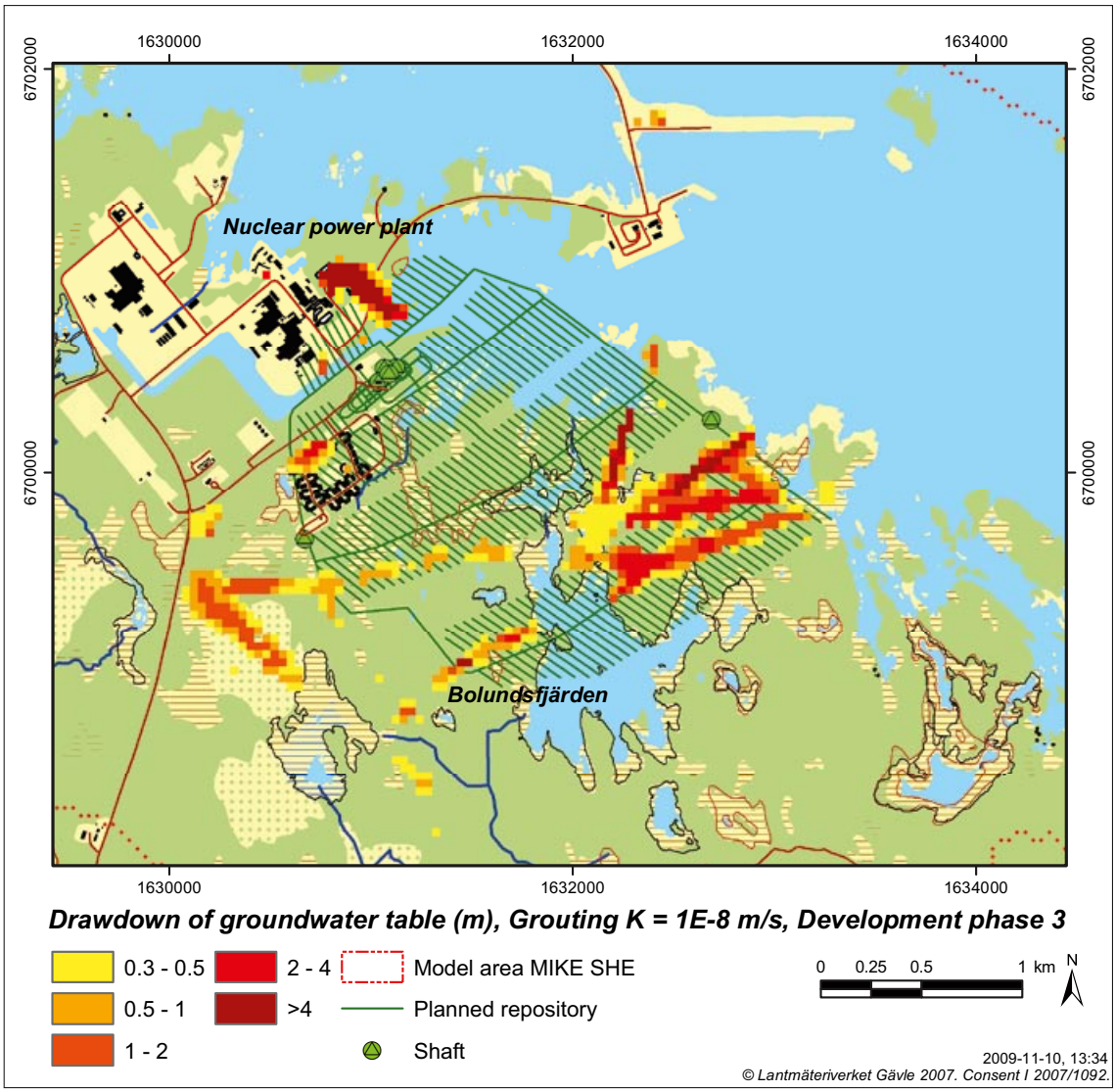

Figure 5-30. *Detailed view of the drawdown of the groundwater table during development phase 3, average for 2006, with a grouting level of K=1·10^{-8} m/s.*

Table 5-14. Influence areas (km^2) with different drawdowns of the groundwater table for different development phases and for a grouting level of K= 1·10^{-8} m/s. The areas are calculated from the average drawdown during 2006.

Case	Maximum lowering of the groundwater table, (m)	Influence area, draw-down >0.3 m	Influence area, draw-down >0.5 m	Influence area, draw-down >1 m	Influence area, draw-down >2 m	Influence area, draw-down >4 m
Phase 1	12.1	0.69	0.47	0.25	0.12	0.06
Phase 2	12.6	0.83	0.57	0.34	0.17	0.08
Phase 3	13.7	0.93	0.63	0.40	0.20	0.09
Full construction (hypothetical case)	14.9	1.02	0.75	0.46	0.25	0.12

5.4.5 Development of steady state groundwater table drawdown

The results presented in the previous sections are all based on a simulation period of two years, 2005 and 2006, where the year of 2005 has been used as an initialisation period. However, in reality the repository will be open for many decades, and the groundwater table drawdown will have time to be fully developed to steady state conditions (in reality, conditions will not be fully steady, since there are short-term temporal variations in the meteorological and hydrological conditions and variations in the extent of the repository during the different development phases). In practice, it would take too long time to simulate the full construction and operation period, so in order to save simulation time a rather short simulation period has been applied in most simulations (two years).

The drawback of this approach is the risk that the influence area and the drawdown are underestimated. In order to investigate this, simulations have been performed for an eight-year period with a fully open repository, and with a grouting level of $K= 1 \cdot 10^{-8}$ m/s. The input data for this simulation is a periodic cycling of the input data for 2005 and 2006, i.e. these years are repeated four times. All results presented are for the second years in the cycles, which are based on input data for 2006, in order to make them comparable to results presented in earlier sections. The results are summarised in Table 5-15.

The first line in Table 5-15, labelled 1st cycle, corresponds to the results presented in the previous sections. The second line in the table shows the result after another two-year cycle. The influence area in the second cycle is somewhat larger; it is approximately 13% larger for a groundwater table drawdown > 0.3 m. Already during the second cycle, steady-state conditions are more or less reached, with effectively no additional changes in the third and fourth cycles. The influence area after the third cycle is approximately 17% larger than after the first cycle, and after the fourth cycle approximately 18% larger. The influence area based on the first cycle is compared with the fourth cycle in Figure 5-31. The results for the two cycles show the same overall patterns, only the size differs slightly. This means that no new influence areas are developed in the fourth cycle compared to the first.

The temporal variation from the short term variations in the meteorology during a year is however much larger than the effect from the development of the groundwater table drawdown over several years. This is clearly seen in Table 5-16, where the minimum, maximum and average influence areas for different drawdown limits are presented. The maximum influence area is two to three times larger than the minimum influence area, depending on which drawdown limit is studied. The maximum and minimum influence areas are also presented in Figure 5-13 in Section 5.4.1, where this subject is further discussed.

5.4.6 Recovery of groundwater table after closure of the repository

When the operational phase of the open repository is finished, the pumping from the repository will cease and the repository will be closed. In order to evaluate how fast the drawdown of the groundwater table will recover, i.e. return to its normal undisturbed conditions, a simulation was done without tunnels and shafts, but initialised from the conditions with an open repository. This means that the open repository simply is replaced with the original bedrock, and that the initial conditions are given by the open repository simulation.

The initial conditions were taken from simulations with a grouting level of $K=1 \cdot 10^{-8}$ m/s, after the third two-year cycle according to Section 5.4.5. The simulation was done for a two-year period (using data from 2005–2006), and compared with the fourth two-year cycle from the reference simulation with undisturbed conditions, when calculating the drawdown of the groundwater table (see also Section 4.2, where all simulation cases are described).

In Table 5-17, the influence areas for different drawdown limits are presented for different times after repository closure. The results show that the size of the influence area decreases rather quickly in the beginning. After half a year, the influence area is approximately one third of the size compared to the same part of the year in a simulation with an open repository (columns 1 and 2 in the table). One year after repository closure, the influence area is reduced to less than 5% of the influence area with an open repository, concentrated to an area of c 0.06 km^2 north-east of Lake Bolundsfjärden, rather close to the coast line. A full recovery is estimated to take approximately one and a half year.

Table 5-15. Influence areas (km²) after different lengths of simulation periods with a grouting level of K= 1·10⁻⁸ m/s. The results are taken from the average groundwater table drawdown during 2006, after different numbers of cycles of the years 2005–2006.

	Influence area, drawdown >0.3 m	Influence area, drawdown >0.5 m	Influence area, drawdown >1 m
Average 2006, 1st cycle	1.02	0.75	0.46
Average 2006, 2nd cycle	1.15	0.92	0.63
Average 2006, 3rd cycle	1.19	0.93	0.65
Average 2006, 4th cycle	1.20	0.93	0.65

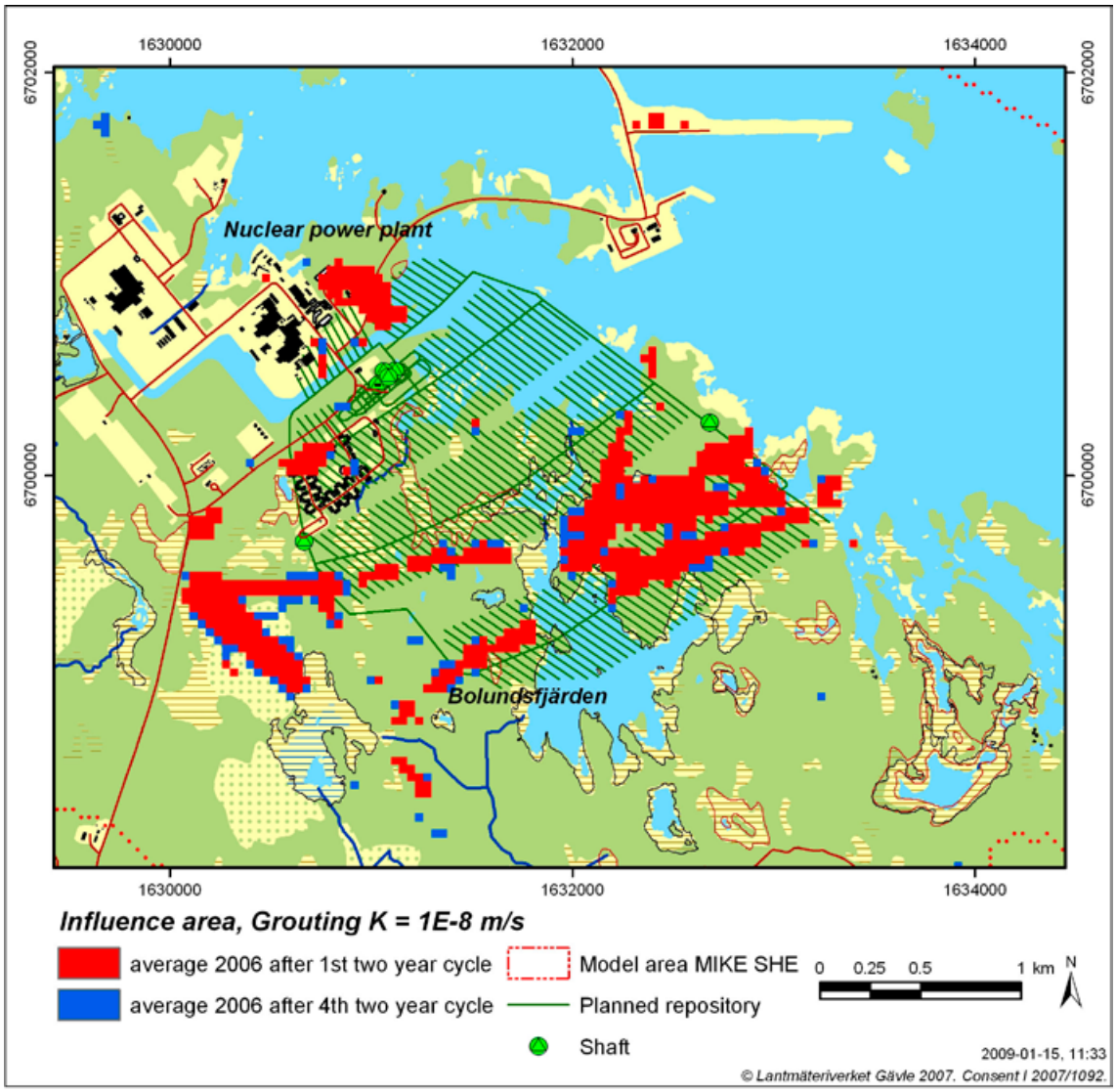

Figure 5-31. *The influence areas (defined as the areas with an average groundwater table drawdown larger than 0.3 m during 2006) after the first two-year cycle (red areas) compared with the fourth two-year cycle (red and blue areas), with a grouting level of K=1·10⁻⁸ m/s.*

Table 5-16. Minimum, maximum and average influence areas (km^2) during 2006, 1st cycle, with a grouting level of K= $1 \cdot 10^{-8}$ m/s.

	Influence area, drawdown >0.3 m	Influence area, drawdown >0.5 m	Influence area, drawdown >1 m
Average 2006, 1st cycle	1.02	0.75	0.46
Maximum 2006, 1st cycle	1.81	1.42	0.70
Minimum 2006, 1st cycle	0.75	0.51	0.28

Table 5-17. Influence areas (km^2) at different times after closure of the repository, starting from conditions with a grouting level of K= $1 \cdot 10^{-8}$ m/s (right side), compared to the influence area for an open repository (same grouting level), for each month during 2006 (left side).

Simulation with an open repository		Simulation of recovery after closure	
Date from 2006	Influence area, drawdown >0.3 m	Days after closure, January 1st 2005	Influence area, drawdown >0.3 m
January 17th 2006	1.46	10	1.30 (89%)
February 16th 2006	1.52	40	1.02 (67%)
March 18th 2006	1.22	70	0.60 (49%)
April 17th 2006	1.73	100	0.49 (28%)
May 17th 2006	0.75	130	0.39 (52%)
June 16th 2006	0.79	160	0.39 (49%)
July 16th 2006	0.80	190	0.25 (31%)
August 15th 2006	0.91	220	0.30 (33%)
September 14th 2006	1.05	250	0.20 (19%)
October 14th 2006	1.28	280	0.16 (13%)
November 18th 2006	1.81	315	0.21 (12%)
December 18th 2006	1.78	345	0.10 (6%)
January 17th 2006	1.46	375	0.06 (4%)

Observe that the results above show how fast the drawdown of the groundwater table will recover, i.e. how long it will take for the groundwater table to return to its normal undisturbed elevation. The results do not show how long time it takes to recover the groundwater head in the bedrock at the repository depth, neither how long it will take until the head inside the tunnels is the same as in the surrounding bedrock. The recovery of heads in the repository takes longer time than the time required for recovery of the groundwater table. Detailed modelling of the groundwater head recovery is performed by SKB using the DarcyTools code. The results will be presented as a part of the SR-Site safety assessment.

6 Sensitivity analysis for open repository conditions

The third and final step in the modelling process was to analyse the sensitivity of the model to the properties of the upper bedrock and the properties of the interface between the Quaternary deposits and the bedrock, with respect to the effects of an open repository. Also, the importance of the sediments under the sea, the lakes and the wetland areas was analysed in the sensitivity analysis (Section 6.1 and 6.2). Finally, the applied method for calculating the inflow to the open repository with MOUSE SHE has been compared to the analytical solution, by comparing calculated inflow to a tunnel with the two methods (Section 6.3).

6.1 Definition of simulation cases

Nine different sensitivity cases have been studied for open repository conditions and compared with corresponding cases without a repository. The sensitivity cases are all based on changes of the hydraulic properties of the bedrock or the interface between QD and bedrock. The nine cases are summarised in Table 6-1. The reference model is the updated version of the MIKE SHE SDM-Site Forsmark model (Chapter 3).

During the calibration of the MIKE SHE SDM-Site Forsmark model /Bosson et al. 2008/, a number of changes in the hydraulic properties of the bedrock were made, as compared to the original dataset delivered from the hydrogeological modelling performed using the ConnectFlow (CF) tool /Follin et al. 2007/. The delivered data set from ConnectFlow originates from the CF simulation case referred to as

SDM23_HCD2h100A2b_HRD5r1_phi4F_HSD5d_IC3Mat_MD2_MOW18

In the following text this is referred to as “the original bedrock model”. The differences between the original bedrock model and the bedrock model used in the MIKE SHE model described in /Bosson et al. 2008/ are:

- The horizontal conductivity in the sheet joints was increased with a factor of 10 (i.e. within the area where the sheet joints are present only).
- The vertical conductivity in the upper 200 m of the bedrock was decreased with a factor of 10 (in the whole model area).

These changes were included in order to optimize the model performance compared to observed data on groundwater elevations in the QD and the bedrock, as well as observed data from pumping tests.

The significance of these changes for the open repository results are of interest to quantify, which explains the first three sensitivity cases in Table 6-1 (*BRO-H*, *BRO-V*, and *BRO-HV*). In these cases the bedrock conductivities are reset to those in the original bedrock model in three different ways: only the horizontal conductivity is reset (i.e. decreased), only the vertical conductivity is reset (i.e. increased), or both conductivities are reset to the values in the original bedrock model.

The hydraulic properties of the upper 20 m of the bedrock and the properties of the interface between the QD and the bedrock seem to be very important for the head changes due to the open repository in the deeper bedrock, and how they are spread and reflected on the groundwater table in the QD (see Section 5.4.2). This hypothesis is the background to the next six sensitivity cases. Two of these deal with the conductivity in the QD/bedrock interface layer (*Z6-low* and *Z6-high*), and the other four with the conductivity of the upper 20 m of the bedrock: two with the horizontal (*BR1-H-high* and *BR1-SJ*) and two with the vertical conductivity (*BR1-V-low* and *BR1-V-high*).

The low-permeable sediment layers under the lakes in the model can be expected to have a strong influence on lake-water levels, and to prevent a lowering of the water level in the lakes. It is therefore of interest to evaluate whether the above-mentioned assumption is correct or not. Likewise, the importance of the sediments under the sea is also of interest to analyse, especially with respect

Table 6-1. Definition of simulation cases in the sensitivity analysis. Changes are compared to the reference model (i.e. the updated version of the MIKE SHE SDM-Site Forsmark model).

Name of the simulation case	Short description	Changes for conductivity in the interface layer Z6	Changes for horizontal conductivity in the bedrock	Changes for vertical conductivity in the bedrock
BRO-HV	Original bedrock model	-	Kh / 10 in sheet joints	Kv × 10 in upper 200 m
BRO-H	Original bedrock model with regard to horizontal conductivity	-	Kh / 10 in sheet joints	-
BRO-V	Original bedrock model with regard to vertical conductivity	-	-	Kv × 10 in upper 200 m
Z6-low	Less permeable interface layer	K / 20	-	-
Z6-high	More permeable interface layer	K × 10	-	-
BR1-SJ	Sheet joints also in upper 20 m of bedrock	-	Upper sheet joint extended to top of bedrock	-
BR1-H-high	Increased horizontal conductivity in upper 20 m of bedrock	-	Kh × 10 in upper 20 m	-
BR1-V-low	Decreased vertical conductivity in upper 20 m of bedrock	-	-	Kv / 10 in upper 20 m
BR1-V-high	Increased vertical conductivity in upper 20 m of bedrock	-	-	Kv x 10 in upper 20 m
S0	No sediments	-	-	-

to the inflow to the repository. The last sensitivity case (*S0*), where the sea, lake and wetland sediments simply are removed from the model and replaced by the underlying geological materials, is motivated by the need to study the role of sediments.

The names of the simulation cases are based on the following abbreviations: BRO = original bedrock, -H = horizontal conductivity, -V = vertical conductivity, Z6 = the QD/bedrock interface layer, -low = lower conductivity, -high = higher conductivity, BR1 = upper (first) bedrock layer, SJ = sheet joint properties included, S0 = no sediments.

In all cases, the period 2005 to 2006 is simulated (in accordance with Section 3.1.2). All of the sensitivity cases are modelled for both undisturbed conditions and for open repository conditions, in order to enable calculations of drawdowns and influence areas. The open repository conditions have been simulated with a grouting level of $K = 1 \cdot 10^{-8}$ m/s only.

6.2 Results from the sensitivity analysis

6.2.1 Parameters in the evaluation

The simulation results from the different sensitivity cases have been analysed with respect to the inflow to the open repository, the impact on the surface water system, and the drawdown of the groundwater table. The results are summarised in Table 6-2, where evaluation key numbers according to the list below are calculated and tabulated. The names of the key parameters are based on the following abbreviations: OR = Open Repository, Q = Discharge, H = Water level, S = Surface water, G = Groundwater.

In order to estimate how realistic the changes in the hydraulic properties in a certain sensitivity case are, the deviations between observed data and simulated undisturbed conditions are analysed as well; the results are shown in Table 6-2. The names of these deviation key numbers are based on the following abbreviations: R = Correlation coefficient between observed and simulated values, ME = Mean error between observed and simulated values, MAE = Mean absolute error between observed and simulated values, PFM = Surface water discharge monitoring station, SFM = Groundwater monitoring well in QD, HFM = Groundwater monitoring well (percussion borehole) in bedrock.

The upper part of Table 6-2 shows the influence of the open repository. The lower part of Table 6-2 shows how reasonable the changes in hydraulic properties are, by comparing the simulated undisturbed conditions with observed data. The numbers that differs the most from the reference case are highlighted in Table 6-2.

Table 6-2. Summary of results for key parameters defined in the text for the different sensitivity cases. Highlighted numbers are those that differ the most from the corresponding reference cases.

Key number	Reference	BRO-HV	BRO-H	BRO-V	Z6-low	Z6-high	BR1-SJ	BR1-H-high	BR1-V-low	BR1-V-high	S0
OR Q (L/s)	20.7	25.6	20.2	26.2	20.7	20.7	20.8	20.8	19.7	20.9	20.7
OR G 0.3 (km²)	1.02	1.58	0.96	1.67	1.02	1.09	1.07	1.00	0.63	1.15	1.02
OR G 1.0 (km²)	0.46	0.65	0.37	0.62	0.46	0.46	0.46	0.41	0.21	0.48	0.46
OR S dH (m)	0.009	0.011	0.009	0.015	0.009	0.010	0.011	0.010	0.008	0.011	0.009
OR S dQ (%)	–7	–3	–6	–5	–7	–7	–7	–8	–8	–7	–7
R PFM S (-)	0.75	0.76	0.75	0.76	0.65	0.75	0.75	0.76	0.75	0.76	0.75
ME SFM S (m)	0.03	0.02	0.03	0.02	0.02	0.02	0.03	0.02	0.03	0.02	0.03
MAE SFM S (m)	0.06	0.06	0.06	0.07	0.07	0.06	0.06	0.06	0.07	0.06	0.06
ME SFM G (m)	0.02	0.01	0.02	0.00	0.00	0.03	0.02	–0.01	0.00	0.03	0.02
MAE SFM G (m)	0.26	0.25	0.26	0.24	0.24	0.25	0.26	0.26	0.24	0.25	0.26
ME HFM G (m)	–0.09	–0.74	–0.54	–0.02	–0.02	–0.09	–0.05	–0.06	–0.02	–0.19	–0.08
MAE HFM G (m)	0.42	0.75	0.58	0.42	0.42	0.42	0.41	0.42	0.42	0.43	0.42

- OR Q: Total inflow to the open repository tunnels, including access tunnels, transport tunnels and deposition tunnels (excluding shafts), annual average for 2006.
- OR G 0.3: Influence area with drawdown of groundwater table larger than 0.3 m due to the open repository, annual average for 2006. In the text below, this is generally what is referred to as the influence area.
- OR G 1.0: Influence area with drawdown of groundwater table larger than 1.0 m due to the open repository, annual average for 2006.
- OR S dH: Drawdown of surface water level in Lake Bolundsfjärden due to the open repository, annual average for 2006.
- OR S dQ: Relative change in surface water discharge between undisturbed and open repository conditions upstream Lake Bolundsfjärden, annual average for 2006.
- R PFM S: Average correlation coefficient (between observed and simulated flows) for the four surface water discharge monitoring stations, undisturbed conditions 2005–2006.
- ME SFM S: Average mean error (between observed and simulated levels) for the four surface water level monitoring stations, undisturbed conditions 2005–2006.
- MAE SFM S :Average mean absolute error (between observed and simulated levels) for the four surface water level monitoring stations, undisturbed conditions 2005–2006.
- ME SFM G: Average mean error (between observed and simulated levels) for the SFM groundwater monitoring wells, undisturbed conditions 2005–2006.
- MAE SFM G: Average mean absolute error (between observed and simulated levels) for the SFM groundwater monitoring wells, undisturbed conditions 2005–2006.
- ME HFM G: Average mean error (between observed and simulated head elevations) for the HFM groundwater monitoring wells, undisturbed conditions 2005–2006.
- MAE HFM G: Average mean absolute error (between observed and simulated head elevations) for the HFM groundwater monitoring wells, undisturbed conditions 2005–2006.

6.2.2 Sensitivity in terms of deviations from measured data

The sensitivity cases with original bedrock (*BRO-HV*) and original bedrock with regard to horizontal conductivities (*BRO-H*) give too high head elevations in the bedrock, which was stated already during the model calibration /Bosson et al. 2008/. All other cases give more or less the same calibration results, except the case with a less permeable QD/bedrock interface layer (*Z6-low*), which gives slightly poorer result for the surface discharge. The case with original bedrock with regard to vertical conductivities (*BRO-V*) on the other hand, giving the largest influence of the repository (upper part of the table), presents as good calibration results as the reference case, even a bit better.

The reason for the decrease of the vertical conductivities in the upper 200 m of the bedrock during the calibration of the SDM model can instead be found in the calibration against a pumping test /Bosson et al. 2008/. Higher vertical conductivities would not give the drawdown observed in the pumping test, which means that the parameterisation of the rock associated with sensitivity case *BRO-V* has lower confidence compared to the reference case.

6.2.3 Sensitivity to the presence of sediments

The influence on the surface water is very small, and more or less the same in all cases. The case *S0* was expected to give impact on the surface water, as well as on the inflow to the open repository, but this was not the case.

In Table 6-3, a summary of changes in flow components, contributing to the open repository inflow, is presented for the reference case and the case *S0*. As can be seen, the flow components contributing to the open repository inflow remain more or less unchanged when the sediments are removed from the model.

In Table 6-4, the overland-water balance for Lake Bolundsfjärden is presented for the reference case and the *S0* case. As can be seen, the different flow components still remain more or less unchanged when the sediments are removed from the model. None of the flow components changes more than 1%, except for the infiltration, which increases with 3%.

All in all, it seems like the sediment layers are not that important for the water balance, neither for the surface water, nor for the inflow to the bedrock when introducing the open repository. It is most likely rather the properties of the till and the bedrock layers that are of importance for the influence of the open repository. The explanation for this is partly the thickness of the sediments, which in general is rather small (especially the clay sediments on the land side), and partly the given hydraulic conductivities for the sediments, being set to $3 \cdot 10^{-7}$ m/s for most of the peat and gyttja (which is rather permeable) and $1.5 \cdot 10^{-8}$ m/s for the clay. Figure 6-1 shows the thickness of the peat, gyttja and clay sediment layers that were removed from the model in the *S0* case.

Table 6-3. Summary water balance for 2006 (L/s) showing the changes in flow components in the bedrock when introducing the open repository, in the reference case and the case without sediments (*S0*).

Changes in flow components due to the open repository:	Reference (L/s)	relative contribution	S0 (L/s)	relative contribution
Vertical net inflow to bedrock from the land area	12.2	55%	12.1	55%
Vertical net inflow to bedrock from the sea area	8.2	37%	8.3	38%
Horizontal net inflow to bedrock from the sea boundary	1.0	5%	1.0	5%
Storage change in bedrock	–0.29	1%	–0.29	1%
Reduced inflow to SFR	–0.4	2%	–0.4	2%
Inflow to the open repository	22.1		22.1	

Table 6-4. Overland-water balances during 2006 (L/s) for Lake Bolundsfjärden for the reference case and the case without sediments (*S0*).

	Reference, with open repository, K=1·10^{-8} m/s	*S0*, with open repository, K=1·10^{-8} m/s	Difference
Net precipitation (incl evaporation and storage)	4.70	4.68	–0.01
Net overland inflow to lake	4.33	4.29	–0.04
Net subsurface discharge to lake	1.71	1.73	0.02
Infiltration	2.03	2.09	0.06
Net river outflow from lake (excl inflow from upstream water course)	8.70	8.62	–0.08
Inflow from the upstream water course	23.61	23.37	–0.24

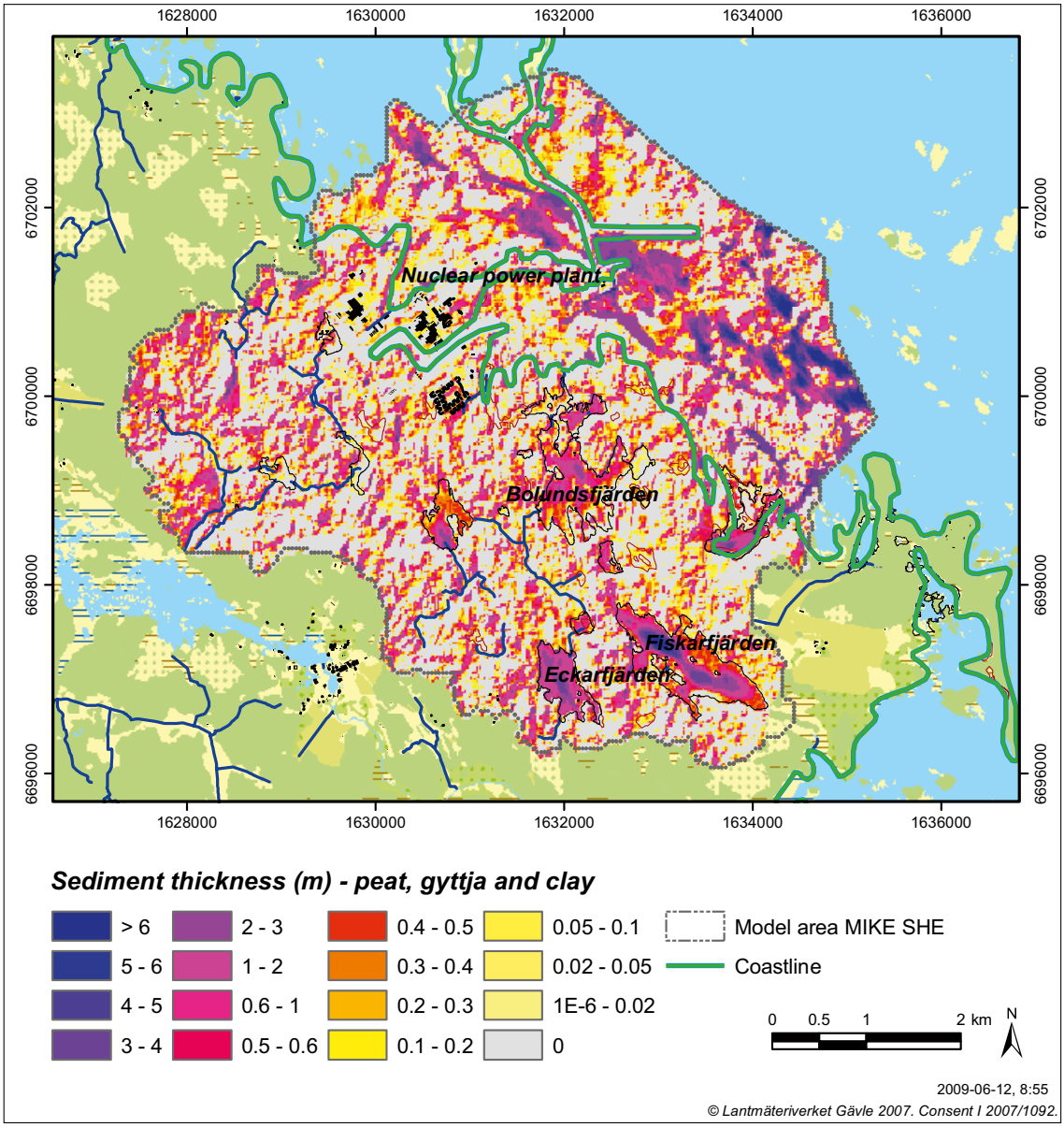

Figure 6-1. *The thickness of the peat, gyttja and clay sediment layers being removed from the model in the S0 sensitivity case.*

The average thickness of these sediments is 0.67 m on land, and 1.32 m for the sea sediments (in both cases only based on the areas where the sediments exist, according to Figure 6-1). The average thickness of the sediments under Lake Bolundsfjärden is 0.59 m (based on the whole lake area). More relevant is, however, the thickness of the clay sediment layer only, presented in Figure 6-2, due to its low hydraulic conductivity ($1.5 \cdot 10^{-8}$ m/s). The average thickness of the clay sediments (based on the areas where any sediment exists, according to Figure 6-1) is 0.05 m for the land part and 0.98 m for the sea sediments. Under Lake Bolundsfjärden, the clay sediment thickness is on average only 0.02 m (based on the whole lake area), which explains the results in the overland-water balances presented in Table 6-4.

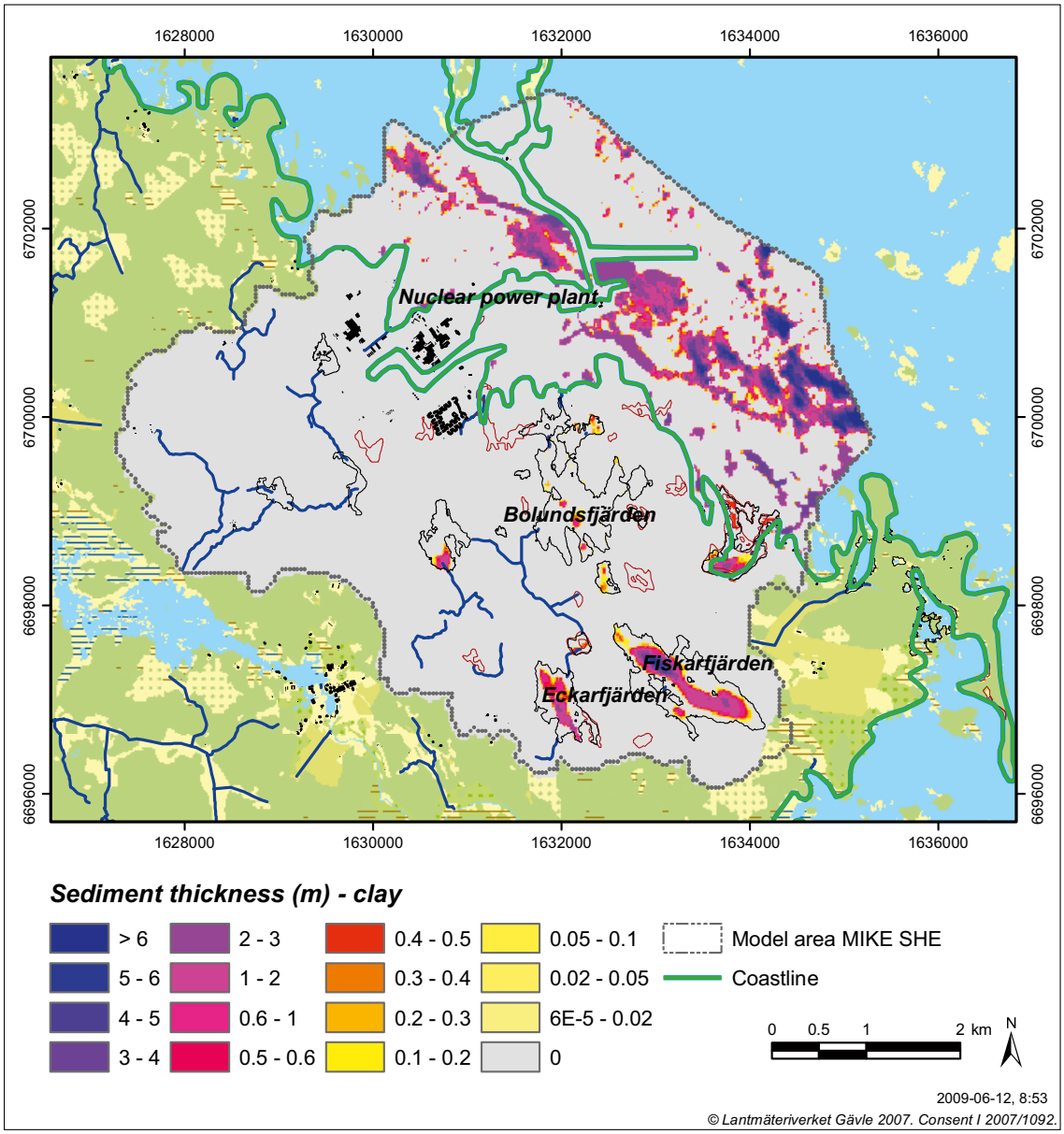

Figure 6-2. *The thickness of the clay sediment layer being removed from the model in the S0 sensitivity case.*

6.2.4 Sensitivity to the bedrock properties

The largest influence area and the largest inflow to the repository are found in case *BRO-V*, where vertical conductivities from the original bedrock model are used. The influence area is 64% larger than in the reference case. The case *BRO-H*, where horizontal conductivities from the original bedrock model are used, gives a slightly reduced influence area; 6% less than the reference case. The case *BRO-HV*, where both horizontal and vertical conductivities from the original bedrock model are used, shows the combined effect of the two cases above, with the increase in vertical conductivity being the most sensitive parameter.

The sensitivity to changes in vertical conductivities are further evaluated in the cases *BR1-V-low* and *BR1-V-high*, where the vertical conductivities in the upper 20 m of the bedrock are decreased and increased by a factor of 10, respectively. The influence area of the case *BR1-V-high* is however much smaller than the influence area in case *BRO-V*, where the vertical conductivity of the upper 200 m was increased by a factor 10. The case *BR1-V-high* gives an increase of 13% compared to the reference case, while the case *BRO-V* gives 64%. The impact on the groundwater table is not only controlled by the properties of the uppermost bedrock layer, but also to a very large extent by the properties in the deeper bedrock down to the repository level.

When decreasing the vertical conductivities in the upper 20 m of the bedrock, i.e. case *BR1-V-low*, the impact is larger, with a decrease of the influence area by 38%. The reason for this is that the upper bedrock layer now acts as a shield compared to the bedrock below, while in the case of *BR1-V-high*, the deeper bedrock layers act as a shield, and the response to the change was less. The conclusion from this, which perhaps could be regarded as basic hydraulics, is that the most impermeable layer, or rather the compartment with the lowest leakage coefficient, controls the effect on the groundwater table. The influence areas from the cases that deal with the vertical conductivities, i.e. case *BRO-V*, *BR1-V-high* and *BR1-V-low*, are shown together with the reference case in Figure 6-3.

The case *BR1-SJ*, where the upper sheet joint was extended to cover also the upper 20 m of the bedrock, was expected to give larger impact, but the influence area was only increased by 5%. The reason for this is most likely that the sheet joints only appear in the horizontal plane, not increasing the vertical conductivities, which seem to be the most important parameter with regard to impact on the groundwater table. Similar results were expected for the case *BR1-H-high*, where the horizontal conductivities in the upper 20 m of the bedrock were increased by a factor of 10. However, this change also increased the connection with the sea, which resulted in a larger inflow from the sea and a somewhat reduced influence on land.

6.2.5 Sensitivity to the properties of the QD/bedrock interface zone

None of the cases that deal with the conductivity in the QD/bedrock interface layer show any significant sensitivity with regard to the influence from the repository. The case *Z6-high* gives a slightly increased influence area, 7%, due to better contact between the QD and the bedrock. Consequently, a small reduction would have been expected in the opposite case *Z6-low*, but no such changes can be seen in the results.

6.2.6 Conclusions of the sensitivity analysis

The following can be concluded from the sensitivity analysis with regard to the influence from the open repository:

- The most sensitive property with regard to influence on the groundwater table, as well as the inflow to the repository, appears to be the vertical conductivity of the bedrock.
- The effects are not only controlled by the properties of the uppermost part of the bedrock, but also to a very large extent by the properties of the deeper bedrock.
- The sensitivity to the properties of the QD/bedrock interface zone is small.
- The most impermeable layer, or rather the model compartment with the lowest leakage coefficient, controls the impact on the groundwater table.
- The influence on the surface water is very small in all cases.
- It seems like the sediment layers are not important for the effects of the open repository, including the influence on the surface water. This is most likely because of the rather thin sediments, especially the clay sediments, in the area influenced by the repository.

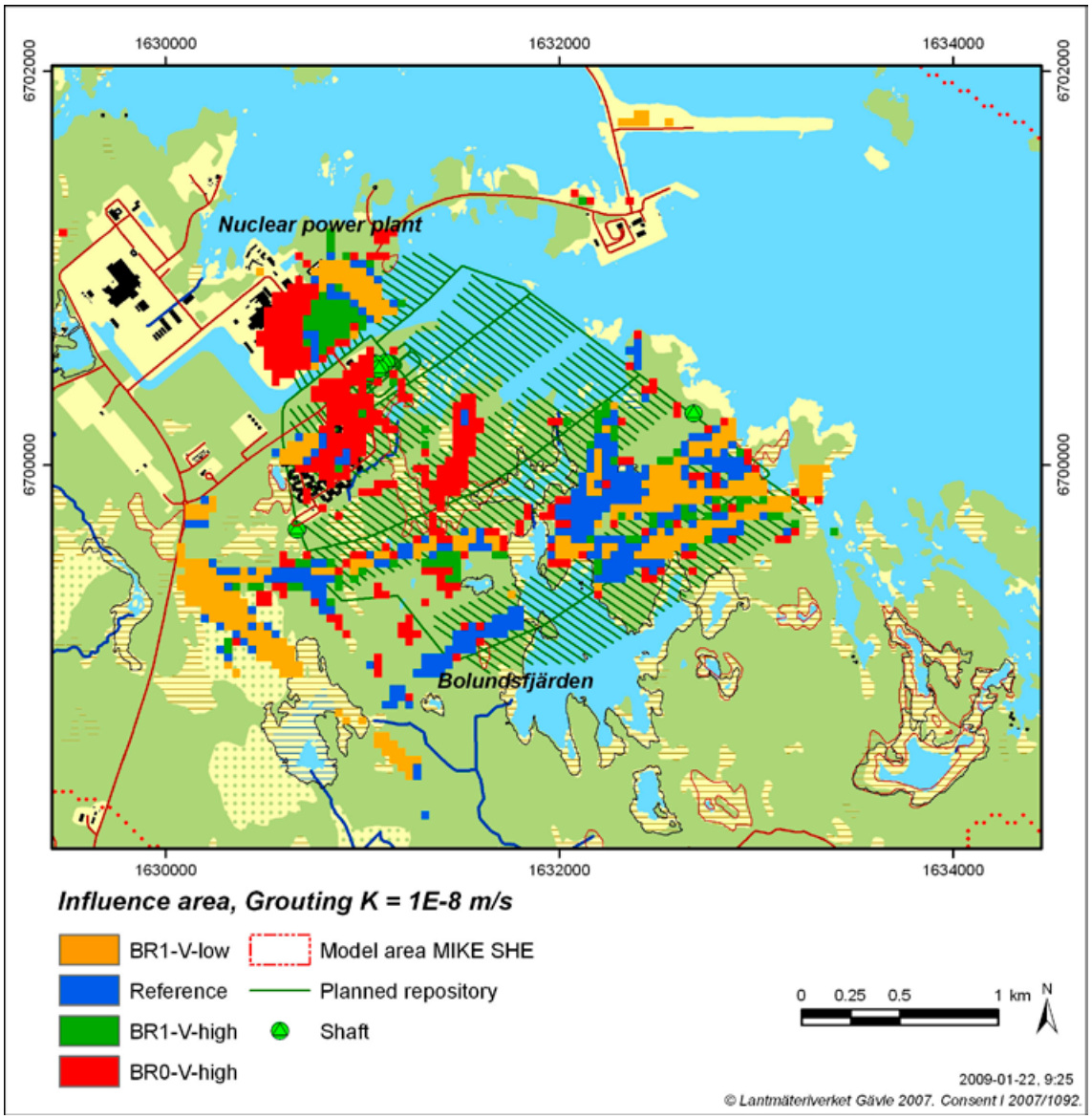

Figure 6-3. *The influence areas (defined as the areas with average groundwater table drawdowns larger than 0.3 m during 2006) for case BR1-V-low (orange areas), the reference case (orange and blue areas), case BR1-V-high (orange, blue and green areas), and case BRO-V (orange, blue, green and red areas), calculated with a grouting level of* $K=1 \cdot 10^{-8}$ *m/s.*

6.3 Comparison between MOUSE SHE and analytical solution

The expected influence area of the open repository is in the order of square kilometres, and the numerical grid cells in MIKE SHE are set to 40 m in both the vertical and the horizontal directions at repository depth. However, the gradients around the tunnels may change on the metre scale, which implies that there may be a spatial resolution problem in the numerical MIKE SHE model and in the coupling to the MOUSE model where the tunnels are described. Also, the coupling routine between MOUSE and MIKE SHE was originally developed for small pipe dimensions with thin concrete walls, typically much smaller and thinner than the size of the grid cells in MIKE SHE. In the case of the open repository modelling, both the tunnel dimensions and the grouted zone are in the same order of magnitude as the grid cell.

Because of these differences, and a general need to quantify uncertainties in the open repository modelling, it is of interest to evaluate how accurate the numerical MIKE SHE/MOUSE solution of the inflow to the tunnels is. To test the accuracy, a number of test simulations were performed and the results were compared with the analytical solution. The following sections describe the analytical solution, the model test setup in MIKE SHE and MOUSE, and the simulation results.

6.3.1 Analytical solution

The analytical solution for leakage flow from bedrock to a grouted tunnel is described by Equation 6-1 /Svensson and Follin 2009/. This solution assumes that the bedrock can be interpreted as a homogeneous porous medium and that the groundwater level is fixed.

$$q_{an} = \frac{2\pi \cdot K_0 \cdot H}{\ln(\frac{2H}{r_w}) + (\frac{K_0}{K_{grout}} - 1) \cdot \ln(1 + \frac{d_{grout}}{r_w})} \qquad \text{(Equation 6-1)}$$

q_{an} Flow from bedrock to grouted tunnel ($m^3/s/m$)

K_0 Average bedrock conductivity (m/s)

K_{grout} Conductivity of grouted zone (m/s)

H Depth from groundwater level to the centre of the tunnel (m)

r_w Tunnel radius (m)

d_{grout} Thickness of the grouted zone (m)

6.3.2 Model setup

A relatively simple test model is defined in MIKE SHE, according to Figure 6-4. The model domain has the dimensions 4,000 m in horizontal direction (x) and 2,000 m in vertical direction (z). The grid size is set to 40 m in all three dimensions. In the second horizontal direction (y) only three grids are used (120 m), out of which 2 grid rows form the model boundary. At the ground surface a fixed pressure is applied while all other boundaries are given a zero-flux condition (i.e. a no-flow boundary). A MOUSE tunnel link with atmospheric pressure and a radius of 2.5 m is placed with its centre at a depth of 500 m.

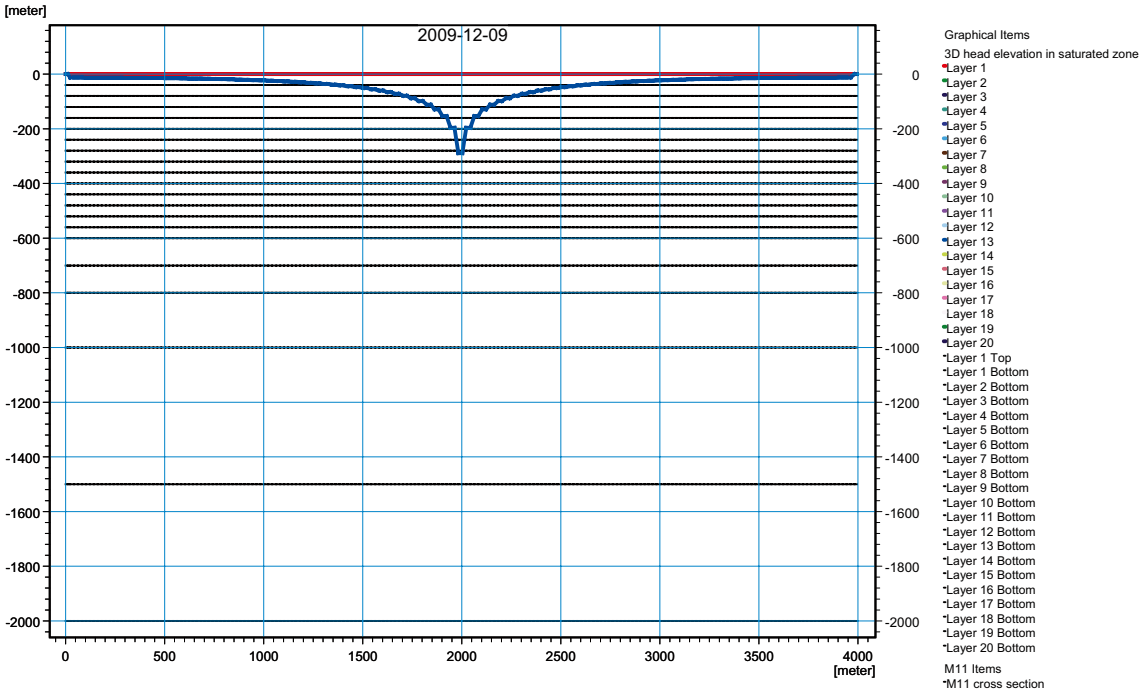

Figure 6-4. *A cross-section through the model test setup defined in MIKE SHE. The groundwater level is fixed at 0 m. The horizontal black lines shows the lower level of each calculation layer. The blue line is an example of the calculated head in the layer where the tunnel is located (with its centre at –500 m).*

The bedrock conductivity is set to $1 \cdot 10^{-7}$, $1 \cdot 10^{-8}$ or $1 \cdot 10^{-9}$ m/s, in both the horizontal and the vertical direction. All these bedrock parameterisations are combined with three different grouting conductivities: $1 \cdot 10^{-7}$, $1 \cdot 10^{-8}$ or $1 \cdot 10^{-9}$ m/s. The grouting thickness is set to 4 m. All in all, this gives nine different simulation cases. This is done in order to evaluate the model accuracy for different combinations of bedrock conductivity and grouting material. In order to reach steady state conditions, all cases are simulated for a time period of 10 years. The inflow of water to the tunnel is calculated as the flow between the MIKE SHE model and the MOUSE model (in which the tunnel is described as a pipe link) according to the method and the equations described in Section 2.3.1 (Equation 2-4 to Equation 2-7).

6.3.3 Results

The calculated inflows to the tunnel for the nine different simulation cases are presented in Table 6-5 together with the results from the analytical solution. The results show that MIKE SHE underestimates the inflow with 20 to 40% compared to the analytical solution. A highly conductive aquifer together with a low grouting conductivity, as in simulation cases 2 and 3, gives the largest deviation from the analytical solution. The best agreement is found in cases 7 and 8 where the grouting conductivity is higher than the aquifer conductivity.

The most likely reason for these discrepancies between the MIKE SHE results and the analytical solution is that the flow resistance in the grouted zone is added to the bedrock properties in the present MIKE SHE code, instead of replacing the bedrock with the grouted zone. If the grouting material is thin, like in the case of a concrete pipe, this will not be a problem. However, in the case of a relatively thick grouted zone (several metres) a considerable part of the grid cell will be changed. This explains the larger deviations observed in the cases where the grouted zone has a much lower conductivity than the bedrock.

Table 6-5. Comparison of tunnel inflows calculated with MIKE SHE and the analytical solution for the nine different simulation cases.

	Simulation case								
	1	2	3	4	5	6	7	8	9
Bedrock conductivity (m/s)	$1 \cdot 10^{-7}$	$1 \cdot 10^{-7}$	$1 \cdot 10^{-7}$	$1 \cdot 10^{-8}$	$1 \cdot 10^{-8}$	$1 \cdot 10^{-8}$	$1 \cdot 10^{-9}$	$1 \cdot 10^{-9}$	$1 \cdot 10^{-9}$
Grouting conductivity (m/s)	$1 \cdot 10^{-7}$	$1 \cdot 10^{-8}$	$1 \cdot 10^{-9}$	$1 \cdot 10^{-7}$	$1 \cdot 10^{-8}$	$1 \cdot 10^{-9}$	$1 \cdot 10^{-7}$	$1 \cdot 10^{-8}$	$1 \cdot 10^{-9}$
MIKE SHE solution ($m^3/s/m$)	$3.7 \cdot 10^{-5}$	$1.4 \cdot 10^{-5}$	$1.9 \cdot 10^{-6}$	$4.5 \cdot 10^{-6}$	$3.7 \cdot 10^{-6}$	$1.4 \cdot 10^{-6}$	$4.8 \cdot 10^{-7}$	$4.7 \cdot 10^{-7}$	$3.9 \cdot 10^{-7}$
Analytical solution ($m^3/s/m$)	$5.2 \cdot 10^{-5}$	$2.2 \cdot 10^{-5}$	$3.1 \cdot 10^{-6}$	$6.1 \cdot 10^{-6}$	$5.2 \cdot 10^{-6}$	$2.2 \cdot 10^{-6}$	$6.2 \cdot 10^{-7}$	$6.1 \cdot 10^{-7}$	$5.2 \cdot 10^{-7}$
Relation between MIKE SHE and analytical solution (%)	71%	64%	61%	73%	71%	64%	77%	77%	74%

7 Conclusions of the open repository modelling

The conclusions below refer to the case where the whole repository is open, i.e. with all tunnels open at the same time, unless otherwise stated. This is a hypothetical worst-case scenario. In reality, the open repository will be constructed and operated in three development phases, with different parts of the deep rock construction open in each phase.

7.1 Water balance and inflow to the open repository

The inflow of water to the open repository construction affects the total turnover of water in the model area. Depending on the grouting level, the inflow to the repository is on the order of 7 to 25% of the total runoff under undisturbed conditions, when the land part of the model area is studied. Inside the influence area, the open repository construction creates a major change in the water balance, with an inflow to the repository corresponding to up to 40% out of the precipitation, depending on the grouting level.

The horizontal boundary flows in the bedrock are generally much smaller then the vertical flow between the QD and the bedrock. The vertical net inflow to the bedrock is between 14 and 37 L/s depending on the grouting level (compared to 4 L/s under undisturbed conditions), while the corresponding total horizontal net inflow to the bedrock from the sea boundary is between 0.1 and 1.0 L/s (compared to a net outflow of 0.4 L/s under undisturbed conditions). Under undisturbed conditions, the inflow and outflow numbers are of the same order of magnitude, in both the vertical and the horizontal direction. For the vertical direction, this changes when the open repository is introduced. The vertical outflow from the bedrock to the QD varies between 7 and 5 L/s depending on the grouting level, while the vertical inflow to the bedrock varies between 12 and 42 L/s (first values refer to undisturbed conditions).

The inflow to tunnels and shafts varies between 10 and 36 L/s depending on the grouting level, where grouting levels corresponding to hydraulic conductivities of $1 \cdot 10^{-7}$ m/s, $1 \cdot 10^{-8}$ m/s and $1 \cdot 10^{-9}$ m/s in the grouted zone have been studied. Slightly more than half of the repository inflow comes from increased vertical inflow from the land area, out of which approximately two thirds can be attributed to the influence area where the groundwater table drawdown exceeds 0.3 m. The remaining contribution comes from increased inflow from the sea, with the majority through vertical inflow from the sea area covered by the model.

Compared to the case with the whole repository construction open at the same time, which is a hypothetical situation that will not occur in reality, the inflows during the different construction/operation phases are smaller, between approximately 60 and 90% of the inflow for the full construction depending on the grouting level. The meteorological conditions are hardly reflected in the calculated inflows to the repository, which means that the inflow is more or less the same during periods of dry conditions compared to wet periods with a large amount of precipitation. The small existing temporal variation originates from the inflow to the upper bedrock layers, above the sheet joint layers.

The sensitivity analysis shows that the inflow to the repository is rather insensitive to changes in the analysed properties. The most sensitive parameter seems to be the vertical hydraulic conductivity of the bedrock. The inflow increased with approximately 25% when the vertical conductivity was increased by a factor 10 for the upper 200 m of the bedrock.

7.2 Surface waters

The water levels in the lakes in the area are hardly affected by the repository and tunnel constructions. Not more than a few centimetres, and only in Lake Bolundsfjärden and Lake Gällsboträsket, where a groundwater table drawdown around and head changes under the lakes are found. The low-permeable sediment layers under the lakes are assumed to have a strong influence on lake-water levels and to prevent a lowering of the water levels in the lakes. The water balance for Lake Bolundsfjärden shows that the increased recharge from the lake, through the sediments, is more or less equivalent to the reduced inflow from the upstream water course, and consequently of the same importance for the drawdown of the lake.

The discharges in the water courses are only affected to a small extent by the open repository. The largest, and only noticeable influence on the surface water discharge (out of the four monitoring stations) is observed at Lake Bolundsfjärden, where a level of grouting of $K = 1 \cdot 10^{-7}$ m/s results in a decrease in the accumulated annual discharge by 8%. The reduced inflow to Lake Bolundsfjärden is a consequence of the groundwater table drawdown in the area around Lake Gällsboträsket, located just upstream Lake Bolundsfjärden. Upstream the other surface water monitoring stations, the groundwater table drawdown is much less, or even doesn't exist.

The sensitivity analysis shows that the surface water levels and discharges are rather insensitive to changes in both bedrock properties and the properties at the interface between the Quaternary deposits and the bedrock. In both cases, this was more or less expected, because the surface water discharge is mainly controlled by the topographical conditions and the presence of a high conductive top soil layer, as long as the deeper till layers are less permeable, which they are. What is more unexpected is the fact that the surface water did not show much sensitivity to the sediments under the lakes under disturbed conditions. It seems like the properties of the till layer is more important for the influence on the surface water of the open repository. The likely explanation for this is the rather thin sediments, especially the clay sediments on the land side. The average total thickness of the sediments under Lake Bolundsfjärden is 0.59 m, but the thickness of the low-permeable clay layer is on average only 0.02 m. This is not enough to make any difference.

7.3 Groundwater table drawdown and head changes

The impact of the repository on the free groundwater table in the QD is concentrated to areas associated with vertical fracture zones in the upper c 20 m of the rock. The influence area, defined as a groundwater table drawdown larger than 0.3 m, is between 0.5 and 1.6 km^2, and covers a number of bands north and west of Lake Bolundsfjärden, and one band north-west and partly south-east of Lake Stocksjön. In addition, the influence area covers a number of smaller areas south of the nuclear power plant, and a larger area rather close to and north-east of the power plant. The largest drawdown of the groundwater table is found in the area north-east of the power plant. The drawdown of the groundwater table is here up to approximately 15 m. This is a consequence of the presence of a local vertical fracture zone in this area.

Compared to the earlier presented influence areas obtained in the Forsmark 1.2 MIKE SHE modelling /Bosson and Berglund 2006/, where more or less only the area around the access tunnel was affected, the impact is now spread over a larger area. The reason for this is mainly found in the updated bedrock description. Especially for the upper 200 m of the bedrock, the differences are large between the Forsmark 1.2 model and the updated description in the SDM-Site model. The Forsmark 1.2 bedrock model was sparsely fractured, had no sheet joints, and the conductivity values were generally very low compared to the updated bedrock description in the SDM-Site model.

Another possible reason for the differences between the Forsmark 1.2 MIKE SHE modelling results and the present ones that are based on the SDM-Site model, is the description of the deep bedrock. The bottom boundary in the Forsmark 1.2 MIKE SHE model was at 150 m.b.s.l. with a prescribed head calculated with the DarcyTools model /Svensson 2005/ used as boundary condition. During the calibration of the SDM-Site version of the MIKE SHE model /Bosson et al. 2008/, this method proved to be unsatisfactory and was abandoned in favour of a no-flow boundary at 600 m.b.s.l. or deeper (990 m.b.s.l. is used in the present open repository modelling).

The last potential reason for the differences between the model versions, which comes as a secondary effect of switching to a deeper model, is the fact that only the upper parts of the access tunnel and shafts were directly included in the Forsmark 1.2 MIKE SHE model, because the model only covered the upper 150 m of the bedrock. The rest of the open repository was described in the DarcyTools model, and consequently only indirectly introduced to the MIKE SHE model as a reflection in the prescribed head at 150 m.b.s.l, calculated with the DarcyTools model.

The above two main differences between the Forsmark 1.2 MIKE SHE modelling and the open repository modelling presented here do not necessarily lead to underestimations of the influence area in the Forsmark 1.2 modelling; the deviations can be in either direction.

There are differences in the head changes of the groundwater when considering different depths in the model. The vertical fracture zones connect the deep parts of the open repository with the upper bedrock where the sheet joints are located. When the head change caused by the open repository reaches a layer with sheet joints, it is spread over a large area in the model. According to the hydrogeological site-descriptive model, only vertical fracture zones are present in the upper 20 m of the bedrock. This means that this layer act as a barrier between the upper sheet joint layer and the QD, only having connectivity through the vertical fracture zones. Because the transmissivity of the QD is limited, the head change in the QD is limited to the areas around the underlying vertical fracture zones.

Notable is that the influence area in the uppermost bedrock covers the east part of the nuclear power plant. Depending on the local groundwater head conditions around the nuclear power plant, this means a potential risk for transport from the nuclear power plant to the open repository, as well as a theoretical risk of settlings.

The influence area for the groundwater table has been defined as the area where the drawdown is larger than 0.3 m. A grouting level of $K=1\cdot10^{-7}$ m/s gives an influence area that is three times larger (1.6 km^2) than that for a grouting level of $K=1\cdot10^{-9}$ m/s (0.5 km^2), while the influence area for a grouting level of $K=1\cdot10^{-8}$ m/s is twice that for the best grouting (1.0 km^2). The overall pattern of the influence areas for the groundwater table is the same for all the three grouting levels, which means that it is limited to bands and areas that follow the underlying vertical fracture zones in the upper bedrock.

The above influence areas refer to a hypothetical case of a fully open repository construction. In reality, the open repository will be constructed in three development phases. Simulation results show that phase 3 gives the largest effects, with an influence area of approximately 90% of the impact from a full construction. The corresponding numbers for phase 1 and phase 2 are 70% and 80%, respectively.

The presented results are based on a two-year simulation period, 2005–2006, where the year of 2005 has been used as an initialization period. However, in reality the repository will be open for many decades, and the groundwater table drawdown will have time to be fully developed to stable conditions. When evaluating the effect of this by simulating an eight-year period, the fully developed influence area was found to be approximately 18% larger than that obtained after two years. This stable area was more or less reached after approximately six years.

This enlargement should be taken into account when considering the possible influence area. However, the temporal variation from the short term variations of the meteorological and hydrological conditions during a year is much larger, with a more than twice as large maximum influence area during the year, compared to the minimum influence area during the year (based on the present results for 2006). On the other hand, the durations of these “extreme periods” are short (relative to, for instance, the growing season), which means that they are probably not leading to long term effects.

The closure of the final repository was simulated by simply replacing the repository with bedrock, and initialising the simulation from the situation with an open repository based on a grouting level of $K = 1\cdot10^{-8}$ m/s. The results from this simulation shows that it takes approximately one and a half year to fully recover the drawdown of the groundwater table. After one year from closure, the influence area is reduced to less then 5%, compared to the fully developed influence area with the whole repository open. Observe that these results do not consider the recovery of the groundwater head in the bedrock at the repository depth, which will take longer than that of the groundwater table.

Similarly to the inflow (see above), the sensitivity analysis shows that the groundwater table drawdown is most sensitive to the vertical conductivity of the bedrock. The impact on the groundwater table is not only controlled by the properties in the uppermost part of the bedrock, but also to a very large extent by the properties of the deeper bedrock. The influence area of the groundwater table drawdown only increased by 13% when the vertical conductivity was increased by a factor of 10 in the upper 20 m of the bedrock, but the increase was as large as 64% when the corresponding change was done in the upper 200 m. However, when decreasing the vertical conductivities in the upper 20 m of the bedrock, the influence area decreased by as much as 38%. This means that the most impermeable layer, or rather the model compartment with the lowest leakage coefficient, controls the impact on the groundwater table.

7.4 Uncertainties and discrepancies

Simulations with a simplified test model, consisting of homogeneous bedrock and one grouted tunnel segment, show that the present MIKE SHE model code underestimates the inflow to a tunnel with approximately 30% compared to the analytical solution. This is however under the assumption that the groundwater table is fixed, with unlimited recharge capacity. In practice, the groundwater recharge will be limited, and the consequences of the deviation from the analytical solution will be smaller than indicated by the test performed in this study. Consequently, the effect of the underestimation of the open repository inflow will most likely be less than 30%.

The sensitivity analysis indicates that the uncertainties associated with the vertical hydraulic conductivity are the most important ones. The impact on the groundwater table is not only controlled by the properties of the uppermost part of the bedrock, but also to a very large extent by the properties of the deeper bedrock. The same holds for the open repository inflow. The difference between the original bedrock model (Section 6.1) and the bedrock properties used in the MIKE SHE SDM-Site model, with regard to vertical conductivity, is a factor of 10 for the upper 200 m. This could be seen as a rough indication of the uncertainties in the bedrock properties. The calculated inflow increased with approximately 25% when the vertical conductivity was changed back to its original value, and the influence area of the groundwater table drawdown increased with as much as 64%.

The influence area for a theoretical grouting level of $K=1\cdot10^{-7}$ m/s is 60% larger than that for a grouting level of $K=1\cdot10^{-8}$ m/s. In practice, it appears reasonable that the real grouting conductivity deviates by a factor of approximately 3 from the chosen design criteria. This would give an uncertainty in the influence area in the order of 30%, if a grouting level of $K=1\cdot10^{-8}$ m/s is chosen as design criterion.

However, it should be noted that the temporal variations caused by the short term (seasonal) variations in the meteorological and hydrological conditions during a year are much larger than all the above-mentioned uncertainties, with a discrepancy from the yearly average groundwater drawdown of as much as 80% during some months. On the other hand, the durations of these “extreme periods” are short relative to, for instance, the growing season, which means that they are probably not leading to long term effects.

8 References

Bosson E, Berglund S, 2006. Near-surface hydrogeological model of Forsmark. Open repository and solute transport applications – Forsmark 1.2. SKB R-06-52, Svensk Kärnbränslehantering AB.

Bosson E, Gustafsson L-G, Sassner M, 2008. Numerical modelling of surface hydrology and near-surface hydrogeology at Forsmark. Site descriptive modelling, SDM-Site Forsmark. SKB R-08-09, Svensk Kärnbränslehantering AB.

DHI Software, 2008a. MIKE SHE – User Manual. DHI Water, Environment & Health, Hørsholm, Denmark.

DHI Software, 2008b. MOUSE PIPE FLOW – Reference Manual. DHI Water, Environment & Health, Hørsholm, Denmark.

Follin S, Johansson P-O, Hartley L, Jackson P, Roberts D, Marsic N, 2007. Hydrogeological conceptual model development and numerical modelling using CONNECTFLOW, Forsmark modelling stage 2.2. SKB R-07-49, Svensk Kärnbränslehantering AB.

Follin S, Hartley L, Jackson P, Roberts D, Marsic N, 2008. Hydrogeological conceptual model development and numerical modelling using CONNECTFLOW, Forsmark modelling stage 2.3. SKB R-08-23, Svensk Kärnbränslehantering AB.

Johansson P-O, 2008. Description of surface hydrology and near-surface hydrogeology at Forsmark. Site descriptive modelling, SDM-Site Forsmark. SKB R-08-08, Svensk Kärnbränslehantering AB.

Kristensen K J, Jensen S E, 1975. A model for estimating actual evapotranspiration from potential evapotranspiration. Nordic Hydrology, vol. 6, pp 170–188.

Lindborg T (ed), 2008. Surface system Forsmark. Site descriptive modelling, SDM-Site Forsmark. SKB R-08-11, Svensk Kärnbränslehantering AB.

SKB, 2008. Site description of Forsmark at completion of the site investigation phase. SDM-Site Forsmark. SKB TR-08-05, Svensk Kärnbränslehantering AB.

Svensson U, 2005. The Forsmark repository. Modelling changes in the flow, pressure and salinity fields, due to a repository for spent nuclear fuel. SKB R-05-57, Svensk Kärnbränslehantering AB.

Svensson U, Follin S, 2009. Groundwater flow modelling of the excavation and operation periods – SR-Site Forsmark. SKB R-09-19, Svensk Kärnbränslehantering AB.

Appendix 1

The total conductance of the walls of the shafts is varying with the level of grouting. The values used for each shaft in the different grouting cases are listed in Table A1-1 to A1-15. The calculation of the conductance is described in Section 2.3.2.

Table A1-1. Geometry, hydraulic conductivity (Kh), leakage coefficients (LC) and conductance (C) for shaft SA01 when K=1·10^{-7} m/s in the grouted zone.

Calculation layer	Circum-ference, m	Kh, m/s	Horiz. grid dx, m	Layer thick-ness dz, m	LCaq, s^{-1}	LCp, s^{-1}	LC, s^{-1}	C, m^2/s
1	9.42	8.04E-06	40	2.42	2.01E-07	2.0E-08	1.82E-08	4.15E-07
2	9.42	6.45E-06	40	2.86	1.61E-07	2.0E-08	1.78E-08	4.79E-07
3	9.42	2.72E-09	40	8.65	6.80E-11	2.0E-08	6.78E-11	5.52E-09
4	9.42	3.08E-08	40	19.57	7.69E-10	2.0E-08	7.41E-10	1.37E-07
5	9.42	1.16E-09	40	20.00	2.90E-11	2.0E-08	2.89E-11	5.45E-09
6	9.42	3.31E-07	40	20.00	8.28E-09	2.0E-08	5.86E-09	1.10E-06
7	9.42	3.31E-08	40	20.00	8.28E-10	2.0E-08	7.95E-10	1.50E-07
8	9.42	1.51E-08	40	20.00	3.77E-10	2.0E-08	3.70E-10	6.96E-08
9	9.42	1.54E-08	40	20.00	3.85E-10	2.0E-08	3.78E-10	7.12E-08
10	9.42	9.59E-08	40	20.00	2.40E-09	2.0E-08	2.14E-09	4.03E-07
11	9.42	1.05E-08	40	40.00	2.62E-10	2.0E-08	2.59E-10	9.76E-08
12	9.42	1.58E-06	40	60.00	3.96E-08	2.0E-08	1.33E-08	7.51E-06
13	9.42	3.45E-09	40	110.00	8.63E-11	2.0E-08	8.59E-11	8.90E-08
14	9.42	4.38E-10	40	60.00	1.10E-11	2.0E-08	1.09E-11	6.19E-09
15	9.42	4.38E-10	40	43.58	1.10E-11	2.0E-08	1.09E-11	4.49E-09

Table A1-2. Geometry, hydraulic conductivity (Kh), leakage coefficients (LC) and conductance (C) for shaft SA02 when K=1·10–7 m/s in the grouted zone.

Calculation layer	Circum-ference, m	Kh, m/s	Horiz. grid dx, m	Layer thick-ness dz, m	LCaq, s^{-1}	LCp, s^{-1}	LC, s^{-1}	C, m^2/s
1	9.42	6.15E-07	40	2.45	1.54E-08	2.0E-08	8.69E-09	2.01E-07
2	9.42	1.00E-07	40	1.00	2.50E-09	2.0E-08	2.22E-09	2.09E-08
3	9.42	3.65E-08	40	10.15	9.12E-10	2.0E-08	8.72E-10	8.34E-08
4	9.42	1.03E-07	40	20.00	2.58E-09	2.0E-08	2.28E-09	4.30E-07
5	9.42	3.95E-08	40	20.00	9.87E-10	2.0E-08	9.41E-10	1.77E-07
6	9.42	1.19E-05	40	20.00	2.96E-07	2.0E-08	1.87E-08	3.53E-06
7	9.42	4.15E-09	40	20.00	1.04E-10	2.0E-08	1.03E-10	1.94E-08
8	9.42	9.71E-05	40	20.00	2.43E-06	2.0E-08	1.98E-08	3.74E-06
9	9.42	3.08E-09	40	20.00	7.70E-11	2.0E-08	7.67E-11	1.45E-08
10	9.42	4.63E-09	40	20.00	1.16E-10	2.0E-08	1.15E-10	2.17E-08
11	9.42	1.69E-08	40	40.00	4.21E-10	2.0E-08	4.13E-10	1.55E-07
12	9.42	1.71E-09	40	60.00	4.28E-11	2.0E-08	4.27E-11	2.41E-08
13	9.42	3.22E-09	40	110.00	8.05E-11	2.0E-08	8.02E-11	8.31E-08
14	9.42	4.20E-09	40	60.00	1.05E-10	2.0E-08	1.04E-10	5.90E-08
15	9.42	4.20E-09	40	43.76	1.05E-10	2.0E-08	1.04E-10	4.31E-08

Table A1-3. Geometry, hydraulic conductivity (Kh), leakage coefficients (LC) and conductance (C) for shaft SB00 when K=1·10–7 m/s in the grouted zone.

Calculation layer	Circum-ference, m	Kh, m/s	Horiz. grid dx, m	Layer thick-ness dz, m	LCaq, s^{-1}	LCp, s^{-1}	LC, s^{-1}	C, m^2/s
1	18.85	0.00015	40	2.48	3.75E-06	2.0E-08	1.99E-08	9.30E-07
2	18.85	4.09E-05	40	1.27	1.02E-06	2.0E-08	1.96E-08	4.70E-07
3	18.85	2.09E-08	40	9.96	5.22E-10	2.0E-08	5.09E-10	9.56E-08
4	18.85	1.97E-05	40	19.89	4.93E-07	2.0E-08	1.92E-08	7.21E-06
5	18.85	4.89E-08	40	20.00	1.22E-09	2.0E-08	1.15E-09	4.34E-07
6	18.85	1.81E-07	40	20.00	4.52E-09	2.0E-08	3.69E-09	1.39E-06
7	18.85	3.22E-08	40	20.00	8.04E-10	2.0E-08	7.73E-10	2.91E-07
8	18.85	3.91E-07	40	20.00	9.78E-09	2.0E-08	6.57E-09	2.48E-06
9	18.85	1.03E-05	40	20.00	2.59E-07	2.0E-08	1.86E-08	7.00E-06
10	18.85	3.35E-09	40	20.00	8.38E-11	2.0E-08	8.35E-11	3.15E-08
11	18.85	1.36E-07	40	40.00	3.40E-09	2.0E-08	2.90E-09	2.19E-06
12	18.85	2.51E-08	40	60.00	6.27E-10	2.0E-08	6.08E-10	6.88E-07
13	18.85	4.33E-09	40	110.00	1.08E-10	2.0E-08	1.08E-10	2.23E-07
14	18.85	2.93E-11	40	60.00	7.33E-13	2.0E-08	7.32E-13	8.28E-10
15	18.85	2.93E-11	40	60.00	7.33E-13	2.0E-08	7.32E-13	8.28E-10
16	18.85	1.64E-11	40	6.40	4.10E-13	2.0E-08	4.10E-13	4.95E-11

Table A1-4. Geometry, hydraulic conductivity (Kh), leakage coefficients (LC) and conductance (C) for shaft SC00 when K=1·10^{-7} m/s in the grouted zone.

Calculation layer	Circum-ference, m	Kh, m/s	Horiz. grid dx, m	Layer thick-ness dz, m	LCaq, s^{-1}	LCp, s^{-1}	LC, s^{-1}	C, m^2/s
1	15.71	7.50E-06	40	2.44	1.88E-07	2.0E-08	1.81E-08	6.93E-07
2	15.71	3.29E-06	40	1.00	8.22E-08	2.0E-08	1.61E-08	2.53E-07
3	15.71	8.63E-09	40	10.66	2.16E-10	2.0E-08	2.13E-10	3.57E-08
4	15.71	2.07E-05	40	19.90	5.19E-07	2.0E-08	1.93E-08	6.02E-06
5	15.71	6.95E-08	40	19.60	1.74E-09	2.0E-08	1.60E-09	4.92E-07
6	15.71	3.31E-08	40	20.00	8.28E-10	2.0E-08	7.95E-10	2.50E-07
7	15.71	3.29E-09	40	20.00	8.22E-11	2.0E-08	8.19E-11	2.57E-08
8	15.71	7.37E-08	40	20.00	1.84E-09	2.0E-08	1.69E-09	5.30E-07
9	15.71	2.71E-07	40	20.00	6.78E-09	2.0E-08	5.06E-09	1.59E-06
10	15.71	6.64E-07	40	20.00	1.66E-08	2.0E-08	9.07E-09	2.85E-06
11	15.71	1.32E-06	40	40.00	3.29E-08	2.0E-08	1.24E-08	7.82E-06
12	15.71	3.22E-07	40	60.00	8.04E-09	2.0E-08	5.73E-09	5.40E-06
13	15.71	2.10E-08	40	110.00	5.25E-10	2.0E-08	5.12E-10	8.84E-07
14	15.71	1.00E-11	40	60.00	2.50E-13	2.0E-08	2.50E-13	2.36E-10
15	15.71	1.00E-11	40	60.00	2.50E-13	2.0E-08	2.50E-13	2.36E-10
16	15.71	1.02E-11	40	36.40	2.55E-13	2.0E-08	2.55E-13	1.46E-10

Table A1-5. Geometry, hydraulic conductivity (Kh), leakage coefficients (LC) and conductance (C) for shafts SF00 and ST00 when K=1·10^{-7} m/s in the grouted zone.

Calculation layer	Circum-ference, m	Kh, m/s	Horiz. grid dx, m	Layer thick-ness dz, m	LCaq, s^{-1}	LCp, s^{-1}	LC, s^{-1}	C, m^2/s
1	18.85	7.50E-06	40	2.48	1.88E-07	2.0E-08	1.81E-08	8.45E-07
2	18.85	5.12E-06	40	1.26	1.28E-07	2.0E-08	1.73E-08	4.11E-07
3	18.85	1.21E-08	40	10.13	3.03E-10	2.0E-08	2.98E-10	5.69E-08
4	18.85	1.48E-05	40	19.93	3.70E-07	2.0E-08	1.90E-08	7.13E-06
5	18.85	5.71E-08	40	20.00	1.43E-09	2.0E-08	1.33E-09	5.02E-07
6	18.85	1.29E-07	40	20.00	3.22E-09	2.0E-08	2.77E-09	1.04E-06
7	18.85	2.54E-08	40	20.00	6.34E-10	2.0E-08	6.15E-10	2.32E-07
8	18.85	7.19E-07	40	20.00	1.80E-08	2.0E-08	9.47E-09	3.57E-06
9	18.85	7.66E-08	40	20.00	1.91E-09	2.0E-08	1.75E-09	6.59E-07
10	18.85	8.35E-08	40	20.00	2.09E-09	2.0E-08	1.89E-09	7.12E-07
11	18.85	7.82E-08	40	40.00	1.95E-09	2.0E-08	1.78E-09	1.34E-06
12	18.85	3.94E-08	40	60.00	9.84E-10	2.0E-08	9.38E-10	1.06E-06
13	18.85	6.52E-09	40	110.00	1.63E-10	2.0E-08	1.62E-10	3.35E-07
14	18.85	1.15E-11	40	60.00	2.86E-13	2.0E-08	2.86E-13	3.24E-10
15	18.85	1.15E-11	40	18.40	2.86E-13	2.0E-08	2.86E-13	9.93E-11

Table A1-6. Geometry, hydraulic conductivity (Kh), leakage coefficients (LC) and conductance (C) for shaft SA01 when K=1·10^{-8} m/s in the grouted zone.

Calculation layer	Circum-ference, m	Kh, m/s	Horiz. grid dx, m	Layer thick-ness dz, m	LCaq, s^{-1}	LCp, s^{-1}	LC, s^{-1}	C, m^2/s
1	9.42	8.04E-06	40	2.42	2.01E-07	2.0E-09	1.98E-09	4.51E-08
2	9.42	6.45E-06	40	2.86	1.61E-07	2.0E-09	1.98E-09	5.32E-08
3	9.42	2.72E-09	40	8.65	6.80E-11	2.0E-09	6.58E-11	5.36E-09
4	9.42	3.08E-08	40	19.57	7.69E-10	2.0E-09	5.56E-10	1.02E-07
5	9.42	1.16E-09	40	20.00	2.90E-11	2.0E-09	2.86E-11	5.38E-09
6	9.42	3.31E-07	40	20.00	8.28E-09	2.0E-09	1.61E-09	3.04E-07
7	9.42	3.31E-08	40	20.00	8.28E-10	2.0E-09	5.85E-10	1.10E-07
8	9.42	1.51E-08	40	20.00	3.77E-10	2.0E-09	3.17E-10	5.97E-08
9	9.42	1.54E-08	40	20.00	3.85E-10	2.0E-09	3.23E-10	6.08E-08
10	9.42	9.59E-08	40	20.00	2.40E-09	2.0E-09	1.09E-09	2.05E-07
11	9.42	1.05E-08	40	40.00	2.62E-10	2.0E-09	2.32E-10	8.74E-08
12	9.42	1.58E-06	40	60.00	3.96E-08	2.0E-09	1.90E-09	1.08E-06
13	9.42	3.45E-09	40	110.00	8.63E-11	2.0E-09	8.27E-11	8.57E-08
14	9.42	4.38E-10	40	60.00	1.10E-11	2.0E-09	1.09E-11	6.16E-09
15	9.42	4.38E-10	40	43.58	1.10E-11	2.0E-09	1.09E-11	4.47E-09

Table A1-7. Geometry, hydraulic conductivity (Kh), leakage coefficients (LC) and conductance (C) for shaft SA02 when K=1·10^{-8} m/s in the grouted zone.

Calculation layer	Circum-ference, m	Kh, m/s	Horiz. grid dx, m	Layer thick-ness dz, m	LCaq, s^{-1}	LCp, s^{-1}	LC, s^{-1}	C, m^2/s
1	9.42	6.15E-07	40	2.45	1.54E-08	2.0E-09	1.77E-09	4.08E-08
2	9.42	1.00E-07	40	1.00	2.50E-09	2.0E-09	1.11E-09	1.05E-08
3	9.42	3.65E-08	40	10.15	9.12E-10	2.0E-09	6.26E-10	5.99E-08
4	9.42	1.03E-07	40	20.00	2.58E-09	2.0E-09	1.13E-09	2.12E-07
5	9.42	3.95E-08	40	20.00	9.87E-10	2.0E-09	6.61E-10	1.25E-07
6	9.42	1.19E-05	40	20.00	2.96E-07	2.0E-09	1.99E-09	3.74E-07
7	9.42	4.15E-09	40	20.00	1.04E-10	2.0E-09	9.86E-11	1.86E-08
8	9.42	9.71E-05	40	20.00	2.43E-06	2.0E-09	2.00E-09	3.76E-07
9	9.42	3.08E-09	40	20.00	7.70E-11	2.0E-09	7.41E-11	1.40E-08
10	9.42	4.63E-09	40	20.00	1.16E-10	2.0E-09	1.09E-10	2.06E-08
11	9.42	1.69E-08	40	40.00	4.21E-10	2.0E-09	3.48E-10	1.31E-07
12	9.42	1.71E-09	40	60.00	4.28E-11	2.0E-09	4.19E-11	2.37E-08
13	9.42	3.22E-09	40	110.00	8.05E-11	2.0E-09	7.74E-11	8.02E-08
14	9.42	4.20E-09	40	60.00	1.05E-10	2.0E-09	9.98E-11	5.64E-08
15	9.42	4.20E-09	40	43.76	1.05E-10	2.0E-09	9.98E-11	4.11E-08

Table A1-8. Geometry, hydraulic conductivity (Kh), leakage coefficients (LC) and conductance (C) for shaft SB00 when K=1·10^{-8} m/s in the grouted zone.

Calculation layer	Circum-ference, m	Kh, m/s	Horiz. grid dx, m	Layer thick-ness dz, m	LCaq, s^{-1}	LCp s^{-1}	LC, s^{-1}	C, m^2/s
1	18.85	0.00015	40	2.48	3.75E-06	2.0E-09	2.00E-09	9.34E-08
2	18.85	4.09E-05	40	1.27	1.02E-06	2.0E-09	2.00E-09	4.78E-08
3	18.85	2.09E-08	40	9.96	5.22E-10	2.0E-09	4.14E-10	7.77E-08
4	18.85	1.97E-05	40	19.89	4.93E-07	2.0E-09	1.99E-09	7.47E-07
5	18.85	4.89E-08	40	20.00	1.22E-09	2.0E-09	7.59E-10	2.86E-07
6	18.85	1.81E-07	40	20.00	4.52E-09	2.0E-09	1.39E-09	5.23E-07
7	18.85	3.22E-08	40	20.00	8.04E-10	2.0E-09	5.74E-10	2.16E-07
8	18.85	3.91E-07	40	20.00	9.78E-09	2.0E-09	1.66E-09	6.26E-07
9	18.85	1.03E-05	40	20.00	2.59E-07	2.0E-09	1.98E-09	7.48E-07
10	18.85	3.35E-09	40	20.00	8.38E-11	2.0E-09	8.05E-11	3.03E-08
11	18.85	1.36E-07	40	40.00	3.40E-09	2.0E-09	1.26E-09	9.49E-07
12	18.85	2.51E-08	40	60.00	6.27E-10	2.0E-09	4.77E-10	5.40E-07
13	18.85	4.33E-09	40	110.00	1.08E-10	2.0E-09	1.03E-10	2.13E-07
14	18.85	2.93E-11	40	60.00	7.33E-13	2.0E-09	7.32E-13	8.28E-10
15	18.85	2.93E-11	40	60.00	7.33E-13	2.0E-09	7.32E-13	8.28E-10
16	18.85	1.64E-11	40	6.40	4.10E-13	2.0E-09	4.10E-13	4.95E-11

Table A1-9. Geometry, hydraulic conductivity (Kh), leakage coefficients (LC) and conductance (C) for shaft SC00 when K=1·10^{-8} m/s in the grouted zone.

Calculation layer	Circum-ference, m	Kh, m/s	Horiz. grid dx, m	Layer thick-ness dz, m	LCaq, s^{-1}	LCp, s^{-1}	LC, s^{-1}	C, m^2/s
1	15.71	7.50E-06	40	2.44	1.88E-07	2.0E-09	1.98E-09	7.59E-08
2	15.71	3.29E-06	40	1.00	8.22E-08	2.0E-09	1.95E-09	3.07E-08
3	15.71	8.63E-09	40	10.66	2.16E-10	2.0E-09	1.95E-10	3.26E-08
4	15.71	2.07E-05	40	19.90	5.19E-07	2.0E-09	1.99E-09	6.23E-07
5	15.71	6.95E-08	40	19.60	1.74E-09	2.0E-09	9.30E-10	2.86E-07
6	15.71	3.31E-08	40	20.00	8.28E-10	2.0E-09	5.86E-10	1.84E-07
7	15.71	3.29E-09	40	20.00	8.22E-11	2.0E-09	7.90E-11	2.48E-08
8	15.71	7.37E-08	40	20.00	1.84E-09	2.0E-09	9.59E-10	3.01E-07
9	15.71	2.71E-07	40	20.00	6.78E-09	2.0E-09	1.54E-09	4.85E-07
10	15.71	6.64E-07	40	20.00	1.66E-08	2.0E-09	1.79E-09	5.61E-07
11	15.71	1.32E-06	40	40.00	3.29E-08	2.0E-09	1.89E-09	1.18E-06
12	15.71	3.22E-07	40	60.00	8.04E-09	2.0E-09	1.60E-09	1.51E-06
13	15.71	2.10E-08	40	110.00	5.25E-10	2.0E-09	4.16E-10	7.19E-07
14	15.71	1.00E-11	40	60.00	2.50E-13	2.0E-09	2.50E-13	2.36E-10
15	15.71	1.00E-11	40	60.00	2.50E-13	2.0E-09	2.50E-13	2.36E-10
16	15.71	1.02E-11	40	36.40	2.55E-13	2.0E-09	2.55E-13	1.46E-10

Table A1-10. Geometry, hydraulic conductivity (Kh), leakage coefficients (LC) and conductance (C) for shafts SF00 and ST00 when K=1·10^{-8} m/s in the grouted zone.

Calculation layer	Circum-ference, m	Kh, m/s	Horiz. grid dx, m	Layer thick-ness dz, m	LCaq, s^{-1}	LCp, s^{-1}	LC, s^{-1}	C, m^2/s
1	18.85	7.50E-06	40	2.48	1.88E-07	2.0E-09	1.98E-09	9.25E-08
2	18.85	5.12E-06	40	1.26	1.28E-07	2.0E-09	1.97E-09	4.68E-08
3	18.85	1.21E-08	40	10.13	3.03E-10	2.0E-09	2.63E-10	5.02E-08
4	18.85	1.48E-05	40	19.93	3.70E-07	2.0E-09	1.99E-09	7.47E-07
5	18.85	5.71E-08	40	20.00	1.43E-09	2.0E-09	8.33E-10	3.14E-07
6	18.85	1.29E-07	40	20.00	3.22E-09	2.0E-09	1.23E-09	4.65E-07
7	18.85	2.54E-08	40	20.00	6.34E-10	2.0E-09	4.81E-10	1.81E-07
8	18.85	7.19E-07	40	20.00	1.80E-08	2.0E-09	1.80E-09	6.79E-07
9	18.85	7.66E-08	40	20.00	1.91E-09	2.0E-09	9.78E-10	3.69E-07
10	18.85	8.35E-08	40	20.00	2.09E-09	2.0E-09	1.02E-09	3.85E-07
11	18.85	7.82E-08	40	40.00	1.95E-09	2.0E-09	9.88E-10	7.45E-07
12	18.85	3.94E-08	40	60.00	9.84E-10	2.0E-09	6.60E-10	7.46E-07
13	18.85	6.52E-09	40	110.00	1.63E-10	2.0E-09	1.51E-10	3.13E-07
14	18.85	1.15E-11	40	60.00	2.86E-13	2.0E-09	2.86E-13	3.24E-10
15	18.85	1.15E-11	40	18.40	2.86E-13	2.0E-09	2.86E-13	9.93E-11

Table A1-11. Geometry, hydraulic conductivity (Kh), leakage coefficients (LC) and conductance (C) for shaft SA01 when K=1·10^{-9} m/s in the grouted zone.

Calculation layer	Circum-ference, m	Kh, m/s	Horiz. grid dx, m	Layer thick-ness dz, m	LCaq, s^{-1}	LCp, s^{-1}	LC, s^{-1}	C, m^2/s
1	9.42	8.04E-06	40	2.42	2.01E-07	2.0E-10	2.00E-10	4.55E-09
2	9.42	6.45E-06	40	2.86	1.61E-07	2.0E-10	2.00E-10	5.38E-09
3	9.42	2.72E-09	40	8.65	6.80E-11	2.0E-10	5.07E-11	4.13E-09
4	9.42	3.08E-08	40	19.57	7.69E-10	2.0E-10	1.59E-10	2.93E-08
5	9.42	1.16E-09	40	20.00	2.90E-11	2.0E-10	2.53E-11	4.77E-09
6	9.42	3.31E-07	40	20.00	8.28E-09	2.0E-10	1.95E-10	3.68E-08
7	9.42	3.31E-08	40	20.00	8.28E-10	2.0E-10	1.61E-10	3.03E-08
8	9.42	1.51E-08	40	20.00	3.77E-10	2.0E-10	1.31E-10	2.46E-08
9	9.42	1.54E-08	40	20.00	3.85E-10	2.0E-10	1.32E-10	2.48E-08
10	9.42	9.59E-08	40	20.00	2.40E-09	2.0E-10	1.85E-10	3.48E-08
11	9.42	1.05E-08	40	40.00	2.62E-10	2.0E-10	1.13E-10	4.28E-08
12	9.42	1.58E-06	40	60.00	3.96E-08	2.0E-10	1.99E-10	1.12E-07
13	9.42	3.45E-09	40	110.00	8.63E-11	2.0E-10	6.03E-11	6.24E-08
14	9.42	4.38E-10	40	60.00	1.10E-11	2.0E-10	1.04E-11	5.87E-09
15	9.42	4.38E-10	40	43.58	1.10E-11	2.0E-10	1.04E-11	4.26E-09

Table A1-12. Geometry, hydraulic conductivity (Kh), leakage coefficients (LC) and conductance (C) for shaft SA02 when K=1·10^{-9} m/s in the grouted zone.

Calculation layer	Circum-ference, m	Kh, m/s	Horiz. grid dx, m	Layer thick-ness dz, m	LCaq, s^{-1}	LCp, s^{-1}	LC, s^{-1}	C, m^2/s
1	9.42	6.15E-07	40	2.45	1.54E-08	2.0E-10	1.97E-10	4.56E-09
2	9.42	1.00E-07	40	1.00	2.50E-09	2.0E-10	1.85E-10	1.74E-09
3	9.42	3.65E-08	40	10.15	9.12E-10	2.0E-10	1.64E-10	1.57E-08
4	9.42	1.03E-07	40	20.00	2.58E-09	2.0E-10	1.86E-10	3.50E-08
5	9.42	3.95E-08	40	20.00	9.87E-10	2.0E-10	1.66E-10	3.13E-08
6	9.42	1.19E-05	40	20.00	2.96E-07	2.0E-10	2.00E-10	3.77E-08
7	9.42	4.15E-09	40	20.00	1.04E-10	2.0E-10	6.83E-11	1.29E-08
8	9.42	9.71E-05	40	20.00	2.43E-06	2.0E-10	2.00E-10	3.77E-08
9	9.42	3.08E-09	40	20.00	7.70E-11	2.0E-10	5.56E-11	1.05E-08
10	9.42	4.63E-09	40	20.00	1.16E-10	2.0E-10	7.33E-11	1.38E-08
11	9.42	1.69E-08	40	40.00	4.21E-10	2.0E-10	1.36E-10	5.11E-08
12	9.42	1.71E-09	40	60.00	4.28E-11	2.0E-10	3.52E-11	1.99E-08
13	9.42	3.22E-09	40	110.00	8.05E-11	2.0E-10	5.74E-11	5.95E-08
14	9.42	4.20E-09	40	60.00	1.05E-10	2.0E-10	6.89E-11	3.89E-08
15	9.42	4.20E-09	40	43.76	1.05E-10	2.0E-10	6.89E-11	2.84E-08

Table A1-13. Geometry, hydraulic conductivity (Kh), leakage coefficients (LC) and conductance (C) for shaft SB00 when K=1·10^{-9} m/s in the grouted zone.

Calculation layer	Circum-ference, m	Kh, m/s	Horiz. grid dx, m	Layer thick-ness dz, m	LCaq, s^{-1}	LCp, s^{-1}	LC, s^{-1}	C, m^2/s
1	18.85	0.00015	40	2.48	3.75E-06	2.0E-10	2.00E-10	9.35E-09
2	18.85	4.09E-05	40	1.27	1.02E-06	2.0E-10	2.00E-10	4.79E-09
3	18.85	2.09E-08	40	9.96	5.22E-10	2.0E-10	1.45E-10	2.72E-08
4	18.85	1.97E-05	40	19.89	4.93E-07	2.0E-10	2.00E-10	7.50E-08
5	18.85	4.89E-08	40	20.00	1.22E-09	2.0E-10	1.72E-10	6.48E-08
6	18.85	1.81E-07	40	20.00	4.52E-09	2.0E-10	1.92E-10	7.22E-08
7	18.85	3.22E-08	40	20.00	8.04E-10	2.0E-10	1.60E-10	6.04E-08
8	18.85	3.91E-07	40	20.00	9.78E-09	2.0E-10	1.96E-10	7.39E-08
9	18.85	1.03E-05	40	20.00	2.59E-07	2.0E-10	2.00E-10	7.53E-08
10	18.85	3.35E-09	40	20.00	8.38E-11	2.0E-10	5.91E-11	2.23E-08
11	18.85	1.36E-07	40	40.00	3.40E-09	2.0E-10	1.89E-10	1.42E-07
12	18.85	2.51E-08	40	60.00	6.27E-10	2.0E-10	1.52E-10	1.71E-07
13	18.85	4.33E-09	40	110.00	1.08E-10	2.0E-10	7.02E-11	1.46E-07
14	18.85	2.93E-11	40	60.00	7.33E-13	2.0E-10	7.30E-13	8.25E-10
15	18.85	2.93E-11	40	60.00	7.33E-13	2.0E-10	7.30E-13	8.25E-10
16	18.85	1.64E-11	40	6.40	4.10E-13	2.0E-10	4.09E-13	4.94E-11

Table A1-14. Geometry, hydraulic conductivity (Kh), leakage coefficients (LC) and conductance (C) for shaft SC00 when K=1·10^{-9} m/s in the grouted zone.

Calculation layer	Circum-ference, m	Kh, m/s	Horiz. grid dx, m	Layer thick-ness dz, m	LCaq, s^{-1}	LCp, s^{-1}	LC, s^{-1}	C, m^2/s
1	15.71	7.50E-06	40	2.44	1.88E-07	2.0E-10	2.00E-10	2.00E-10
2	15.71	3.29E-06	40	1.00	8.22E-08	2.0E-10	2.00E-10	2.00E-10
3	15.71	8.63E-09	40	10.66	2.16E-10	2.0E-10	1.04E-10	1.04E-10
4	15.71	2.07E-05	40	19.90	5.19E-07	2.0E-10	2.00E-10	2.00E-10
5	15.71	6.95E-08	40	19.60	1.74E-09	2.0E-10	1.79E-10	1.79E-10
6	15.71	3.31E-08	40	20.00	8.28E-10	2.0E-10	1.61E-10	1.61E-10
7	15.71	3.29E-09	40	20.00	8.22E-11	2.0E-10	5.83E-11	5.83E-11
8	15.71	7.37E-08	40	20.00	1.84E-09	2.0E-10	1.80E-10	1.80E-10
9	15.71	2.71E-07	40	20.00	6.78E-09	2.0E-10	1.94E-10	1.94E-10
10	15.71	6.64E-07	40	20.00	1.66E-08	2.0E-10	1.98E-10	1.98E-10
11	15.71	1.32E-06	40	40.00	3.29E-08	2.0E-10	1.99E-10	1.99E-10
12	15.71	3.22E-07	40	60.00	8.04E-09	2.0E-10	1.95E-10	1.95E-10
13	15.71	2.10E-08	40	110.00	5.25E-10	2.0E-10	1.45E-10	1.45E-10
14	15.71	1.00E-11	40	60.00	2.50E-13	2.0E-10	2.50E-13	2.50E-13
15	15.71	1.00E-11	40	60.00	2.50E-13	2.0E-10	2.50E-13	2.50E-13
16	15.71	1.02E-11	40	36.40	2.55E-13	2.0E-10	2.55E-13	2.55E-13

Table A1-15. Geometry, hydraulic conductivity (Kh), leakage coefficients (LC) and conductance (C) for shafts SF00 and ST00 when $K=1 \cdot 10^{-9}$ m/s in the grouted zone.

Calculation layer	Circum-ference, m	Kh, m/s	Horiz. grid dx, m	Layer thick-ness dz, m	LCaq, s^{-1}	LCp, s^{-1}	LC, s^{-1}	C, m^2/s
1	18.85	7.50E-06	40	2.48	1.88E-07	2.0E-10	2.00E-10	9.34E-09
2	18.85	5.12E-06	40	1.26	1.28E-07	2.0E-10	2.00E-10	4.74E-09
3	18.85	1.21E-08	40	10.13	3.03E-10	2.0E-10	1.20E-10	2.30E-08
4	18.85	1.48E-05	40	19.93	3.70E-07	2.0E-10	2.00E-10	7.51E-08
5	18.85	5.71E-08	40	20.00	1.43E-09	2.0E-10	1.75E-10	6.61E-08
6	18.85	1.29E-07	40	20.00	3.22E-09	2.0E-10	1.88E-10	7.10E-08
7	18.85	2.54E-08	40	20.00	6.34E-10	2.0E-10	1.52E-10	5.73E-08
8	18.85	7.19E-07	40	20.00	1.80E-08	2.0E-10	1.98E-10	7.46E-08
9	18.85	7.66E-08	40	20.00	1.91E-09	2.0E-10	1.81E-10	6.83E-08
10	18.85	8.35E-08	40	20.00	2.09E-09	2.0E-10	1.83E-10	6.88E-08
11	18.85	7.82E-08	40	40.00	1.95E-09	2.0E-10	1.81E-10	1.37E-07
12	18.85	3.94E-08	40	60.00	9.84E-10	2.0E-10	1.66E-10	1.88E-07
13	18.85	6.52E-09	40	110.00	1.63E-10	2.0E-10	8.98E-11	1.86E-07
14	18.85	1.15E-11	40	60.00	2.86E-13	2.0E-10	2.86E-13	3.23E-10
15	18.85	1.15E-11	40	18.40	2.86E-13	2.0E-10	2.86E-13	9.91E-11